EAST HARTFORD, CONNECTICUT

H-910093-46

Investigation of Gaseous Nuclear Rocket Technology -- Summary Technical Report

NASA Contract No. NASw-847

UNITED AIRCRAFT CORPORATION

United Aircraft Research Laboratories

EAST HARTFORD, CONNECTICUT

United Aircraft Research Laboratories

UNITED AIRCRAFT CORPORATION

EAST HARTFORD, CONNECTICUT

H-910093-46

Investigation of Gaseous Nuclear Rocket Technology -- Summary Technical Report

NASA Contract No. NASw-847

REPORTED BY G. H. McLafferty

G. H. McLafferty

DATE November 1969

NO. OF PAGES 136

COPY NO. 65

FOREWORD

An exploratory experimental and theoretical investigation of gaseous nuclear rocket technology was conducted during the period between September 15, 1963 and November 15, 1969 under Contract NASw-847 with the joint AEC-NASA Space Nuclear Propulsion Office. The Technical Supervisor of the Contract for NASA during the period between 1963 and 1967 was Captain W. A. Yingling (USAF), and during the period from 1967 through 1969 was Captain C. E. Franklin (USAF). The present report represents the final technical report under the contract. Work on gaseous nuclear rockets at the United Aircraft Research Laboratories is now being continued under Contract SNPC-70.

Report H-910093-46

Investigation of Gaseous Nuclear Rocket Technology --

Summary Technical Report

TABLE OF CONTENTS

Report H-910093-46

Investigation of Gaseous Nuclear Rocket Technology --

Summary Technical Report

SUMMARY

The experimental and theoretical investigations conducted under Contract NASw-847 during the period from September 1963 through November 1969 have been designed to obtain information applicable to determining the feasibility of two gaseous nuclear rocket engine concepts: the open-cycle vortex-stabilized engine and the closed-cycle nuclear light bulb engine. It became apparent from results of investigations conducted up to 1967 that the fuel-containment characteristics of the open-cycle engine were too low for economic fuel containment; therefore, all work since 1967 has been directed toward the nuclear light bulb engine. This latter engine is based on the transfer of energy by thermal radiation from gaseous nuclear fuel suspended in a neon vortex through an internally cooled transparent wall to seeded hydrogen propellant. Such an engine offers the possibility of providing values of specific impulse greater than 1500 sec, values of thrust-to-weight ratio greater than 1, and containment of the gaseous nuclear fuel without loss of fuel or fission products in the exhaust from the engine. In addition, it may be possible to obtain many reuses from such an engine by replenishing the spent recirculating fuel. Removal of the spent fuel and fission products from the engine would also reduce the radiation hazards during multiple-rendezvous missions.

The work under this contract has resulted in the issuance of 50 technical reports. The present report summarizes the key results discussed in these 50 reports and provides information which permits cross-referencing between the reports. The work under the contract has included investigations of the following: the characteristics of one-component and two-component vortex flows, both unheated and r-f induction heated; the characteristics of coaxial flows (this work has application to both the propellant region of a nuclear light bulb engine and the coaxial-flow engine being investigated at the NASA Lewis Research Center); the spectral and total radiant energy emitted from the fuel-containment region; the transmission characteristics of fused silica before, during and after being exposed to nuclear radiation; and various analytical studies designed to interpret the results of these programs in terms of the characteristics of full-scale engines.

RESULTS

1. Analyses of the characteristics of nuclear light bulb engines have resulted in selection of a reference engine design having the following characteristics: seven unit cavities, each having a length of 6 ft; cavity pressure of 500 atm; engine weight of 70,000 lb; effective fuel radiating temperature of 15,000 R; total power of 4600 megw; propellant-exit temperature of 12,000 R; specific impulse of 1870 sec (including allowance for propellant seeds and transpiration nozzle coolant flow); and thrust of 92,000 lb.

2. An r-f heated light source has been developed for simulating the nuclear fuel light source in a full-scale engine. This source has radiated a total of 156 kw or 37 kw/in.^{2}; this radiant flux is equal to the black-body radiant flux for a temperature of 10,200 R.

3. Internally cooled transparent-wall models having wall thicknesses of 0.005 in. (the same thickness as that required in a full-scale engine) have been developed and tested adjacent to the r-f heated plasma at plasma powers up to 50 kw. The power levels used in these tests were limited because of damage to the copper injectors used to drive the vortex within the transparent walls rather than because of damage to the transparent walls themselves.

4. Preliminary tests were conducted in which seeded simulated propellant was heated by thermal radiation from the r-f light source. These tests were at power levels up to 3 kw with associated temperature rises in a seeded propellant gas of about 200 F. The power levels and temperature rises were limited primarily by deposition of seed material on the transparent walls. Future investigations will concentrate on developing aerodynamic configurations for keeping the seed material off the wall and on raising the radiant power during the propellant heating tests.

5. The use of vortex flows in two-component gas tests has significantly increased the concentration of simulated nuclear fuel near the centerline relative to that near the wall. This effect is particularly evident in vortexes with radial temperature gradients in which the wall is colder than the center of the flow.

6. The stability of coaxial flows has been significantly improved by the use of porous foam materials in the inlet region upstream of a test section in which there is a velocity difference between the flows. These results are applicable to the propellant stream of a nuclear light bulb engine as well as to the coaxial-flow engine under investigation at the NASA Lewis Research Center.

7. Calculations of the radiant energy spectrum emitted by the nuclear fuel of a full-scale nuclear light bulb engine indicate that the spectrum is shifted toward the ultraviolet relative to the spectrum corresponding to a black-body temperature

defined by the total radiant flux. However, calculations also indicate that the energy in the ultraviolet portion of the spectrum can be reduced by the use of selected seeds in the fuel-containment region.

8. Results of several different experiments indicate that the equilibrium absorption at the center of the 2150-Å band in the fused silica transparent wall will be on the order of 3 to 8 cm^{-1} under the neutron and gamma flux encountered in a full-scale engine if no photon flux is present. The intense photon flux in a full-scale engine may substantially reduce this absorption. If not, the transparent wall thickness will have to be reduced from 0.005 to 0.003 to 0.004 in. if the temperature difference across the transparent wall is to be kept at the nominal design value of 200 F.

9. Preliminary calculations indicate that the control of a full-scale nuclear light bulb engine can be obtained by adjustment of the fuel flow injection rate into the multiple cavities.

INTRODUCTION

One of the most interesting propulsion concepts for space travel in the post-1975 time period is the gaseous nuclear rocket engine in which heat is transferred from a gaseous fissioning fuel to a propellant such as hydrogen. Because of the high temperatures obtainable in the gaseous fuel, such engines can theoretically provide values of specific impulse on the order of 1500 to 3000 sec and thrust-to-weight ratios greater than unity. The primary problems associated with such engines are the containment of the gaseous fuel in a cavity and the transfer of heat from the fuel to the propellant working fluid. The containment and heat transfer must be accomplished in a manner such that conventional materials and cooling techniques may be used in the containment vessel and exhaust nozzle.

Research on the characteristics of gaseous nuclear rockets has been carried out at a number of Government laboratories (notably the NASA Lewis Research Center, the Jet Propulsion Laboratory, the Aerospace Corporation, the AEC Oak Ridge National Laboratory, and the Los Alamos Scientific Laboratory) and at several industrial research laboratories. The largest research effort in a Government laboratory is being conducted at the NASA Lewis Research Center; this organization has concentrated on investigations of the coaxial-flow reactor concept. The largest research effort in an industrial laboratory has been conducted at the United Aircraft Research Laboratories. The purpose of this research has been to investigate the feasibility of two different gaseous nuclear rocket engine concepts. The first of these--the open-cycle, vortex-stabilized engine concept--is based on the transfer of energy by thermal radiation from gaseous nuclear fuel contained in a vortex to seeded hydrogen propellant passing external to the fuel-containment region. This concept, like the coaxial-flow reactor, relies on fluid mechanics to minimize loss of nuclear fuel in the exhaust. The second concept under investigation at the Research Laboratories, the nuclear light bulb engine, is similar to the open-cycle, vortex-stabilized engine, except that an internally-cooled transparent wall is located between the fuel-containment and propellant regions. Because of this physical barrier between the fuel and propellant, the nuclear light bulb offers the possibility of perfect containment of fuel and fission products.

The work on vortex containment of simulated gaseous nuclear fuel conducted in the first portion of the work under Contract NASw-847 resulted in the conclusion that the achievable levels of containment in a full-scale engine were insufficient to provide economical space transportation. As a result, all work after 1967 under this contract has been directed toward determining the feasibility of the nuclear light bulb engine.

A total of 50 reports have been issued to describe the technical results obtained under Contract NASw-847 (Refs. 1 through 50). The summary pages of these reports are reproduced in the Appendix. In addition, Table I indicates the category of technical information contained in each of these 50 reports.

Work on gaseous nuclear rocket technology at the United Aircraft Research Laboratories has been conducted under four contracts other than Contract NASw-847. These other contracts were: Contract NASw-768 with the Space Nuclear Propulsion Office; Contract NAS3-3382 with the NASA Lewis Research Center; and Contracts AF 04(611)7448 and AF 04(611)8189 with the USAF Rocket Propulsion Laboratory at Edwards Air Force Base. The results obtained under these contracts are described in Refs. 51 through 67, and the key technical areas covered in these reports are also indicated in Table I. Publications in technical journals and presentations at technical meetings which have been an outgrowth of work conducted under these five contracts are given as Refs. 68 through 93; all of this information is included in the reports issued under the contracts. In addition, the technology of gaseous nuclear rockets has received major support from United Aircraft's corporate-sponsored programs. Some of the reports issued under these programs are given as Refs. 94 to 97.

The progress made at UARL during investigations of gaseous nuclear rocket technology has been enhanced by interaction with a number of other organizations working on these problems. A selected list of reports which have been of particular relevance is given by Refs. 98 through 235; the primary area of technology for each of these reports is also indicated in Table I.

The following sections of the present report describe some of the key results obtained during the course of the work under Contract NASw-847.

DESCRIPTION OF VORTEX-STABILIZED NUCLEAR LIGHT BULB ENGINE

A small fraction of the total effort expended under Contract NASw-847 has been devoted to studies of the details of the characteristics of full-scale gaseous nuclear rocket engines; the majority of the effort has been devoted to the study of component technology problems, primarily fluid mechanics. However, these studies of engine characteristics are necessary to provide goals for the studies of component technology. Therefore, a large portion of the present summary report is devoted to the following descriptions of the characteristics of a nuclear light bulb engine in order to provide guidelines for the work in component technology described in following sections.

Principle of Operation

Sketches illustrating the principle of operation of the nuclear light bulb engine are given in Fig. 1. Energy is transferred by thermal radiation from gaseous nuclear fuel suspended in a neon vortex to seeded hydrogen propellant. The vortex and propellant regions are separated by an internally-cooled transparent wall. A seven-cavity configuration is shown in Fig. 1 rather than a single-cavity configuration in order to increase the total surface radiating area at the edge of the fuel. The total radiating surface area for the seven-unit configuration is approximately 2.2 times that for a single-unit cavity configuration having the same total cavity volume.

Neon is injected to drive the vortex, passes axially toward the end walls, and is removed through a port at the center of one or both end walls. The resulting aerodynamic configuration is referred to as a "radial-inflow" vortex (see Refs. 31, 32, 33, and 46). The neon discharging from the cavity, along with any entrained fuel and fission products, is cooled by being mixed with low-temperature neon, thus causing condensation of the nuclear fuel into liquid form. The liquid fuel is centrifugally separated from the neon and pumped back into the vortex region. The neon is then further cooled and pumped back to drive the vortex.

Reference Configuration at Design Point

A reference engine design has been chosen (Ref. 37) for use in evaluating the results of various component studies in terms of the characteristics of a full-scale nuclear light bulb rocket engine. The general configuration of the reference design is based on seven decisions which, although somewhat arbitrary in nature, appear logical on the basis of engine studies made using the component information available to date. These seven decisions are:

(1) Overall configuration: seven separate unit cavities with moderator-reflector material located between each cavity and surrounding the assembly of cavities.

(2) Size: length of individual cavity equal to 6.0 ft and volume of all seven cavities equal to 169.8 ft^3 (equal to the volume of a single cavity having a diameter of 6 ft and a length of 6 ft).

(3) Vortex volume for seven cavities: equal to half of the total cavity volume or 84.9 ft^3. The corresponding volume within the transparent wall of each of the seven unit cavities is 12.1 ft^3.

(4) Cavity pressure: a value of cavity pressure of 500 atm is chosen on the basis of criticality and fuel density ratio considerations.

(5) Fuel-containment region: the radius of the fuel-containment region is assumed to be 85 percent of the radius of the transparent wall.

(6) Effective fuel black-body radiating temperature: assumed to be equal to 15,000 R.

(7) Propellant exit temperature: assumed to be equal to 80 percent of the fuel radiating temperature, or 12,000 R.

Sketches showing the dimensions and conditions in a unit cavity of the reference nuclear light bulb engine are given in Figs. 2 and 3, and a side-view drawing of the complete reference engine configuration is given in Fig. 4.

Engine Power

The black-body heat flux at the outside edge of the fuel-containment region for the assumed black-body radiating temperature of 15,000 R is 24,300 Btu/sec-ft^2 (178 kw/$in.^2$). The "surface area" at the edge of the cylindrical fuel-containment region of all seven unit cavities is 179.8 ft^2. Therefore, the total energy radiated outward from the fuel is the product of these two quantities, or 4.37×10^6 Btu/sec (4600 megw).

Surface reflection at the transparent walls will result in approximately 15 percent of the incident energy being reflected back toward the fuel-containment region. Thus, the net heat transfer by radiation through the transparent wall to the propellant region will be 85 percent of that indicated in the preceding paragraph. However, the energy lost from the fuel-containment region by thermal radiation represents only approximately 85 percent of the total energy created in the fission process. The remaining 15 percent of the energy created in the fission process is

convected away from the fuel-containment region by neon flow (see following sections) or is deposited in the moderator walls by neutrons and gamma rays. Therefore, it has been assumed that the total energy created in the engine is equal to that corresponding to black-body radiation at 15,000 R (i.e., a total power of 4.37×10^6 Btu/sec or 4600 megw). The engine size and radiating temperature chosen provide an engine power which is approximately equal to that which has been considered for advanced solid core nuclear rockets.

Hydrogen Propellant Stream Properties

At the assumed hydrogen exit temperature of 12,000 R, the enthalpy according to Ref. 26 is 1.033×10^5 Btu/lb. If the total engine power is divided by this value of hydrogen enthalpy, a resulting hydrogen flow rate of 42.3 lb/sec is indicated for all seven units, which yields a value of 6.04 lb/sec for each unit cavity.

Since the hydrogen propellant must absorb approximately 15 percent of the total energy created in the process of removing heat from the engine walls and the neon recycle system, the hydrogen inlet enthalpy must be 15 percent of the hydrogen exit enthalpy, or 15,500 Btu/lb (see Fig. 3). The corresponding hydrogen inlet temperature according to Ref. 26 is 4050 R. This temperature is approximately the same as that considered for the hydrogen exit temperature in solid-core nuclear rockets.

The hydrogen flow cross-sectional area in the propellant region has been assumed to be proportional to the local average hydrogen enthalpy. Thus, the cross-sectional area at the inlet is 15 percent of the cross-sectional area at the exit. The corresponding values of hydrogen velocity at the inlet and exit are 35.5 and 23.7 ft/sec, respectively (Fig. 3). It might be desirable to increase the inlet area and decrease the exit area in order to provide a uniform hydrogen velocity of approximately 30 ft/sec in the propellant region. However, insufficient information is available at present to properly design the geometry of the propellant region.

The calculated dynamic pressure of the hydrogen at the inlet to the propellant region is less than 0.05 lb/in.^{2} (see Fig. 3). This dynamic pressure is much less than that usually considered in solid-core nuclear rockets. The dynamic pressure at the exit of the propellant region is less than that at the entrance of the propellant region primarily because of the change of hydrogen density.

Propellant Seed Characteristics

It is assumed in the following discussion that the required normal "optical depth" of the seeds at the propellant inlet station is 3.0. If all of the light emitted from the fuel-containment region passed only in a direction normal to the propellant region, the energy transmitted through the propellant region would be $1/e^3$, or 5 percent of the incident energy. However, many of the light rays emitted

from the fuel-containment region pass in an oblique direction through the propellant region. According to Fig. 3 of Ref. 57, the percentage of light which is emitted from a black body and which would pass through a region having an optical depth of 3.0 is approximately 2 percent of the incident energy. It is also expected that a large portion of the energy which passes through the seeded propellant region and impinges on the outer wall will be reflected back into the propellant stream.

It is also assumed in the following discussion that the hydrogen seed is composed of tungsten particles having a diameter of 0.05 micron. Information on the absorption characteristics of such tungsten particles is given in Fig. 19 of Ref. 22. Integration of the spectral absorption parameters in this figure yields an average absorption parameter weighted by the black-body spectrum at 15,000 R of approximately 5000 cm^2/gm or 2440 ft^2/lb. The distance across the propellant stream at the duct inlet is 0.0931 ft or 2.84 cm (see Fig. 2). Thus, the absorption coefficient required to provide an optical depth of 3.0 must be 1.06 cm^{-1} or 32.2 ft^{-1}. The required seed density, obtained by dividing the required absorption coefficient by the absorption parameter, is 1.32×10^{-2} lb/ft^3. This seed density is equal to 3.9 percent of the inlet propellant density.

As noted in Ref. 22, it is expected that the opacity obtainable by using thin plates will be greater than that obtainable by using spherical particles. However, the data on spherical particles rather than flat plates has been used in the preceding analysis because no information is available on the absorption characteristics of these thin flat plates, whereas data on absorption of light in streams containing spherical tungsten particles is available in Refs. 6, 119, 125, and 183.

Neon Characteristics

The reason for injecting neon coolant between the nuclear fuel and the transparent wall is to prevent diffusion of the nuclear fuel toward the wall, thereby preventing fuel plating on the wall and preventing fission fragments from impinging on the wall. If the neon coolant is to serve this purpose, the thickness of the diffusion layer at the outside edge of the fuel-containment region must be less than the distance between the edge of the fuel-containment region and the transparent wall. This diffusion layer thickness is related to the thickness of the viscous layer in this region. In the following calculations it is assumed that the thickness of the viscous layer evaluated on the basis of the conditions at the edge of the fuel-containment region is 0.05 ft. The actual thickness of the viscous layer would be considerably less than 0.05 ft because of the decrease in temperature (and the corresponding decrease in diffusivity) with increasing radius in this region. In addition, the thickness of the diffusion layer will be less than the thickness of the viscous boundary layer because the Schmidt number is greater than unity for low fuel concentrations (see Ref. 4).

The thickness of the viscous boundary layer at the outside edge of the fuel-containment region is a function of the axial velocity in this region and the turbulence level of the flow. It is assumed in the following discussion that the flow in this region is laminar because of the stabilizing effect of radial temperature gradients (see following section). It was determined on the basis of the calculations procedures in Ref. 61 that a viscous boundary layer thickness at the edge of the fuel region of 0.05 ft would require an axial velocity in this region of 1.95 ft/sec near the end walls. (The axial velocity increases linearly from zero at the midplane to a specified value near the end wall according to the analysis of Ref. 61.) It was also assumed in the analysis of Ref. 61 that the axial dynamic pressure is constant in the region between the outside edge of the fuel-containment region and the peripheral wall (neglecting boundary layer effects at both boundaries of this region). Since density increases by a factor of 7.5 between the outside edge of the fuel-containment region and the peripheral wall, the velocity must decrease by a factor of $(7.5)^{0.5} = 2.74$ in order to provide a constant axial dynamic pressure. The corresponding axial velocity of the neon next to the peripheral wall is 0.71 ft/sec.

Insufficient information is available at present to determine the variation of temperature with radius in the neon region (this temperature distribution can be controlled to some extent by proper selection of seeds in the neon). However, sample calculations were carried out assuming a linear variation of temperature with radius between the values of 15,000 R at the edge of the fuel and 2000 R at the wall. This assumed variation of temperature permitted calculation of a variation of density with radius and, from the assumption of constant axial dynamic pressure, a variation of axial velocity with radius. The total flow passing towards both end walls, obtained by integrating the resulting mass flow distribution, is equal to 2.96 lb/sec per cavity. The total energy carried away by this fluid was determined by integrating the product of density, axial velocity, specific heat, and the neon temperature rise as a function of radius. The total energy carried away from each unit by the neon flow passing towards both end walls was determined to be 4120 Btu/sec (a constant neon specific heat of 0.253 was assumed in this analysis). The total energy carried away by the neon in all seven units is equal to 28,900 Btu/sec. This energy removal rate is approximately 0.7 percent of the total energy created in the engine.

It will probably be necessary to provide a tangential velocity within the transparent wall of the nuclear light bulb engine which is somewhat greater than the axial neon velocity in order to provide the stabilizing effect necessary to create laminar flow at the edge of the fuel-containment region. It has been arbitrarily assumed in the following calculations that this tangential velocity is 10 ft/sec, or approximately 5 times the maximum axial velocity. The corresponding dynamic pressure of the neon at the inside edge of the transparent wall is approximately 0.075 $lb/in.^2$.

The centrifugal acceleration corresponding to the tangential velocity at the inside edge of the transparent wall is 3.9 g's. Insufficient information is available at present to determine whether this centrifugal acceleration is sufficient to prevent problems resulting from axial vehicle accelerations. If such problems should arise, it will be necessary to increase the tangential velocity at the outer periphery of the vortex tube. However, the dynamic pressures at injection are sufficiently low in the present reference design that relatively large increases in velocity can be tolerated without encountering intolerably high dynamic pressures due to this tangential velocity.

Fuel Region Characteristics

The neutron transport theory studies of Ref. 44 have indicated a critical mass requirement for the reference engine of approximately 30.9 lb. This critical mass is less than that for a single-cavity engine because of the moderating effect of the material located between adjacent cavities. The average fuel density based on the volume inside the edge of the fuel-containment region of the seven cavities in the reference engine is 0.505 lb/ft^3 (8.1×10^{-3} gm/cm^3). Thus, the average density of the fuel is only 54 percent of the density of the neon at the outside edge of the fuel-containment region. The gases in the fuel-containment region are considerably hotter than the gases at the outside edge of the fuel-containment region. On the basis of the studies of Ref. 24, the average temperature in the fuel-containment region is approximately 44,000 R. The resulting average neon density in the fuel-containment region is approximately 0.19 lb/ft^3 (accounting for the fuel partial pressure but neglecting neon ionization). Thus, the average total density (the sum of average fuel density and average neon density) in the fuel-containment region is approximately 0.70 lb/ft^3. This total density is only 75 percent of the density of the neon at the outside edge of the fuel-containment region.

The volume flow of neon passing through the cavity obtained by dividing the neon mass flow of 2.96 lb/sec by the neon density at the outside edge of the fuel-containment region of 0.924 lb/ft^3 is 3.2 ft^3/sec. The resulting average neon dwell time obtained by dividing the vortex volume of 12.1 ft^3 by the neon volume flow rate is 3.8 sec. If the average fuel dwell time is equal to 5 times the average neon dwell time (see Refs. 31, 32, 33, and 46), the average fuel dwell time would be approximately 19 sec. Since the nuclear fuel mass per unit cavity is approximately 4.4 lb, this fuel retention time would correspond to a fuel flow rate of approximately 0.23 lb/sec per unit cavity.

An estimate of the energy carried away by the fuel passing through the cavity can be obtained by multiplying the fuel flow rate by the average fuel exit enthalpy. This average fuel exit enthalpy can be estimated by multiplying the average fuel temperature of 44,000 R by a specific heat of 0.1 Btu/lb-deg R. The corresponding energy removal rate is approximately 1000 Btu/sec per unit cavity, or 7000 Btu/sec for the seven unit cavities. This energy removal rate is approximately 0.16 percent of the total energy creation rate in the engine.

Specific Impulse and Thrust

The exhaust velocity which would be created by converting all of the hydrogen enthalpy of 1.033×10^5 Btu/lb to kinetic energy would be 71,900 ft/sec. This exhaust velocity would correspond to a specific impulse of 2230 sec. This ideal specific impulse has been reduced to account for the following factors:

(1) The specific impulse has been reduced by 8 percent to allow for incomplete expansion due to an area ratio of 545 rather than infinity (corresponding pressure ratio equals 1000; see Ref. 26).

(2) The specific impulse has been reduced by 6 percent to account for the requirement for approximately 12 percent transpiration coolant flow for the nozzle (see Ref. 97).

(3) The specific impulse has been reduced by 1.95 percent to allow for the 3.9 percent mass fraction of tungsten seeds.

(4) The specific impulse has been reduced by 1 percent to allow for friction and recombination losses in the nozzle.

The final specific impulse on the basis of these four corrections is 84 percent of the ideal specific impulse, or 1870 sec.

The total flow passing through the nozzle exit (including an allowance for 3.9 percent seed and 12 percent transpiration cooling for the nozzle) is 49.3 lb/sec. The thrust produced by this flow at a specific impulse of 1870 sec would be 92,000 lb.

According to Ref. 26, the hydrogen flow per unit area at the throat for a stagnation temperature of 12,000 R and a stagnation pressure of 500 atm is 1062 $lb/sec\text{-}ft^2$. If the flow area occupied by the seed flow is neglected, and half of the transpiration coolant flow is assumed to be injected upstream of the throat, the corresponding throat flow area would be 0.0422 ft^2. If a single nozzle were employed, the throat diameter would be 0.232 ft. For the nozzle area ratio of 545 assumed in calculating the loss in specific impulse due to a finite area ratio, the nozzle exit area would be 23.0 ft^2. The corresponding diameter of the exit of a single nozzle would be 5.40 ft, which is substantially less than the overall engine diameter. For the seven-nozzle configuration shown in Figs. 1 and 4, the throat and exit diameters would be 0.0875 ft (1.05 in.) and 2.04 ft, respectively.

Limitations on Specific Impulse

The specific impulse of a gaseous-core nuclear rocket engine is greater than that of a solid-core nuclear rocket engine because of the greater propellant-exit temperature in the gaseous nuclear rocket engine. This increased propellant-exit temperature

is due to the fact that the hydrogen propellant is heated by thermal radiation from gaseous nuclear fuel, rather than being heated by conduction and convection from solid nuclear fuel. There are three limitations on the specific impulse which can be obtained from a gaseous nuclear rocket. The first limitation is due to the fact that not all of the energy deposited in the propellant is transferred by thermal radiation; instead, some is transferred by conduction and convection due to various other mechanisms of heat loss from the fuel-containment region. For instance, in the reference engine discussed in the preceding subsections, fifteen percent of the energy created is assumed to be absorbed in the hydrogen propellant before it is injected into the engine. Therefore, the exhaust enthalpy of the hydrogen propellant is equal to $1/0.15 = 6.67$ times the enthalpy of the hydrogen propellant as it is injected into the propellant region. Since this propellant-injection temperature is also limited by the same factors which limit the propellant-exit temperature in a solid-core engine, the exhaust enthalpy and temperature are also limited.

The effect on specific impulse of cavity propellant inlet temperature and the fraction of the energy transferred to the propellant by thermal radiation is illustrated in Fig. 5. In calculating the results shown in Fig. 5, the specific impulse was taken as 84 percent of the ideal specific impulse corresponding to the propellant-exit enthalpy (see preceding section). The reference engine, for which the propellant-inlet temperature is 4050 R and 85 percent of the energy is transferred to the propellant by thermal radiation, is indicated by the upper symbol on Fig. 5. If the propellant-inlet temperature were raised to 6000 R (a probable upper limit for the material walls of the moderator portion of a nuclear rocket engine), and the percent energy transferred by internal radiation remained at 85 percent, the specific impulse would be raised from 1870 sec for the reference engine to 2330 sec.

One technique by which this limitation on specific impulse could be overcome is by the use of space radiators to reject the waste heat from the engine. If all of the waste heat (i.e., the heat deposited directly in the engine walls) could be removed by the use of a space radiator, the limitation on specific impulse indicated by Fig. 5 would be removed. However, the use of a space radiator would result in a penalty in weight. If the radiator temperature were 4000 R, then all the waste energy from the reference engine (690 megw) could be rejected with a radiator surface area of 5300 ft^2. If the weight of the radiator is assumed to be 5 lb/ft^2 of radiating area, then the resulting penalty in engine weight would be 26,500 lb.

A second limitation on the maximum specific impulse of a nuclear light bulb engine occurs because of the need to match the wavelength spectrum radiated from the nuclear fuel to the wavelength range over which the transparent wall will transmit this energy. For a fuel black-body radiating temperature of 15,000 R and a fused silica wall, there is a reasonable match between these two spectra (see following section). There is some indication that single-crystal beryllium oxide will be transparent to a much shorter wavelength (on the order of 0.12 microns) than fused silica. Therefore,

transparent walls made from single-crystal beryllium oxide should permit the use of fuel radiating spectra which are centered more in the ultraviolet than is permitted by the use of fused silica walls. However, as the propellant exit temperature increases, the required fuel radiating temperature also increases, and eventually will reach the point where too large a fraction of the energy radiated from the fuel will lie in the ultraviolet portion of the spectrum where no known materials are transparent.

A third limitation on specific impulse is due to the necessity of providing transpiration cooling for the exhaust nozzle. Analyses of the transpiration cooling flow requirements necessary to protect the exhaust nozzle from convective and radiative energy deposition are given in Ref. 97. These studies indicate that the limiting specific impulse of any type of gaseous nuclear rocket engine will be between approximately 3,000 and 5,000 sec because of nozzle cooling requirements.

The development of a nuclear light bulb engine having the characteristics of the reference engine would clearly provide performance which is superior to that of any solid core nuclear rocket engine for most applications. It is also possible that substantial advantages can be obtained by the use of a nuclear light bulb engine with significantly poorer performance than that given by the reference engine. Such a "derated" engine might have a fuel black-body radiating temperature of 10,000 R and a propellant-exit temperature of 8000 R. According to Fig. 5, this would provide a specific impulse of 1160 sec, which might be sufficiently greater than that of a solid-core nuclear rocket to make it a desirable engine for use in many applications. Also, according to Fig. 5, it would be permissible to allow the fraction of energy transferred to the propellant before injection to increase from 15 percent for the reference engine to 25 percent, and still require a propellant inlet temperature of only 2800 R. This reduction in propellant inlet temperature would substantially reduce the materials development effort associated with development of a nuclear light bulb engine.

One of the problems which may be encountered as a result of further research on the nuclear light bulb engine is an increase in the fraction of the energy which is transferred to the propellant before injection into the cavity. This fraction, which is calculated to be 15 percent for the reference engine, could increase because of increased convection from the propellant to the wall, increased heat load in the fuel recycle system, or increased radiant heat transfer to the structure due to either degraded seed characteristics or degraded wall reflectivity. The resulting reduction in specific impulse for a fixed propellant inlet temperature can be obtained from Fig. 5. However, it may be desirable, if this penalty should become too severe, to employ a space radiator for rejection of this waste heat. As noted in a preceding paragraph, it may be possible to reject 15 percent of the total energy by the use of a space raditor weighing approximately 26,000 lb.

VORTEX FLUID MECHANICS

Motivation for Employing Vortex Flows

The gaseous nuclear fuel must be kept separated from the transparent wall in a nuclear light bulb engine in order to prevent condensation of the fuel on the wall and to prevent impingement of fission fragments on the wall. Two aerodynamic configurations have been considered to provide this separation: a coaxial flow of nuclear fuel and buffer gas, and a "radial-inflow" vortex. In all work at the United Aircraft Research Laboratories, a vortex has been chosen to provide this separation for the reasons discussed in the following paragraphs. However, there is no inherent reason why a coaxial flow pattern similar to the flow pattern in an open-cycle coaxial-flow reactor (but with more evenly matched velocities) could not be employed.

Vortex flows have been considered for use in gas-core nuclear rockets for three reasons. The first reason was to provide centrifugal diffusion of the heavy fuel atoms relative to a radial-inward flow of light hydrogen atoms (see Ref. 143). This is unimportant for application to a nuclear light bulb and has also proven to be impractical for use in a gas-core nuclear rocket in which the hydrogen propellant is heated as it is diffused through the fuel. The second reason for employing a vortex in a gas-core nuclear rocket is to provide preferential containment of the gaseous nuclear fuel relative to the hydrogen propellant. Such containment is required for the open-cycle vortex-stabilized gaseous nuclear rocket; however, the fuel retention characteristics of the vortex have proven to be insufficient to provide economical fuel containment (see Ref. 31). Although minimization of the fuel flow rate relative to the neon flow rate in a nuclear light bulb reactor is desirable, it is not an overriding necessity; an increase in the fuel flow rate will only result in an increase in the heat load on the fuel recycle system. The third reason for employing a vortex in a gaseous nuclear rocket is to take advantage of the resultant laminar flow patterns in order to keep the gaseous nuclear fuel separated from the outer containing wall. This third reason is the primary reason for employing a vortex in a nuclear light bulb engine.

Unheated Vortex Flows

The first indications of laminar vortex flow evidenced during investigations of gaseous nuclear rocket technology were found in water vortex tests conducted during 1961 (Ref. 54). During these tests, a radial-inflow vortex was employed in which a favorable radial gradient of angular momentum (increasing angular momentum with increasing radius) existed at intermediate radii. This radial momentum gradient resulted in stabilization of the flow and the appearance of fine laminar dye patterns

in water vortex tests. Photographs from Ref. 13 of typical dye patterns illustrating this effect are shown in Fig. 6. The flow in the thin boundary layer immediately adjacent to the peripheral wall is not stabilized in such tests since the angular momentum gradient in this region is destabilizing. However, the angular momentum gradient is sufficiently stabilizing at intermediate radii to eliminate the turbulence present near the outer periphery of the tube.

Vortex flows may be stabilized by a favorable radial gradient of density (increasing density with increasing radius) as well as by a favorable radial gradient of angular momentum. Results of two-component gas tests conducted to illustrate this favorable effect of radial density gradient are given in Fig. 7. These tests were conducted with air injected near the outer periphery of the vortex to drive the vortex, and mixtures of different simulated-fuel gases injected near the vortex centerline to form a simulated fuel cloud. When helium "marked" with iodine was injected near the vortex centerline, a steep radial gradient in gas concentration near the outer region of the simulated fuel cloud was formed, as evidenced in Fig. 7. This steep concentration gradient was not encountered with near-zero radial density gradients (tests with a mixture of nitrogen and iodine) or with destabilizing density gradients (tests with sulfur hexafluoride and iodine).

According to Fig. 3, the neon density near the outer periphery of the vortex in a full-scale engine is 7.5 times the neon density at the outer edge of the fuel-containment region. This neon density gradient, by analogy with the results shown in Fig. 7, should provide essentially laminar flow in this region. This laminar flow should result even though turbulence will exist in the layer immediately adjacent to the outer periphery of the vortex tube as a result of the unstable radial gradient of angular momentum near the peripheral wall and as a result of the turbulence associated with neon injection. In the laminar region between the edge of the fuel and the edge of the peripheral-wall boundary layer, the neon should "blow away" any nuclear fuel diffusing radially outward. The axial velocities shown in Fig. 3 have been selected to cause this effect.

One difficulty which has been encountered in tests of vortex flows is that in many cases it is difficult to inject a substantial quantity of simulated fuel into the central region of the vortex without creating high levels of turbulence. One problem which must be overcome in future work, therefore, is to develop techniques which will permit injection of simulated fuel into the fuel-containment region without generating unacceptable turbulence.

R-F-Heated Vortex Flows

It became apparent in 1966 that nuclear tests of a gas-core rocket should be conducted only after small-scale tests had been conducted at temperatures and heat fluxes similar to those expected in a full-scale engine. This was particularly true for the nuclear light bulb engine, where it is necessary to demonstrate that the thin internally-cooled transparent walls will stay intact in a region of high heat flux. A number of different techniques were considered for creating the desired conditions, including the use of both radio-frequency induction heaters and arc heaters. The r-f heat source was chosen for creating the conditions necessary to simulate a nuclear light bulb engine because it would add energy directly to the center of the stream without energy addition in the boundary layers adjacent to electrodes, as would occur with an arc configuration. Although emphasis has been placed on r-f heating experiments during tests conducted under Contract NASw-847, some tests have also been conducted using an arc (Ref. 45).

The r-f equipment required for these tests was developed under a corporate-sponsored program. The power supply for this r-f device provides up to 1.2 megw of d-c power at approximately 25 kv. With allowance for losses in the r-f equipment and the r-f work coils, it is anticipated that it will eventually be possible to deposit 500 kw in a small-diameter gas load (deposition of this energy in a large-diameter gas load is relatively easy, but does not provide as high a value of radiant heat flux from the r-f heated plasma region). The highest power deposited in a gas load to date using this equipment in tests conducted under Contract NASw-847 has been 216 kw in a plasma having a diameter of 0.82 in. Additional details of the characteristics of the gas and cooling flow in this particular test is given in Fig. 8. As noted on Fig. 8, the total power radiated through the inner peripheral wall during this test was 156 kw. Additional information relative to r-f light source test results is given in Fig. 9, where the output radiant energy flux is plotted as a function of discharge power. The highest flux noted on this figure, 36.7 kw/in.^{2}, corresponds to the data point illustrated in Fig. 8. This radiant flux is equal to the radiant flux from a black body at a temperature of 10,200 R. Additional details of this test are given in Ref. 45.

One of the purposes of developing the light source shown in Fig. 8 is to permit testing of thin-walled, internally-cooled models which represent the transparent wall of a full-scale nuclear light bulb engine. Photographs of two such models which have been employed in the tests described in Ref. 45 are given in Fig. 10. The thickness of the transparent-wall tubes in these models is 0.005 in., which is equal to the nominal wall thickness of the tubes chosen for the full-scale engine. The main problem encountered in the development of models such as those shown in Fig. 10 was to prevent model breakage at the joints between the transparent walls and the metal structure. This problem was solved by employing a silicone rubber sealant in this region.

Models similar to those shown in Fig. 10 were tested in the r-f discharge at power levels up to approximately 50 kw. These tests were terminated because of damage to the copper vortex injector tubes, not damage to the transparent walls. These copper injector tubes were cooled only by the argon flow which passed through the tubes to drive the vortex. Vortex-injection configurations with water cooling as well as the internal argon cooling have now been developed. It is expected that future experiments will permit tests of these transparent-wall models at significantly higher power levels. It should be noted that the energy fluxes deposited on the transparent wall in these tests were, in some cases, greater than that exptected in a full-scale engine because of the smaller dimensions of the model as compared to the full-scale engine.

Preliminary tests were also initiated to heat seeded simulated propellant by thermal radiation passing through a transparent-wall model. These tests were conducted at low power levels (on the order of 3 kw) and resulted in a maximum propellant temperature rise of approximately 200 F. The main difficulty encountered in these tests was coating of the particle seed material on the outside of the transparent walls. Better control of the flow in the simulated propellant stream is necessary to keep the seeded portion of the stream separated from the transparent wall (see following section).

Two-component gas vortex tests were conducted using an 80-kw r-f power supply (Ref. 46). These tests indicated that the radial temperature gradient in an r-f heated vortex resulted in a reduction of simulated-fuel concentration near the peripheral wall relative to tests with no r-f energy addition.

COAXIAL-FLOW FLUID MECHANICS

The investigation of gaseous nuclear rocket technology conducted under Contract NASw-847 has included investigations of coaxial-flow fluid mechanics in support of the NASA Lewis Research Center work on the coaxial-flow reactor, as well as work on vortex flows such as the work described in the preceding section. Tests have been conducted with a range of geometrical configurations, with different molecular weight ratios between the heavy and light gases, and with different velocity ratios between these gas streams. The most significant result of these tests is an indication of the effect of the use of foam inlets in minimizing the mixing between the high-velocity simulated-propellant stream and the low-velocity simulated-fuel stream (see Fig. 11 and Ref. 49). These foam inlets serve to reduce the initial stream turbulence, particularly in the boundary layers on the surfaces separating the initial high-velocity stream from the initial low-velocity stream.

The results of the coaxial-flow tests have application to the propellant stream of a nuclear light bulb engine as well as to an open-cycle coaxial-flow engine. To prevent impingement of propellant seed on the reflecting outer wall and the transparent inner wall of a nuclear light bulb engine, it is necessary to employ a seed-free buffer region between the main seeded propellant stream and each of these walls. If the thickness of these buffer regions is to be minimized, then the turbulence associated with the interface between these two streams must also be minimized. Therefore, the foam inlet technology is also important for application to the nuclear light bulb propellant stream. This fact was emphasized by test results described in the preceding section in which propellant heating experiments were severely limited by coating of seed on the transparent wall.

RADIANT HEAT TRANSFER

Calculations and experiments have been performed to determine the spectral absorption coefficients of several gases and solid materials which might be employed in different regions of the nuclear light bulb engine, and to determine the resulting radiant heat transfer characteristics of the engine. One portion of this effort has been directed toward calculation of the spectral absorption coefficients of the gaseous nuclear fuel. This has been accomplished for several different analytical fuel models using two different sets of fuel ionization potentials. The fuel absorption coefficients have, in turn, been used to calculate the temperature distributions in the fuel-containment region. Typical results indicating centerline temperatures are given in Fig. 12 as a function of average fuel density for several different values of radiant heat transfer per unit length. The radiant heat transfer per unit length for the reference nuclear light bulb engine is 104,000 Btu/sec-ft, and the average fuel density is 8.1×10^{-3} gm/cm^3 (see preceding section). It can be seen from Fig. 12 that this will result in a centerline temperature on the order of 64,000 R (36,000 K).

Calculations have been made to determine the spectral distribution of energy emitted from the fuel-containment region. The absorption coefficient of nuclear fuel in the ultraviolet portion of the spectrum is usually much less than that in the visible portion of the spectrum. Therefore, an observer "sees further into" the nuclear fuel in the ultraviolet portion of the spectrum and, hence, the output ultraviolet radiation is increased relative to the visible radiation. A discussion of these results is given in Ref. 47. These results are undesirable, since they place more of the energy in the ultraviolet portion of the spectrum where the transparent walls are more opaque (see following section). Therefore, it is desirable to reduce this effect as much as possible. One method by which the energy in the ultraviolet portion of the spectrum can be reduced is by the use of seed materials in the neon to increase the absorption preferentially in the ultraviolet portion of the spectrum. One such possible seed is diatomic oxygen, which is extremely opaque in the ultraviolet portion of the spectrum (as evidenced by the poor transmission of the atmosphere to ultraviolet energy), yet is transparent in the visible portion of the spectrum. The use of diatomic oxygen could have two effects. First, it would absorb the ultraviolet energy before it impinges on the transparent wall, thereby reducing the heat load on this wall. However, this would still require that the energy be removed from the oxygen-seeded neon in the fuel recycle system. A much more desirable circumstance is one in which the oxygen retains its absorption at edge-of-fuel conditions. Under this circumstance, the oxygen would reradiate its energy back into the fuel region, and a minimum of energy would have to be removed in the fuel recycle system. Only preliminary calculations have been conducted to date to determine the effect of neon seeding (Ref. 47).

Calculations and measurements have also been made to determine the spectral absorption coefficients of various propellant seed materials. The theoretical calculations to determine the absorption characteristics of particle seeds have employed experimentally determined values of the complex index of refraction, in conjunction with the Mie theory, to determine spectral absorption coefficients as a function of wavelength and particle diameter. Many different particle materials have been considered. Although carbon particles provide the highest absorption per unit weight, these particles react with hydrogen at relatively low temperatures (Ref. 8); therefore, tungsten particles have been assumed to be employed in the full-scale engine.

Results of theoretical and experimental studies of the extinction characteristics of tungsten particles are given in Fig. 13. The extinction parameter is the sum of the absorption parameter and the scattering parameter; the scattering is usually much lower than the absorption. Although the nominal radius of these particles is 0.01 microns, they normally prove to be agglomerated into effectively much larger diameter particles. This increase in effective diameter results in a decrease in the extinction parameter due to the fact that some of the particles "hide behind" other particles. As noted in Fig. 13, the passage of particle-containing streams through a small-diameter passage at high stream velocities results in breaking up of particle agglomerates, and a resulting increase in extinction parameter. The highest value of extinction parameter measured for tungsten particles during this program was 8200 cm^2/gram, and was obtained at a high reservoir pressure upstream of the passage, a relatively long passage, and with helium used as the carrier gas to maximize the velocity gradients within the stream. This high value of extinction parameter is only ten percent lower than the theoretical value for a particle radius of 0.16 microns. The experimental data shown in Fig. 13 were obtained from Ref. 6, while the theoretical value was obtained from Ref. 5. The extinction parameters employed in the propellant-heating tests (Ref. 45) have been lower than those shown in Fig. 13 because less turbulence was employed to break up particle agglomeration in these tests. The ultimate particle seed system has a high initial degree of turbulence to break up particle agglomerates, followed by a settling chamber which removes the turbulence (to prevent mixing of the coaxial streams), yet which has a dwell time short enough so that the particles are not re-agglomerated.

TRANSPARENT WALLS

The spectral distribution of energy radiated by a black body is illustrated in Fig. 14 for several different radiating temperatures. For a radiating temperature of 15,000 R, 1 percent of the energy falls below a wavelength of 0.18μ, and 1 percent of the energy falls above a wavelength of 2.7μ. Thus, it is desirable that the transparent wall be substantially transparent at wavelengths between approximately 0.18 and 2.7μ. Three candidate materials fulfill this requirement: fused silica, alumina, and beryllium oxide. It is known also that transparent materials will color when exposed to a radiation field at room temperature (Refs. 186 to 190).

Measured (Ref. 52) spectral absorption characteristics of high-quality fused silica are shown in Fig. 15. An increase in the temperature of an unirradiated specimen results in a shift of the ultraviolet cutoff to a higher wavelength. Results of room-temperature nuclear irradiation are primarily evidenced by the appearance of an absorption band centered at a wave-length of 0.21μ. Verification of the transmission characteristics of unirradiated fused silica has been obtained from Ref. 132. The transmission characteristics of fused silica shown in Fig. 15 with and without the radiation-induced absorption band have been used in a study of the absorption of radiant energy in a transparent wall and the resulting effect on permissible wall thickness (Ref. 96).

It is well known (Refs. 186 to 190) that radiation-induced absorption in transparent materials will ammend rapidly during heat treatment of high temperatures. Therefore, investigations have been conducted under NASA contracts NASw-768 and NASw-847 to determine the equilibrium absorption which may be present in the wall of an operating nuclear light bulb engine by examining the relationship between the irradiation parameters (particle flux and dose) and the temperature of the optical material. Since it is not possible to perform a single irradiation test in which the reactor operating conditions simulate an operating nuclear light bulb engine in both neutron and ionizing radiation flux and dose, the investigations have been conducted using several techniques which do not simulate all of the engine characteristics. These can conveniently be grouped into two categories: (1) the measurement of the effects of irradiation on the transmission of optical materials after the irradiation process and (2) the measurement of the effects of irradiation during the irradiation process upon the transmission of optical materials.

Tests using the first of these categories of techniques were conducted using the Union Carbide 5-megw facility and a Co-60 gamma ray source (Refs. 34 and 52). The optical materials were simultaneously exposed to high temperatures (in the range of 700 to 1100 C) and nuclear irradiation for times sufficiently long to simulate the nuclear light bulb dose. Transmission measurements were made following the

irradiations and indicated that there was no significant coloration at 0.215 and 0.163 microns (Ref. 52). The actual induced absorption coefficient present during the reactor irradiation process may not have been determined, however, because of two competing processes which occurred after the removal of the capsule from the reactor core: (1) bleaching of short-lived defects during the cool-down process and (2) gamma coloration of the defects due to containment within the radioactive capsule.

The measurement of transmission during the irradiation was conducted in several facilities, since it was not possible to perform a single irradiation under operating conditions which completely simulate an operating nuclear light bulb in dose rate and dose of neutrons and ionizing radiation. These facilities included the TRIGA Mark II reactor located at the University of Illinois (Refs. 35 and 38), the Dynamitron electron accelerator located at the Space Radiation Effects Laboratory at NASA Langley (Ref. 50), and the Nuclear Engineering Test Reactor (NETR) of the Air Force Institute of Technology located at Wright-Patterson Air Force Base (Ref. 50). The TRIGA facility can provide simulation of the neutron and ionizing dose rates in a full-scale nuclear light bulb engine, but for very short periods of time; the NETR provides simulation of the dose of neutrons and ionizing radiation, but at low flux levels; and the Dynamitron provides simulation of the dose and dose rate of ionizing radiation, but without neutron flux.

Representative data obtained in the experiments using the above facilities are illustrated in Fig. 16 together with calculated values. The calculated values were obtained using the following equation:

$$\alpha = G\dot{D}\tau \qquad (1)$$

In evaluating this equation, the color generation factor, G, was taken as 0.045 cm^{-1}/Mrad on the basis of Co-60 irradiation experiments (Ref. 34), and the decoloration rate, τ, was taken from data from post-reactor annealing experiments quoted in Fig. 21 of Ref. 34. It can be seen from Fig. 16 that the calculated absorption coefficients are in reasonable agreement with the experimentally measured absorption coefficients for the NETR tests. However, the calculated absorption coefficients are higher than the absorption coefficients measured in the Dynamitron experiments by a factor of between two and eleven. Similarly, the absorption coefficients predicted for the full-scale engine based on extrapolation of Dynamitron data (dashed lines in Fig. 16) are lower than the calculated values. Resolution of these differences is obviously an important endeavor to undertake.

Data from TRIGA experiments (Ref. 35) indicated a value of the color generation factor, G, only slightly higher than the value of 0.045 cm^{-1}/Mrad obtained from the Co-60 experiments. However, the time constants determined from the TRIGA experiments were approximately two orders of magnitude shorter than determined from the post-reactor annealing experiments (see also Fig. 21 of Ref. 34). The time constant data determined from the TRIGA experiment may be in error, however, because of transient specimen temperature changes immediately after the TRIGA pulse.

An additional factor (optical bleaching) was investigated during the last contract period (Ref. 50); this factor may reduce the magnitude of the absorption present in the wall of an operating nuclear light bulb engine. The time for the induced absorption coefficient to decay to 1/e of its original value as a result of optical bleaching was determined with a specimen, which had been electron irradiated, using a hydrogen lamp as a light source and was found to be 4800 sec. Since the photon flux in this experiment was approximately 10^{-7} of that expected in a full-scale nuclear rocket engine, the expected optical bleaching time constant in the engine is approximately 0.48 x 10^{-3} sec. In order for optical bleaching to be effective, the time constant for creation of coloration must be longer than 0.48 x 10^{-3} sec. If the time constant associated with Eq. (1) (34 to 61 sec; see Ref. 50) is related to the same physical phenomenon as optical bleaching, then optical bleaching will cause a very large reduction in the equilibrium induced coloration in a full-scale nuclear light bulb engine. However, this may not be the case, as indicated by the following. The creation and decoloration rates associated with Eq. (1) may be related to either material defects or coloration of these defects, whereas optical bleaching is almost certainly related only to decoloration of defects. Thus it is possible that Eq. (1) is related to a different phenomenon than optical bleaching, and the re-coloration time constant for optically bleached centers may be different than for thermally annealed damage centers. Additional experiments are obviously required to resolve this question.

The allowable thickness of the walls in the fused silica tubes in the reference nuclear light bulb engine has been calculated to be 0.005 in. in the basis of an assumed allowable temperature difference across the wall of 200 F (Ref. 96) and on the basis of no radiation-induced coloration. According to the results shown on Fig. 16, the equilibrium radiation-induced absorption coefficient in the center of the 2150 Å downstream band would be between 3 and 8 cm^{-1} with no optical bleaching. According to Ref. 96, this would result in a reduction in allowable wall thickness to between 0.003 and 0.004 in. If further tests indicate that photon bleaching is important, then there may be little or no effect of nuclear radiation damage on allowable wall thickness.

REFERENCES

1. Johnson, B. V.: Analysis of Secondary-Flow-Control Methods for Confined Vortex Flows. United Aircraft Research Laboratories Report C-910091-1, September 1964. Also issued as NASA CR-276.

2. Travers, A. and B. V. Johnson: Measurements of Flow Characteristics in a Basic Vortex Tube. United Aircraft Research Laboratories Report C-910091-2, September 1964. Also issued as NASA CR-278.

3. Travers, A. and B. V. Johnson: Measurements of Flow Characteristics in an Axial-Flow Vortex Tube. United Aircraft Research Laboratories Report C-910091-3, September 1964. Also issued as NASA CR-277.

4. Schneiderman, S. B.: Theoretical Viscosities and Diffusivities in High-Temperature Mixtures of Hydrogen and Uranium. United Aircraft Research Laboratories Report C-910099-1, September 1964. Also issued as NASA CR-213.

5. Krascella, N. L.: Theoretical Investigation of the Absorption and Scattering Characteristics of Small Particles. United Aircraft Research Laboratories Report C-910092-1, September 1964. Also issued as NASA CR-210.

6. Marteney, P. J.: Experimental Investigation of the Opacity of Small Particles. United Aircraft Research Laboratories Report C-910092-2, September 1964. Also issued as NASA CR-211.

7. McLafferty, G. H. and W. G. Burwell: Theoretical Investigation of the Temperature Distribution in the Propellant Region of a Vortex-Stabilized Gaseous Nuclear Rocket. United Aircraft Research Laboratories Report C-910093-10, September 1964. Also issued as NASA CR-279.

8. Roback, R.: Thermodynamic Properties of Coolant Fluids and Particle Seeds for Gaseous Nuclear Rockets. United Aircraft Research Laboratories Report C-910092-3, September 1964. Also issued as NASA CR-212.

9. McLafferty, G. H.: Analytical Study of Moderator Wall Cooling of Gaseous Nuclear Rocket Engines. United Aircraft Research Laboratories Report C-910093-9, September 1964. Also issued as NASA CR-214.

10. Mensing, A. E. and J. S. Kendall: Experimental Investigation of Containment of a Heavy Gas in a Jet-Driven Light-Gas Vortex. United Aircraft Research Laboratories Report D-910091-4, March 1965. Also issued as NASA CR-68926.

11. McFarlin, D. J.: Experimental Investigation of the Effect of Peripheral Wall Injection Technique on Turbulence in an Air Vortex Tube. United Aircraft Research Laboratories Report D-910091-5, September 1965. Also issued as NASA CR-68867.

12. Johnson, B. V.: Analytical Study of Propellant Flow Requirements for Reducing Heat Transfer to the End Walls of Vortex-Stabilized Gaseous Nuclear Rocket Engines. United Aircraft Research Laboratories Report D-910091-6, September 1965.

13. Travers, A.: Experimental Investigation of Peripheral Wall Injection Techniques in a Water Vortex Tube. United Aircraft Research Laboratories Report D-910091-7, September 1965. Also issued as NASA CR-68866.

14. Johnson, B. V. and A. Travers: Analytical and Experimental Investigation of Flow Control in a Vortex Tube by End-Wall Suction and Injection. United Aircraft Research Laboratories Report D-910091-8, September 1965. Also issued as NASA CR-68927.

15. Mensing, A. E. and J. S. Kendall: Experimental Investigation of the Effect of Heavy-to-Light-Gas Density Ratio on Two-Component Vortex Tube Containment Characteristics. United Aircraft Research Laboratories Report D-910091-9, September 1965. Also issued as NASA CR-68926.

16. Williamson, H. A., H. H. Michels and S. B. Schneiderman: Theoretical Investigation of the Lowest Five Ionization Potentials of Uranium. United Aircraft Research Laboratories Report D-910099-2, September 1965. Also issued as NASA CR-69002.

17. Krascella, N. L.: Theoretical Investigation of the Opacity of Heavy-Atom Gases. United Aircraft Research Laboratories Report D-910092-4, September 1965. Also issued as NASA CR-69001.

18. Kesten, A. S. and R. B. Kinney: Theoretical Effect of Changes in Constituent Opacities on Radiant Heat Transfer in a Vortex-Stabilized Gaseous Nuclear Rocket. United Aircraft Research Laboratories Report D-910092-5, September 1965.

19. Marteney, P. J., N. L. Krascella and W. G. Burwell: Experimental Refractive Indices and Theoretical Small-Particle Spectral Properties of Selected Metals. United Aircraft Research Laboratories Report D-910092-6, September 1965. Also issued as NASA CR-68865.

20. McLafferty, G. H., H. H. Michels, T. S. Latham and R. Roback: Analytical Study of Hydrogen Turbopump Cycles for Advanced Nuclear Rockets. United Aircraft Research Laboratories Report D-910093-19, September 1965.

21. McLafferty, G. H.: Analytical Study of the Performance Characteristics of Vortex-Stabilized Gaseous Nuclear Rocket Engines. United Aircraft Research Laboratories Report D-910093-20, September 1965.

22. Krascella, N. L.: Theoretical Investigation of the Absorptive Properties of Small Particles and Heavy-Atom Gases. United Aircraft Research Laboratories Report E-910092-7, September 1966. Also issued as NASA CR-693.

23. Kinney, R. B.: Theoretical Effect of Seed Opacity and Turbulence on Temperature Distributions in the Propellant Region of a Vortex-Stabilized Gaseous Nuclear Rocket. United Aircraft Research Laboratories Report E-910092-8, September 1966. Also issued as NASA CR-694.

24. Kesten, A. S. and N. L. Krascella: Theoretical Investigation of Radiant Heat Transfer in the Fuel Region of a Gaseous Nuclear Rocket Engine. United Aircraft Research Laboratories Report E-910092-9, September 1966. Also issued as NASA CR-695.

25. McLafferty, G. H., H. E. Bauer and D. E. Sheldon: Preliminary Conceptual Design Study of a Specific-Vortex-Stabilized Gaseous Nuclear Rocket Engine. United Aircraft Research Laboratories Report E-910093-29, September 1966. Also issued as NASA CR-698.

26. Roback, R.: Theoretical Performance of Rocket Engines Using Gaseous Hydrogen in the Ideal State at Stagnation Temperatures up to 200,000 R. United Aircraft Research Laboratories Report E-910093-30, September 1966. Also issued as NASA CR-696.

27. Latham, T. S.: Nuclear Criticality Study of a Specific Vortex-Stabilized Gaseous Nuclear Rocket Engine. United Aircraft Research Laboratories Report E-910375-1, September 1966. Also issued as NASA CR-697.

28. Travers, A.: Experimental Investigation of Flow Patterns in Radial-Outflow Vortexes Using a Rotating-Peripheral-Wall Water Vortex Tube. United Aircraft Research Laboratories Report F-910091-10, May 1967. Also issued as NASA CR-991.

29. Johnson, B. V.: Exploratory Flow and Containment Experiments in a Directed-Wall-Jet Vortex Tube with Radial Outflow and Moderate Superimposed Axial Flows. United Aircraft Research Laboratories Report F-910091-11, May 1967. Also issued as NASA CR-992.

30. Kendall, J. S., A. E. Mensing and B. V. Johnson: Containment Experiments in Vortex Tubes with Radial Outflow and Large Superimposed Axial Flows. United Aircraft Research Laboratories Report F-910091-12, May 1967. Also issued as NASA CR-993.

31. Clark, J. W., J. S. Kendall, B. V. Johnson, A. E. Mensing and A. Travers: Summary of Gaseous Nuclear Rocket Fluid Mechanics Research Conducted Under Contract NASw-847. United Aircraft Research Laboratories Report F-910091-13, May 1967.

32. Travers, A.: Experimental Investigation of Radial-Inflow Vortexes in Jet-Injection and Rotating-Peripheral-Wall Water Vortex Tubes. United Aircraft Research Laboratories Report F-910091-14, September 1967. Also issued as NASA CR-1028.

33. Kendall, J. S.: Experimental Investigation of Heavy-Gas Containment in Constant-Temperature Radial-Inflow Vortexes. United Aircraft Research Laboratories Report F-910091-15, September 1967. Also issued as NASA CR-1029.

34. Douglas, F. C., R. Gagosz and M. A. DeCrescente: Optical Absorption in Transparent Materials Following High Temperature Reactor Irradiation. United Aircraft Research Laboratories Report F-910485-2, September 1967. Also issued as NASA CR-1031.

35. Gagosz, R., J. Waters, F. C. Douglas and M. A. DeCrescente: Optical Absorption in Fused Silica During TRIGA Reactor Pulse Irradiations. United Aircraft Research Laboratories Report F-910485-1, September 1967. Also issued as NASA CR-1032.

36. Latham, T. S.: Nuclear Criticality Studies of Specific Nuclear Light Bulb and Open Cycle Gaseous Nuclear Rocket Engines. United Aircraft Research Laboratories Report F-910375-2, September 1967.

37. McLafferty, G. H. and H. E. Bauer: Studies of Specific Nuclear Light Bulb and Open-Cycle Vortex-Stabilized Gaseous Nuclear Rocket Engines. United Aircraft Research Laboratories Report F-910093-37, September 1967. Also issued as NASA CR-1030.

38. Gagosz, R. M. and J. Waters: Optical Absorption and Fluorescence in Fused Silica During TRIGA Pulse Irradiation. United Aircraft Research Laboratories Report G-910485-3, April 1968. Also issued as NASA CR-1191.

39. Johnson, B. V.: Experimental Study of Multi-Component Coaxial-Flow Jets in Short Chambers. United Aircraft Research Laboratories Report G-910091-16, April 1968. Also issued as NASA CR-1190.

40. Kendall, J. S., W. C. Roman and P. G. Vogt: Initial Radio-Frequency Gas Heating Experiments to Simulate the Thermal Environment in the Nuclear Light Bulb Reactor. United Aircraft Research Laboratories Report G-910091-17, September 1968. Also issued as NASA CR-1311.

41. Mensing, A. E. and L. R. Boedeker: Theoretical Investigation of R-F Induction Heated Plasmas. United Aircraft Research Laboratories Report G-910091-18, September 1968. Also issued as NASA CR-1312.

42. Krascella, N. L.: Theoretical Investigation of the Composition and Line Emission Characteristics of Argon-Tungsten and Argon-Uranium Plasmas. United Aircraft Research Laboratories Report G-910092-10, September 1968. Also issued as NASA CR-1313.

43. Marteney, P. J., A. E. Mensing and N. L. Krascella: Experimental Investigation of the Spectral Emission Characteristics of Argon-Tungsten and Argon-Uranium Induction Heated Plasmas. United Aircraft Research Laboratories Report G-910092-11, September 1968. Also issued as NASA CR-1314.

44. Latham, T. S.: Nuclear Studies of the Nuclear Light Bulb Rocket Engine. United Aircraft Research Laboratories Report G-910375-3, September 1968. Also issued as NASA CR-1315.

45. Roman, W. C., J. F. Klein and P. G. Vogt: Experimental Investigations to Simulate the Thermal Environment, Transparent Walls and Propellant Heating in a Nuclear Light Bulb Engine. United Aircraft Research Laboratories Report H-910091-19, September 1969. To be issued as NASA CR report.

46. Mensing, A. E. and J. F. Jaminet: Experimental Investigations of Heavy-Gas Containment in R-F Heated and Unheated Two-Component Vortexes. United Aircraft Research Laboratories Report H-910091-20, September 1969. To be issued as NASA CR report.

47. Krascella, N. L.: Theoretical Investigation of the Radiant Emission Spectrum from the Fuel Region of a Nuclear Light Bulb Engine. United Aircraft Research Laboratories Report H-910092-12, September 1969. To be issued as NASA CR report.

48. Latham, T. S., H. E. Bauer and R. J. Rodgers: Studies of Nuclear Light Bulb Start-up Conditions and Engine Dynamics. United Aircraft Research Laboratories Report H-910375-4, September 1969. To be issued as NASA CR report.

49. Johnson, B. V.: Exploratory Experimental Study of the Effects of Inlet Conditions on the Flow and Containment Characteristics of Coaxial Flows. United Aircraft Research Laboratories Report H-910091-21, September 1969. To be issued as NASA CR report.

50. Palma, G. E. and R. M. Gagosz: Measurement of Optical Transmission During Reactor Irradiation. United Aircraft Research Laboratories Report H-930709-1, October 1969. To be issued as NASA CR report.

51. Krascella, N. L.: Tables of the Composition, Opacity and Thermodynamic Properties of Hydrogen at High Temperatures. United Aircraft Research Laboratories Report B-910168-1, September 1963. Also issued as NASA SP-3005.

52. Douglas, F. C. and R. M. Gagosz: Experimental Investigation of Thermal Annealing of Nuclear-Reactor-Induced Coloration in Fused Silica. United Aircraft Research Laboratories Report D-910082-7, March 1965. Also issued as NASA CR-304.

53. Anderson, O.: Theoretical Solutions for the Secondary Flow on the End Wall of a Vortex Tube. United Aircraft Research Laboratories Report R-2494-1, November 1961.

54. Owen, F. S., R. W. Hale, B. V. Johnson and A. Travers: Experimental Investigation of Characteristics of Confined Jet-Driven Vortex Flows. United Aircraft Research Laboratories Report R-2494-2, November 1961.

55. Owen, F. S. and A. E. Mensing: Heat Transfer to Confined Vortex Flows by Means of a Radio-Frequency Gas Discharge. United Aircraft Research Laboratories Report R-2494-3, November 1961.

56. McLafferty, G. H.: Investigations of a Unique Gaseous-Core Nuclear Rocket Concept - Summary Report. United Aircraft Research Laboratories Report R-2494-4, November 1961.

57. Patch, R. W.: Methods for Calculating Radiant Heat Transfer in High-Temperature Hydrogen Gas. United Aircraft Research Laboratories Report M-1492-1, November 1961.

58. Mensing, A. E. and J. S. Kendall: Experimental Investigation of Containment of Gaseous Iodine in a Jet-Driven Vortex. Air Force Systems Command Report RTD-TDR-63-1093 prepared by United Aircraft Research Laboratories, November 1963.

59. Johnson, B. V., A. Travers, and R. W. Hale: Measurements of Flow Patterns in a Jet-Driven Vortex. Air Force Systems Command Report RTD-TDR-63-1094 prepared by United Aircraft Research Laboratories, November 1963.

60. McLafferty, G. H. and G. E. Anderson: Analytical Investigation of Diffusive Loss Rates of Gaseous Iodine from a Helium Vortex. Air Force Systems Command Report RTD-TDR-63-1095 prepared by United Aircraft Research Laboratories, November 1963.

61. McLafferty, G. H.: Summary of Investigations of a Vortex-Stabilized Gaseous Nuclear Rocket Concept. Air Force Systems Command Report RTD-TDR-63-1097 prepared by United Aircraft Research Laboratories, November 1963.

62. Anderson, O. L.: Theoretical Effect of Mach Number and Temperature Gradient on Primary and Secondary Flow in a Jet-Driven Vortex. Air Force Systems Command Report RTD-TDR-63-1098 prepared by United Aircraft Research Laboratories, November 1963.

63. Bisshopp, F. E.: Theoretical Investigation of the Hydromagnetic Stability of a Free Boundary Layer. Air Force Systems Command Report RTD-TDR-63-1099 prepared by United Aircraft Research Laboratories, November 1963.

64. Carta, F. O.: The Effects of Body Force and Finite Electrical Conductivity on the Hydromagnetic Stability of a Discontinuous Shear Flow. Air Force Systems Command Report RTD-TDR-63-1100 prepared by United Aircraft Research Laboratories, November 1963.

65. Saunders, A. R.: Theoretical Investigation of Radiant Heat Transfer in a Vortex-Stabilized Gaseous Nuclear Rocket. Air Force Systems Command Report RTD-TDR-63-1096 prepared by United Aircraft Research Laboratories, November 1963.

66. Krascella, N. L.: Theoretical Investigation of Spectral Opacities of Hydrogen and Nuclear Fuel. Air Force Systems Command Report RTD-TDR-63-1101 prepared by United Aircraft Research Laboratories, November 1963.

67. Marteney, P. J. and N. L. Krascella: Theoretical and Experimental Investigations of Spectral Opacities of Mixtures of Hydrogen and Diatomic Gases. Air Force Systems Command Report RTD-TDR-63-1102 prepared by United Aircraft Research Laboratories, November 1963.

68. Johnson, B. V. and A. Travers: Application of Flow Control to a Confined Vortex. Presented at the AIAA Propulsion Joint Specialist Conference held at the Air Force Academy in Colorado Springs, Colorado, June 14-18, 1965.

69. Mensing, A. E. and J. S. Kendall: Experimental Investigation of the Containment of a Heavy Gas in a Light-Gas Vortex. Presented at the AIAA Propulsion Joint Specialist Conference held at the Air Force Academy in Colorado Springs, Colorado, June 14-18, 1965.

70. Foley, W. M.: Comparison of Simulated and Required Flow Characteristics for a Vortex-Stabilized Gaseous Nuclear Rocket Engine. Presented at the AIAA Propulsion Joint Specialist Conference held at the Air Force Academy in Colorado Springs, Colorado, June 14-18, 1965.

71. Burwell, W. G.: Calculated Temperature Distributions in a Vortex-Stabilized Gaseous Nuclear Rocket Engine. Presented at the AIAA Propulsion Joint Specialist Conference held at the Air Force Academy in Colorado Springs, Colorado, June 14-18, 1965.

72. McLafferty, G. H.: Characteristics of a Gaseous Nuclear Rocket Engine Employing Transparent-Wall Containment. Presented at the AIAA Propulsion Joint Specialist Conference held at the Air Force Academy in Colorado Springs, Colorado, June 14-18, 1965.

73. Latham, T. S. and L. O. Herwig: The Effects of Hot Hydrogen Propellant on the Critical Mass of Gaseous Nuclear Rocket Cavity Reactors. AIAA Paper No. 65-564, presented at the AIAA Propulsion Joint Specialist Conference held at the Air Force Academy in Colorado Springs, Colorado, June 14-18, 1965.

74. Kendall, J. S. and A. E. Mensing: Experimental Investigation of the Effect of Heavy-to-Light-Gas Density Ratio on Vortex Containment Characteristics. Presented at the Second AIAA Propulsion Joint Specialist Conference held at the Air Force Academy in Colorado Springs, Colorado, June 13-17, 1966.

75. Kesten, A. S., N. L. Krascella and R. B. Kinney: Effect of Changes in Constituent Opacities on Calculated Radiant Heat Transfer Rates in a Vortex-Stabilized Gaseous Nuclear Rocket. Presented at the Second AIAA Propulsion Joint Specialist Conference held at the Air Force Academy in Colorado Springs, Colorado, June 13-17, 1966.

76. Latham, T. S.: Heat Generation in Nuclear Fuel During Injection Into a Gaseous Nuclear Rocket Engine. AIAA Paper No. 66-620 presented at the Second AIAA Propulsion Joint Specialist Conference held at the Air Force Academy in Colorado Springs, Colorado, June 13-17, 1966.

77. Clark, J. W., B. V. Johnson, J. S. Kendall, A. E. Mensing and A. Travers: Summary of Gaseous Nuclear Rocket Fluid Mechanics Research. AIAA Paper No. 67-500, presented at the Third AIAA Propulsion Joint Specialist Conference held in Washington, D. C., June 1967.

78. McLafferty, G. H.: Survey of Advanced Concepts in Nuclear Propulsion. AIAA Paper No. 67-783, presented at the Fourth AIAA Annual Meeting and Technical Display held in Anaheim, California, October 23-27, 1967.

79. Travers, A. and J. W. Clark: Experimental Investigation of Flow Stability and Flow Patterns in Radial-Outflow Vortexes. AIAA Paper No. 68-695, presented at the Fourth AIAA Propulsion Joint Specialist Conference held in Cleveland, Ohio, June 1968.

80. Kendall, J. S., A. E. Mensing, A. Travers and P. Vogt: Radio-Frequency Gas Heating Experiment to Simulate the Thermal Environment of the Nuclear Light Bulb Engine. Presented at the Fourth AIAA Propulsion Joint Specialist Conference held in Cleveland, Ohio, June 1968.

81. Johnson, B. V. and A. Travers: Application of Vortex Flow Control to a Confined Vortex. Presented at the Fourth AIAA Propulsion Joint Specialist Conference held in Cleveland, Ohio, June 1968.

82. Latham, T. S.: Criticality Studies of a Nuclear Light Bulb Engine. AIAA Paper No. 68-571, presented at the Fourth AIAA Propulsion Joint Specialist Conference held in Cleveland, Ohio, June 1968.

83. Roman, W. C. and J. F. Klein: Investigation of High-Pressure Vortex-Stabilized R-F Plasma Discharges. AIAA Paper No. 69-695, presented at the Fifth AIAA Propulsion Joint Specialist Conference held in San Francisco, California, June 1969.

84. Clark, J. W., B. V. Johnson, J. S. Kendall, A. E. Mensing and A. Travers: Open-Cycle and Light-Bulb Types of Vortex-Stabilized Gaseous Nuclear Rockets. Journal of Spacecraft and Rockets, Vol. 5, No. 8, August 1968, pp. 941-947.

85. Krascella, N. L.: The Absorption and Scattering of Radiation by Small Solid Particles. Journal of Quantitative Spectroscopy and Radiative Transfer, Vol. 5, 1965, p. 245.

86. Herwig, L. O. and T. S. Latham: Nuclear Characteristics of Large Reflector-Moderated Gaseous-Fueled Cavity Reactors Containing Hot Hydrogen. AIAA Journal, Vol. 5, No. 5, May 1967, p. 930.

87. Latham, T. S.: Criticality Studies of a Nuclear Light Bulb Engine. Journal of Spacecraft and Rockets, Vol. 6, No. 10, October 1969.

88. Krascella, N. L.: The Spectral Opacity of High Temperature Hydrogen. Presented at the 1963 Opacity Conference, Kirtland Air Force Base, Albuquerque, New Mexico, April 1963.

89. Krascella, N. L.: The Absorption and Scattering of Radiation by Small Solid Particles. Presented at the 1964 Opacity Conference, Kirtland Air Force Base, Albuquerque, New Mexico, September 1964.

90. Gagosz, R. M.: High-Temperature Long-Wavelength Range Spectrophotometer. Presented at the 1965 Annual Meeting of the Optical Society of America, Philadelphia, Pennsylvania, October 5-8, 1965.

91. Gagosz, R. M. and J. P. Waters: Optical System for In-Reactor Transmission Measurements at Elevated Temperatures. Presented at the 1967 Annual Meeting of the Optical Society of America, Detroit, Michigan, October 10-13, 1967.

92. Palma, G. E.: Measurement of Optical Transmittance of Fused Silica During 1.5 Mev Electron Irradiation. Presented at the 1969 Annual Meeting of the Optical Society of America, Chicago, Illinois, October 21-24, 1969.

93. Johnson, B. V.: Experimental Study of One- and Two-Component Coaxial Flow Jets in Short Chambers. AIChE Paper 25B, presented at Annual Meeting, December 1-5, 1968.

94. Johnson, B. V. and C. P. Van Dine: Laminar Boundary Layer Similarity Solutions for Rotating Flows with Wall Suction. Proceedings of the Ninth Midwestern Mechanics Conference (Madison, Wisconsin, August 16-18, 1965), Wiley, 1967.

95. Kurzweg, U. H.: Criteria for the Stability of Heterogeneous Swirling Flows. United Aircraft Research Laboratories Report UAR-F96, May 1967.

96. McLafferty, G. H.: Absorption of Thermal Radiation in the Transparent Wall of a Nuclear Light Bulb Rocket Engine. Journal of Spacecraft and Rockets, Vol. 4, No. 6, June 1967, pp. 758-761.

97. McLafferty, G. H.: Limitations on Gaseous Nuclear Rocket I_{sp} Due to Nozzle Coolant Requirements. Journal of Spacecraft and Rockets, Vol. 3, No. 10, October 1966, pp. 1515-1522.

98. Evvard, J. C.: Wheel-Flow Gaseous-Core Reactor Concept. NASA TN D-2951, November 1965.

99. Weinstein, H. and R. G. Ragsdale: A Coaxial Flow Reactor -- A Gaseous Nuclear Rocket Concept. ARS Paper 1518-60, 1960.

100. Ragsdale, R. G.: Applicability of Mixing Length Theory to a Turbulent Vortex System. NASA TN D-1051, August 1961.

101. Ragsdale, R. G. and F. E. Rom: NASA Research on the Coaxial Flow Gaseous Nuclear Rocket. Proceedings of Nuclear Propulsion Conference, Naval Postgraduate School, August 1962. USAEC Report TID-7653 (Part I), pp. 110-114.

102. Ragsdale, R. G. and H. Weinstein: On the Hydrodynamics of a Coaxial Flow Gaseous Reactor. Proceedings of Nuclear Propulsion Conference, Naval Postgraduate School, August 1962. USAEC Report TID-7653 (Part I), pp. 82-88.

103. Rom, F. E. and R. G. Ragsdale: Advanced Concepts for Nuclear Rocket Propulsion. Nuclear Rocket Propulsion, NASA SP-20, 1962, pp. 3-15.

104. Weinstein, H. and C. A. Todd: A Numerical Solution of the Problem of Mixing of Laminar Coaxial Streams of Greatly Different Densities - Isothermal Case. NASA TN D-1534, February 1963.

105. Ragsdale, R. G., H. Weinstein, and C. D. Lanzo: Correlation of a Turbulent Air-Bromine Coaxial-Flow Experiment. NASA TN D-2121, February 1964.

106. Weinstein, H. and C. A. Todd: Analysis of Mixing of Coaxial Streams of Dissimilar Fluids Including Energy-Generation Terms. NASA TN D-2123, March 1964.

107. Ragsdale, R. G. and Edwards, O. J.: Turbulent Coaxial Mixing of Dissimilar Gases at Nearly Equal Stream Velocities. NASA TM X-52082, 1965.

108. Ragsdale, R. G.: Effects of Momentum Buffer Region on Coaxial Flow of Dissimilar Fluids. NASA TM X-520098, 1965.

109. Ragsdale, R. G.: Effects of a Momentum Buffer Region on the Coaxial Flow of Dissimilar Gases. NASA TN D-3138, December 1965.

110. Ragsdale, R. G. and O. J. Edwards: Data Comparisons and Photographic Observations of Coaxial Mixing of Dissimilar Gases at Nearly Equal Stream Velocities. NASA TN D-3131, December 1965.

111. Ragsdale, R. G. and F. E. Rom: Gas-Core Reactor Work at NASA/Lewis. AIAA Paper No. 67-499, July 1967.

112. Donovan, L. F.: Similarity Solution for Turbulent Mixing Between a Jet and a Faster Moving Coaxial Stream. NASA TN D-4441, March 1968.

113. Donovan, L. F. and C. A. Todd: Computer Program for Calculating Isothermal, Turbulent Jet Mixing of Two Gases. NASA TN D-4378, March 1968.

114. Ragsdale, R. G.: Are Nuclear Rockets Attainable? AIAA Paper No. 68-570, June 1968.

115. Taylor, M. F. and C. C. Masser: Photographic Study of a Bromine Jet in a Coaxial Airstream. NASA TN D-4660, July 1968.

116. Masser, C. C. and M. F. Taylor: Photographic Study of a Bromine Jet Flowing in a Coaxial Airstream and Impinging on a Stagnation Surface. NASA TN D-5209, May 1969.

117. Lanzo, C. D.: A Curved Porous Wall Gaseous Nuclear Reactor Concept. Transactions, American Nuclear Society, Vol. 12, No. 1, June 1969, p. 2.

118. Ragsdale, R. G. and C. D. Lanzo: Some Recent Gaseous-Reactor Fluid Mechanics Experiments. Preprint 69-477 for Fifth AIAA Propulsion Joint Specialist Conference, June 1969.

119. Lanzo, C. D.: A Flow Experiment on a Curved-Porous-Wall Gas-Core Reactor Geometry. NASA TM X-1852, August 1969.

120. Ragsdale, R. G. and C. D. Lanzo: Summary of Recent Gaseous Reactor Fluid Mechanics Experiments. NASA TM X-1847, August 1969.

121. Masser, C. C.: A Photographic Study of a Bromine Jet in a Coaxial Airstream with Honeycombs at the Injection Plane. NASA TM X-1900, October 1969.

122. Lanzo, C. D. and Ragsdale, R. G.: Experimental Determination of Spectral and Total Transmissivities of Clouds of Small Particles. NASA TN D-1405, September 1962.

123. Einstein, T. H.: Radiant Heat Transfer to Absorbing Gases Enclosed in a Circular Pipe with Conduction, Gas Flow, and Internal Heat Generation. NASA Technical Report R-156, 1963.

124. Einstein, T. H.: Radiant Heat Transfer to Absorbing Gases Enclosed Between Parallel Flat Plates with Flow and Conduction. NASA Technical Report R-154, 1963.

125. Lanzo, C. D. and Ragsdale, R. G.: Heat Transfer to a Seeded Flowing Gas from an Arc Enclosed by a Quartz Tube. Proceedings of 1964 Heat Transfer and Fluid Mechanics Institute, edited by W. H. Geidt and S. Levy, Stanford University Press, 1964.

126. Masser, C. C.: Radiant Heating of a Seeded Gas in a Coaxial-Flow Gaseous Reactor. NASA TN D-3197, January 1966.

127. Patch, R. W.: Effective Absorption Coefficients for Radiant Energy Transport in Nongray, Nonscattering Gases. Journal of Quantitative Spectroscopy and Radiative Transfer, Vol. 7, No. 4, 1967, p. 611.

128. Patch, R. W.: Approximation for Radiant Energy Transport in Nongray, Nonscattering Gases. NASA TN D-4001, June 1967.

129. Patch, R. W.: Components of a Hydrogen Plasma Including Minor Species. NASA TN D-4993, January 1969.

130. Ragsdale, R. G. and A. F. Kascak: Simple Equations for Calculating Temperature Distributions in Radiating Gray Gases. NASA TN D-5226, May 1969.

131. Patch, R. W.: Interim Absorption Coefficients and Opacities for Hydrogen Plasma at High Pressure. NASA TM X-1902, October 1969.

132. Edwards, O. J.: Optical Absorption Coefficients of Fused Silica in the Wavelength Range 0.17 to 3.5 Microns from Room Temperature to 980 C. NASA TN D-3257, February 1966.

133. Ragsdale, R. G. and R. E. Hyland: Some Nuclear Calculations of U-235 D_2O Gaseous Core Cavity Reactors. NASA TN D-475, October 1961.

134. Hyland, R. E., R. G. Ragsdale and E. J. Gunns: Two-Dimensional Criticality Calculations of Gaseous-Core Cylindrical-Cavity Reactors. NASA TN D-1575, March 1963.

135. Ragsdale, R. G.: Outlook for Gas-Core Nuclear Rockets. Astronautical Aerospace Engineering, Vol. 1, August 1963, pp. 88-91.

136. Hyland, R. E., G. D. Pincock, J. F. Kunze and R. E. Wood: Experimental Results from Large Cavity Reactor Critical. Transactions, American Nuclear Society, Vol. 10, No. 1, June 1967, p. 8.

137. Synge, J. L.: The Stability of Heterogeneous Liquids. Transactions of the Royal Society of Canada, Vol. 27, 1933, pp. 1-18.

138. Chandrasekhar, S.: The Stability of Viscous Flow Between Rotating Cylinders in the Presence of a Radial Temperature Gradient. Journal of Rational Mechanics and Analysis, 1954.

139. Stuart, J. T.: On the Effects of Uniform Suction on the Steady Flow Due to a Rotating Disc. Quarterly Journal of Mechanics and Applied Mathematics, 1954.

140. Kerrebrock, J. and R. Meghreblian: An Analysis of Vortex Tubes for Combined Gas-Phase Fission-Heating and Separation of the Fissionable Material. Oak Ridge National Laboratories' Report CF 57-11-3, Rev. 1, 1958.

141. Grey, J.: A Gaseous-Core Nuclear Rocket Utilizing Hydrodynamic Containment of Fissionable Material. ARS Paper 848-59, June 1959.

142. Ludwieg, H.: Stability of Flow in an Annular Space. Zeitschrift für Flugwissenschaften, Vol. 8, 1960, pp. 135-140.

143. Kerrebrock, J. L. and R. V. Meghreblian: Vortex Containment for the Gaseous-Fission Rocket. Journal of the Aerospace Sciences, Vol. 28, 1961, pp. 710-724.

144. Ludwieg, H.: Extension of the Work on the Stability of Flow in an Annular Space. Zeitschrift für Flugwissenschaften, Vol. 9, 1961, pp. 359-361.

145. Stumpf, H. J.: Vortex-Tube and Regenerative-Cooling-Tube Parameters for Gaseous Fission Reactors. Jet Propulsion Laboratory Technical Report No. 32-201, January 22, 1962.

146. Kendall, J. M., Jr.: Experimental Study of a Compressible Viscous Vortex. California Institute of Technology Report No. 32-290, Pasadena, California, 1962.

147. Mack, L. M.: The Laminar Boundary Layer on a Disk of Finite Radius in a Rotating Flow. Part 1: Numerical Integration of the Momentum Integral Equations and Application of the Results to the Flow in a Vortex Chamber. Jet Propulsion Laboratories' Technical Report 32-224, 1962.

148. Hocking, L. M.: An Example of Boundary Layer Formation. AIAA Journal, Vol. 1, No. 5, May 1963, pp. 1222-1223.

149. Ross, D. H.: An Experimental Study of Secondary Flow in Jet-Driven Vortex Chambers. Aerospace Corporation Report No. ATN-64 (9227)-1, El Segundo, California, 1964.

150. Rosenzweig, M. L., W. S. Lewellen and D. H. Ross: Confined Vortex Flows with Boundary Layer Interaction. Aerospace Corporation Report No. ATN-64 (9227)-2, El Segundo, California, February 20, 1964. Also AIAA Journal, Vol. 3, No. 12, December 1964, pp. 2127-2134.

151. Lewellen, W. S.: Linearized Vortex Flows. AIAA Journal, Vol. 3, January 1965.

152. Lewellen, W. S., D. H. Ross and M. L. Rosenzweig: Effects of Secondary Flows on the Containment of a Heavy Gas in a Vortex. Aerospace Corporation Report TDR-469 (9210-01)-3, El Segundo, California, May 1965. Also AIAA Paper No. 65-582, 1965.

153. Johnson, K. P.: A Plasma Core Nuclear Rocket Utilizing a Magnetohydrodynamically-Driven Vortex. AIAA Paper No. 65-583, AIAA Propulsion Joint Specialist Conference, June 1965.

154. Poplawski, R. and A. Pinchak: Aerodynamic Performance of Reversed Flow Vortex Chambers. ARL Report 65-219, 1965.

155. Lewellen, W. S., D. H. Ross and M. L. Rosenzweig: Binary Diffusion in a Confined Vortex. AIAA Journal, Vol. 4, March 1966.

156. Miller, R. A. and R. Poplawski: The ARL Inertial Particle Separator for Military Turbine-Powered Vehicles. Proceedings of the O. A. R. Research Applications Conference, Washington, D. C., April 1966.

157. Pivirotto, T. J.: Mass-Retention Measurements in a Binary Compressible Vortex Flow. California Institute of Technology, Jet Propulsion Laboratories' Report TR 32-864, 1966.

158. Burggraf, O. R.: A Linearized Analysis of Mass Transfer Effects on Confined Laminar Vortex Flows. ARL Report, 1967.

159. Chang, C. C., S. W. Chi and C. M. Chen: Gas-Core Nuclear Rocket Fluid Mechanics Experiments at Catholic University of America. AIAA Paper No. 67-502, 1967.

160. Keyes, J. J., Jr., T. S. Chang and W. K. Sartory: Hydrodynamic Stabilization of Jet-Driven Vortex Flow. Oak Ridge National Laboratory USAEC Report ORNL-TM-1896, 1967.

161. Chang, C. C., S. W. Chi and C. M. Chen: Experimental Exploration of Recirculation Zone in the Gas-Core Nuclear Rocket Concept. Journal of Spacecraft and Rockets, Vol. 5, No. 4, April 1968, pp. 480-481.

162. Textor, R. E.: A Numerical Investigation of a Confined Vortex Problem. Oak Ridge National Laboratory, Computing Technology Center USAEC Report K-1732, 1968.

163. Kidd, G. J., Jr. and G. J. Farris: Potential Vortex Flow Adjacent to a Stationary Surface. ASME Transactions, Journal of Applied Mechanics, Vol. 35, Series E, 1969, pp. 209-215.

164. Thorpe, M. L.: Production of Superheated Hydrogen Plasma Using Induction Heating of Cold Plasma and D-C Plasma Enhancement. NASA CR-657 prepared under Lewis Work Order C69512A by Humphreys Corporation, December 1966.

165. Boehman, L. I.: Mass and Momentum Transport Properties in Isoenergetic Coaxial Flows. Mechanical Engineering Ph.D. Thesis, Illinois Institute of Technology, 1967.

166. Baker, R. L. and H. Weinstein: Experimental Investigation of the Mixing of Two Parallel Streams of Dissimilar Fluids. NASA CR-957, January 1968.

167. Baker, R. L. and H. Weinstein: Analytical Investigation of the Mixing of Two Parallel Streams of Dissimilar Fluids. NASA CR-956, January 1968.

168. D'Souza, G. J., A. Montealegre and H. Weinstein: Measurement of Turbulent Correlations in a Coaxial Flow of Dissimilar Fluids. NASA CR-960, January 1968.

169. Montealegre, A., G. J. D'Souza and H. Weinstein: Evaluation of Turbulence Correlations in a Coaxial Flow of Dissimilar Fluids. NASA CR-961, January 1968.

170. Baker, R. L., T. Rozenman and H. Weinstein: Stability of Shear Flow with Density Gradient and Viscosity. NASA CR-958, February 1968.

171. Zawacki, T. S. and H. Weinstein: Experimental Investigation of Turbulence in the Mixing Region Between Coaxial Streams. NASA CR-959, February 1968.

172. Thorpe, M. L.: Induction Plasma Heating: System Performance, Hydrogen Operation and Gas Core Reactor Simulation Development. NASA CR-1143 prepared under Contract NAS 3-9375 by Humphreys Corporation, August 1968.

173. Rozenman, T.: Experimental Investigation of Recirculation Patterns in the Initial Region of Coaxial Jets. Chemical Engineering Ph.D. Thesis, Illinois Institute of Technology, January 1969.

174. Kulik, R. A., J. J. Leithem and H. Weinstein: Effect of Free Stream Turbulence on Coaxial Mixing. NASA CR-1336, May 1969.

175. Thorpe, M. L. and L. W. Scammon: Induction Plasma Heating: High Power Law Frequency Operation and Pure Hydrogen Heating. NASA CR-1343 prepared under Contract NAS 3-9375 by Humphreys Corporation, May 1969.

176. Leithem, J. J., R. A. Kulik and H. Weinstein: Turbulence in the Mixing Region Between Ducted Coaxial Streams. NASA CR-1335, July 1969.

177. Thorpe, M. L.: Radio-Frequency Plasma Simulation of Gas-Core Reactor. Journal of Spacecraft and Rockets, Vol. 6, No. 8, August 1969, pp. 923-928. Also AIAA Paper No. 68-712, 1968.

178. Mayer, Harris: Methods of Opacity Calculations. Los Alamos Scientific Laboratory Report AECD-1870 (LADC-464), October 1947.

179. Treiman, S. B. and K. W. Ford: Radiative Thermal Conductivity in Gases at High Temperature. Lockheed Aircraft Corporation, Missile Systems Division Report MSD 1299, August 1955.

180. Olfe, D.: Equilibrium Emissivity Calculations for a Hydrogen Plasma at Temperatures up to 10,000 K. Daniel and Florence Guggenheim Jet Propulsion Center, California Institute of Technology Technical Report No. 14, Contract AF 18 (603)-2, May 1960.

181. Viskanta, R.: Heat Transfer in Thermal Radiation Absorbing and Scattering Media. Argonne National Laboratory AEC Research and Development Report, ANL-6170 (TID-4500, 15th Edition), May 1960.

182. Meghreblian, R. V.: Thermal Radiation in Gaseous Fission Reactors for Propulsion. Technical Report No. 32-139, Pasadena, California, July 24, 1961.

183. McAlister, J. A., E. Y. H. Keng and C. Orr, Jr.: Heat Transfer to a Gas Containing a Cloud of Particles. Georgia Institute of Technology Special Report, Project A-635-002, Research Grant NsG-273-62, 1965; prepared for NASA July 30, 1965.

184. Knapp, D. E., V. C. Burkig and J. S. Cory: Flash Heating of Seeded Gases. AIAA Paper No. 67-501, 1967.

185. Parks, D. E., G. Lane, J. C. Stewart and S. Peyton: Optical Constants of Uranium Plasma. Gulf General Atomic Incorporated Report GA-8244, February 1968. Also issued as NASA CR-72348.

186. Levy, P. W.: Reactor and Gamma-Ray Induced Coloring in Crystalline Quartz and Corning Fused Silica. Journal of Chemical Physics, Vol. 23, 1955, p. 764.

187. Mitchell, E. W. J. and E. G. S. Paige: The Optical Effects of Radiation Induced Atomic Damage in Quartz. The Philosophical Magazine, Vol. 1, No. 12, December 1956.

188. Dienes, G. J.: Defects in Silicas. Journal of Physical and Chemical Solids, Vol. 13, 1960, p. 272.

189. Levy, P. W.: Reactor and Gamma-Ray Induced Coloring of Corning Fused Silica. Journal of Physical and Chemical Solids, Vol. 13, 1960, p. 287.

190. Compton, W. D. and G. W. Arnold, Jr.: Radiation Effects in Fused Silica and α-Al_2O_3. Discussions of the Faraday Society, Vol. 31, 1961, p. 130.

191. Ross, F. S. and R. J. Holl: Conceptual Design Study of the Glow Plug Gaseous Core Reactor. Douglas Aircraft Report SM44042, November 1963.

192. Nelson, C. M. and J. H. Crawford, Jr.: Optical Absorption in Irradiated Quartz and Fused Silica. Journal of Physical and Chemical Solids, Vol. 13, 1966, p. 296.

193. Bell, G. I.: Calculations of the Critical Mass of UF_6 as a Gaseous Core with Reflectors of D_2O, Be, and C. Los Alamos Report LA-1874, February 1955.

194. Mills, C. B.: Reflector Moderated Reactors. Nuclear Science and Engineering, Vol. 13, No. 4, August 1962, p. 301.

195. Jarvis, G. A. and C. C. Byers: Critical Mass Measurements for Various Fuel Configurations in the LASL D_2O Reflected Cavity Reactor. AIAA Paper No. 65-555, AIAA Propulsion Joint Specialist Conference, June 1965.

196. Shepherd, L. R. and A. V. Cleaver: The Atomic Rocket--3. Journal of the British Interplanetary Society, Vol. 8, No. 1, January 1949, pp. 23-24, 30-37.

197. Safonov, G.: The Criticality and Some Potentialities of Cavity Reactors (Unabridged). RAND Corporation Report RM-1520, July 17, 1955.

198. Safonov, G.: The Criticality and Some Potentialities of Cavity Reactors. RAND Corporation Research Memorandum RM-1835, July 1955.

199. Safonov, G.: Engineering Test Reactors with Large Central Irradiation Cavities. Nuclear Science and Engineering, Vol. 2, No. 4, July 1957, p. 527.

200. Bussard, R. W. and R. D. DeLauer: Nuclear Rocket Propulsion. McGraw-Hill, New York, 1958.

201. Safonov, G.: Externally Moderated Reactors. Proceedings of the Second International Conference, Peaceful Uses of Atomic Energy, Geneva, P/625, Vol. 12, 1958, pp. 705-718.

202. Meghreblian, R. V.: Gaseous Fission Reactors for Spacecraft Propulsion. Jet Propulsion Laboratories' Technical Report No. 32-42, 1960.

203. Nelson, S. T.: The Plasma Core Reactor. Space Technology Laboratories' Report GM 60-7630.2-9, June 22, 1960.

204. Hallet, R. W. Jr., J. W. McKee and R. J. Faller: Operational Use of Gas Core Nuclear Reactor Propulsion Systems in Large Manned High-Thrust Spacecraft. Douglas Aircraft Company Paper No. DP-1200, 1961.

205. Meghreblian, R. V.: Prospects for Advanced Nuclear Systems. Astronautica Acta, Vol. VII, 1961, pp. 276-289.

206. Meghreblian, R. V.: Gaseous Propulsion Reactors. Nucleonics, Vol. 19, 1961, pp. 95-99.

207. MacLain, R. D. and J. W. McKee: Observations on the Kinetics and Control of Gas Core Reactors. IRE Transactions on Nuclear Science, Vol. NS-9, No. 1, January 1962, p. 212.

208. Spencer, D. F.: Thermal and Criticality Analysis of the Plasma Core Reactor. Jet Propulsion Laboratories' Technical Report 32-189, January 1, 1962.

209. Meghreblian, R. V.: Gaseous Fission Reactors for Booster Propulsion. ARS Journal, Vol. 32, 1962, pp. 13-21.

210. Meghreblian, R. V.: Fuel-Containment Requirements for Gaseous-Fuel Nuclear Rockets. Jet Propulsion Laboratories' Technical Report No. 32-441, September 2, 1963.

211. Hubbard, H. W., A. L. Latter and E. A. Martinelli: Second Report on Propulsion by a Gaseous Fission Reactor. RAND Memorandum RM-3851-AEC, October 1963.

212. Holl, R. J. and T. F. Plunkett: Cavity Nuclear Reactors. Transactions of the American Nuclear Society, Vol. 6, No. 2, 1963. Also issued as Douglas Paper No. DP-1738, 1963.

213. Butler, W. R., H. C. Chang and J. A. Vreeband: A Transport Theory Analysis of a Gaseous Core Concept. Aerojet-General REON Report RN-TM-0190, May 1965.

214. Tumm, G. W. U-235 Resonance Cross Sections and Gaseous Core Reactor Calculations. Plasma Research Laboratory Report No. 22, Columbia University, August 1965.

215. Cooper, R. S.: Advanced Nuclear Propulsion Concepts. AIAA Paper No. 65-531, 1965.

216. Holl, R. J. and T. F. Plunkett: Fuels for Gaseous-Core Nuclear Rockets. Transactions of the American Nuclear Society, Vol. 8, No. 2, 1965; also Douglas Paper No. DP-3613, 1966.

217. Duke, E. E. and W. J. Houghton: Gaseous Fueled Nuclear Rocket Engine. AIAA Paper No. 66-621, Second AIAA Propulsion Joint Specialist Conference, June 1966.

218. Eriksen, J. A., R. M. Kaufman, W. F. Osborn, E. B. Roth, J. R. Simmons and A. H. Foderaro: Gaseous-Fueled Cavity Reactors - Criticality Calculations and Analysis. General Motors Corporation, NASA CR-487, July 1966.

219. Kunze, J. F., J. H. Lofthouse, G. D. Pincock, R. E. Wood and R. E. Hyland: Cavity Reactor Critical Experiment. General Electric Report GEMP-473, October 7, 1966. Also, Transactions, American Nuclear Society, Vol. 9, No. 2, November 1966, p. 340.

220. Podney, W. N., H. P. Smith, Jr. and A. K. Oppenheim: Prompt-Neutron Kinetics of a Spherical Cavity Reactor. Transactions, American Nuclear Society, Vol. 9, No. 2, November 1966, p. 329.

221. Miraldi, F., G. W. Nelson, G. Holmberg and G. Skoff: Neutron Flux Distributions: (Experiment vs. Theory) For a Water Reflected Spherical Cavity System. Case Institute of Technology, NASA CR-72231, December 31, 1966.

222. Plunkett, T. F.: Nuclear Analysis of Gaseous-Core Nuclear Rockets. Nuclear Applications, Vol. 3, No. 3, March 1967, p. 178.

223. Pincock, G. D. and J. F. Kunze: Cavity Reactor Critical Experiment, Vol. 1. General Electric Company, NASA CR-72234, September 6, 1967.

224. Podney, W. N. and H. P. Smith: Neutron Kinetics of a Cylindrical-Cavity Reactor. Transactions, American Nuclear Society, Vol. 10, No. 2, November 1967, p. 422.

225. Masson, L. S., G. D. Pincock, J. F. Kunze, R. E. Wood and R. E. Hyland: Cavity Reactor Gas-Core Critical Experiment. Transactions, American Nuclear Society, Vol. 10, No. 2, November 1967, p. 419. Also issued as NASA CR-72329.

226. Podney, W. N. and H. P. Smith, Jr.: Prompt Neutron Kinetics of a Spherical Cavity Reactor. Nuclear Science and Engineering, Fol. 29, 1967, p. 373.

227. Titus, R. R.: Propulsion System Comparison for Manned Mars Landing Missions. United Aircraft Research Laboratories Report F-110224-3, 1967.

228. Pincock, G. D. and J. F. Kunze: Cavity Reactor Critical Experiment, Vol. 2. General Electric Company, NASA CR-72415, May 31, 1968.

229. McNeill, H. and M. Becker: Acoustic Instability in a Fission Gas. Transactions, American Nuclear Society, Vol. 11, No. 1, June 1968, p. 31.

230. Pincock, G. D., J. F. Kunze, R. E. Wood, R. E. Hyland: Cavity Reactor Engineering Mockup Critical Experiment. Transactions, American Nuclear Society, Vol. 11, No. 1, June 1968, p. 29.

231. Pincock, G. D. and J. F. Kunze: Cavity Reactor Critical Experiment, Vol. 3. General Electric Company, NASA CR-72384, November 15, 1968.

232. Henderson, W. B. and J. F Kunze: Analysis of Cavity Reactor Experiments. General Electric Company, NASA CR-72484, January 1969.

233. Kunze, J. F., G. D. Pincock and R. E. Hyland: Cavity Reactor Critical Experiments. Nuclear Applications, Vol. 6, No. 2, February 1969, p. 104.

234. McNeill, H. and M. Becker: Acoustic Instability with Neutronic Feedback in a Gas Core Nuclear Rocket. Transactions, American Nuclear Society, Vol. 12, No. 1, June 1969, p. 1.

235. Kunze, J. F.: The Physics of Cavity Reactors. Transactions, American Nuclear Society, Vol. 12, No. 2, December 1969.

LIST OF SYMBOLS

A_S	Surface area of r-f discharge plasma (see Fig. 8), $in.^2$
$\dot{D}$	Ionizing dose rate (see Eq. (1)), Mrad/sec
G	Color generation factor (see Eq. (1)), cm^{-1}/Mrad
H_{pe}	Propellant enthalpy at exit of propellant duct, Btu/lb
H_{pi}	Propellant enthalpy at inlet to propellant duct, Btu/lb
I_{sp}	Specific impulse, sec
P	Total pressure, atm
P_D	Gas pressure in r-f discharge, atm
P_F	Local simulated-fuel partial pressure, atm
Q_C	Probable maximum power conducted through peripheral wall in r-f tests (see Fig. 8), kw
Q_E	Power removed by end-wall coolant in r-f tests (see Fig. 8), kw
Q_I	D-C input power in r-f tests (see Fig. 8), kw
Q_L	Power removed by argon thru-flow in r-f tests (see Fig. 8), kw
Q_R	Power radiated through both peripheral walls in r-f tests (see Fig. 8), kw
$Q_{R,T}$	Power radiated through inner peripheral wall in r-f tests (see Fig. 8), kw
Q_T	Total discharge power in r-f tests (see Fig. 8), kw
Q_W	Power removed by peripheral-wall cooling water in r-f tests (see Fig. 8), kw
Q_6	Radiant flux at edge-of-fuel region of full-scale nuclear light bulb engine, Btu/sec-ft^2
r	Distance from vortex centerline, in.
r_1	Inside radius of vortex tube, in.

LIST OF SYMBOLS (CONT'D)

r_6	Radius of fuel-containment region, ft
R_P	Radius of seed particle, microns
T_{pe}	Propellant temperature at exit of propellant duct, deg R
T_{pi}	Propellant temperature at inlet of propellant duct, deg R
T^*	Temperature such that black-body radiating flux is equal to actual radiating flux, deg R
ΔT	Temperature rise in cooling fluid, deg R
V	Discharge volume in r-f tests (see Fig. 8), $in.^3$
W_A	Argon thru-flow in r-f tests (see Fig. 8), lb/sec
W_C	Coolant water flow in r-f tests (see Fig. 8), gpm
α	Absorption coefficient in transparent wall, cm^{-1}
λ	Wavelength, microns
τ	Time constant for thermal removal of radiation-induced coloration in transparent materials, sec
ϕ	Radiant flux at edge of plasma in r-f tests (see Fig. 8), $kw/in.^2$

APPENDIX

COMPILATION OF SUMMARY PAGES FROM 50 TECHNICAL REPORTS ISSUED UNDER CONTRACT NASw-847

Reference 1

Johnson, B. V.: Analysis of Secondary-Flow-Control Methods for Confined Vortex Flows. UARL Report C-910091-1, September 1964. Also issued as NASA CR-276.

SUMMARY

An analysis was performed to determine criteria to prevent flow from the end-wall boundary layers (secondary flow) to the central region (primary flow) of a confined, cylindrical vortex. The secondary flow was analyzed by a boundary layer momentum-integral technique for cases in which primary-flow circulation r (product of tangential velocity and local radius) is proportional to the radius to the n_r power (i.e., $r \alpha r^{n_r}$). Radial variations of local end-wall friction coefficient and end-wall suction were investigated as means to alter the radial distribution of angular momentum in the boundary layers and thereby to control the primary flow - secondary flow interactions.

The results of the analysis yield the radial variation of either local friction or wall suction which must be employed to prevent fluid transfer between the primary and secondary flows. The variation of boundary layer thickness with radius is also calculated. Results are obtained for: (1) a constant-density fluid with n_r = 0.5, 1, 2, 3, and 4, and (2) variable-density fluid with n_r = 3 and four different rates of axial mass transfer between the higher-density primary flow and the lower-density secondary flow.

Travers, A., and B. V. Johnson: Measurements of Flow Characteristics in a Basic Vortex Tube. UARL Report C-910091-2, September 1964. Also issued as NASA CR-278.

SUMMARY

An experimental study was conducted to determine the characteristics of confined vortex flows generated in a cylindrical tube by water injection through a single slot extending along the entire length of the tube. Two configurations were tested: a vortex tube with plain end walls and a vortex tube with suction end walls designed to control the interaction between the flow in the end-wall boundary layers and the primary flow. The flow characteristics were determined from photographs of neutrally buoyant plastic particles and dye which were injected as tracer materials.

The flow patterns in the vortex tube with plain end walls were found to be in general agreement with those predicted by a previously developed theory for interacting primary and end-wall boundary layer flows in a vortex tube. It was determined that the primary-flow tangential velocity distributions and the magnitudes of the axial velocities induced in the primary flow by its interaction with the end-wall boundary layers could be reduced by controlling the end-wall boundary layers with distributed end-wall suction.

Travers, A., and B. V. Johnson: Measurements of Flow Characteristics in an Axial-Flow Vortex Tube. UARL Report C-910091-3, September 1964. Also issued as NASA CR-277.

SUMMARY

An experimental study was conducted to determine the characteristics of confined vortex flows generated in a cylindrical tube by tangential injection of water through a slot extending the length of the peripheral wall of the vortex tube and withdrawal of part or all of the water through an annulus in one of the tube end walls near its outer radius. The remainder of the flow was withdrawn through ports at the center of the end walls. Flow patterns in the vortex tube were determined by photographically recording the traces of neutrally buoyant plastic particles and dye which were injected as tracer materials. Tangential and axial velocity profiles, flow patterns, and the radial extent of the high-axial-velocity region are presented for two different annular exhaust geometries and several flow conditions.

Schneiderman, S. B.: Theoretical Viscosities and Diffusivities in High-Temperature Mixtures of Hydrogen and Uranium. UARL Report C-910099-1, September 1964. Also issued as NASA CR-213.

SUMMARY

Coefficients of viscosity and diffusion were calculated for multicomponent mixtures of hydrogen and uranium in order to provide data for use in studies of gaseous nuclear reactor concepts. These properties were calculated for eighteen fuel partial pressure ratios, P_{FUEL}/P, ranging from 0.0 (pure hydrogen) to 1.0 (pure fuel), for nine temperatures from 20,000 K to 100,000 K, and for pressures of 100, 500, and 1000 atmospheres. Some of the calculations for pure hydrogen were also performed for a temperature of 10,000 K.

The calculated values of viscosity and diffusion coefficients for the multicomponent hydrogen-uranium mixtures were used to calculate the Schmidt number--a dimensionless group which relates the scales of momentum and mass transfer--for each mixture. For values of P_{FUEL}/P greater than approximately 0.03, the Schmidt number was found to be less than unity, thus indicating that, for gradients of the same magnitude in velocity and concentration, mass flux due to diffusion will proceed at a greater rate than momentum flux due to viscosity. For values of P_{FUEL}/P less than approximately 0.03, the Schmidt number exceeded unity, thus indicating a reversal in the relative magnitudes of momentum and diffusive flux.

Krascella, N. L.: Theoretical Investigation of the Absorption and Scattering Characteristics of Small Particles. UARL Report C-910092-1, September 1964. Also issued as NASA CR-210.

SUMMARY

A theoretical investigation was conducted to determine the absorption, scattering, and extinction characteristics of small solid spherical particles which might be employed as seeding agents to control radiant heat transfer in gaseous nuclear rocket engines. The calculations were made using the Mie theory to determine the effect of particle size, wavelength, and particle temperature on particle opacity in those regions of the ultraviolet, visible, and infrared spectra for which complex index of refraction information was available. The following materials were considered: aluminum, carbon, cobalt, iridium, molybdenum, niobium, palladium, platinum, rhenium, rhodium, silicon, tantalum, titanium, tungsten, and vanadium.

Marteney, P. J.: Experimental Investigation of the Opacity of Small Particles. UARL Report C-910092-2, September 1964. Also issued as NASA CR-211.

SUMMARY

An experimental investigation was conducted to develop a technique for producing dispersions of submicron-radius solid particles in a carrier gas and to determine the optical parameters of these particles as a function of the wave length of electromagnetic radiation incident upon the particles. A dispersion system was devised which permitted (a) mixing of measured amounts of agglomerated submicron particles with metered quantities of preselected carrier gases, (b) application of de-agglomerative aerodynamic shear forces in a restrictive flow passage (nozzle) through which the carrier gas-particle mixture was passed, and (c) measurement of the extinction and scattering characteristics of the de-agglomerated particles downstream of the nozzle. Tests were conducted with carbon and tungsten particles having nominal radii of 0.0045 and 0.01 microns, respectively, as specified by the manufacturer. Helium and nitrogen were used as carrier gases.

The application of aerodynamic shear forces in the tests resulted in an increase in the extinction parameter for carbon particles from approximately 10,000 cm^2/gm to 58,000 cm^2/gm and for tungsten particles from approximately 2000 cm^2/gm to 8000 cm^2/gm. These increases in extinction parameter are believed to be caused by a reduction in the size of particle agglomerates since, for the sizes of agglomerates encountered in the test program, a reduction in the average agglomerate size should theoretically result in an increase in extinction parameter. Particle photographs qualitatively indicated that the sizes of particle agglomerates were reduced by the application of aerodynamic shear. The maximum theoretical extinction parameters for carbon and tungsten particles at a wavelength of 0.4 microns are 68,000 cm^2/gm and 20,000 cm^2/gm, and occur for particles having radii of 0.1 and 0.05 microns, respectively. The differences between theoretical and experimental maximum extinction parameters can be explained by the presence of a range of particle agglomerate sizes in the experimental program and by the theoretical variation of extinction parameter with particle size.

McLafferty, G. H., and W. G. Burwell: Theoretical Investigation of the Temperature Distribution in the Propellant Region of a Vortex-Stabilized Gaseous Nuclear Rocket. UARL Report C-910093-10, September 1964. Also issued as NASA CR-279.

SUMMARY

A theoretical investigation was conducted to determine the effect of changes in particle seed characteristics on the temperature distributions in the propellant region of a vortex-stabilized gaseous nuclear rocket engine. An engine of this type is based on the transfer of heat by thermal radiation from gaseous nuclear fuel suspended in a vortex to seeded hydrogen propellant passing axially over the fuel-containment region. The investigation included calculation of temperature and heat flux distributions in the propellant region for two or more values of each of the following parameters: hydrogen pressure, hydrogen propellant flow rate, seed vaporization temperature, and ratio of particle seed density to propellant density. Most of the calculations were made using hydrogen opacities and particle opacities which were allowed to vary as a function of temperature but which were averaged over the wavelength spectrum. However, several calculations were made to determine the temperatures and heat flux distributions resulting from use of a more complicated procedure which integrates spectral heat flux. All calculations neglected any contribution to opacity from vaporized particle seeds.

Roback, R.: Thermodynamic Properties of Coolant Fluids and Particle Seeds for Gaseous Nuclear Rockets. UARL Report C-910092-3, September 1964. Also issued as NASA CR-212.

SUMMARY

Thermodynamic properties and equilibrium chemical composition were calculated for various materials which could serve as moderator coolants or as particle seeds designed to control radiant heat transfer in gaseous nuclear rocket engines. The materials which were considered as moderator coolants were hydrogen, methane, water, ammonia, deuterium, heavy water, and helium. Materials which were considered as possible particle seeds were several elemental species which have high boiling points, such as graphite, tungsten, and molybdenum, and the oxides, carbides, nitrides, and borides of titanium and zirconium.

The results of the calculations indicate that the use of graphite as a seed material is impractical because graphite reacts readily with hydrogen, and, consequently, excessive quantities of graphite must be added to the hydrogen stream in order to maintain even very small concentrations of seed particles at high temperatures. Also, the limited thermodynamic data currently available indicate that no significant increase in particle vaporization temperature would result from using oxides, carbides, nitrides, or borides of such high-melting-point metals as titanium and zirconium as seeds in place of the metals themselves.

McLafferty, G. H.: Analytical Study of Moderator Wall Cooling of Gaseous Nuclear Rocket Engines. UARL Report C-910093-9, September 1964. Also issued as NASA CR-214.

SUMMARY

An analytical study was conducted to investigate cooling problems in high-thrust cavity-type gaseous nuclear rocket engines resulting from (a) heat deposition within the interior of the moderator-reflector surrounding the cavity by neutrons and gamma rays and (b) heat deposition on the surface of the cavity by fission fragments, beta particles, radiant heat transfer, and convection. The study included determination of the size and spacing of coolant tube passages required in the wall of the moderator-reflector and the pressure drop of the coolant fluid in these passages. A number of different coolant flow cycles were considered.

The results of the study indicate that more heat will be deposited in the interior of the moderator than on the surface of the cavity, but that the heat deposited on the surface of the cavity may be more difficult to remove. Removal of the energy deposited in the interior of the moderator will require the use of a large number of small-diameter coolant passages. The major causes of cavity surface heating will be beta-particle impingement and thermal radiation, but calculations indicate that heating by beta-particle impingement can be reduced by the use of a magnetic field and that heating by thermal radiation can be reduced by the use of seeds in the propellant.

In addition to a description of the moderator cooling study in the main body of the report, three additional studies are described in the appendices: determination of the fuel-containment characteristics of a gaseous nuclear rocket in which no attempt is made to separate propellant and fuel; determination of the effect of different propellants on the specific impulse of gaseous nuclear rockets; and a description of a facility concept which might be employed for testing gaseous nuclear rockets.

Mensing, A. E., and J. S. Kendall: Experimental Investigation of Containment of a Heavy Gas in a Jet-Driven Light-Gas Vortex. UARL Report D-910091-4, March 1965. Also issued as NASA CR-68926.

SUMMARY

An experimental study of the containment of a heavy gas in a jet-driven light-gas vortex was conducted as part of a program to establish the feasibility of a vortex-stabilized gaseous nuclear rocket. Helium or air was employed as the light gas (simulated propellant) and mixtures of iodine with other gases were employed as the heavy gas (simulated fuel). Most of the tests were conducted in a basic vortex tube, i.e., with the light gas injected through a slot at the periphery extending the length of the vortex tube and with the majority of this light gas removed after one revolution through a perforated plate extending the length of the vortex tube. The amount of heavy gas contained in the vortex and the loss rate of this heavy gas were found to depend strongly on the method and rate of its injection into the vortex and the vortex flow Reynolds numbers. Of the several injection configurations tested, injection of the heavy gas along the vortex centerline yielded the best performance in terms of minimization of loss rate and maximization of the amount of contained heavy gas.

McFarlin, D. J.: Experimental Investigation of the Effect of Peripheral Wall Injection Technique on Turbulence in an Air Vortex Tube. UARL Report D-910091-5, September 1965. Also issued as NASA CR-68867.

SUMMARY

Experiments were conducted to investigate the effect of the peripheral-wall injection technique used to drive an air vortex on the level of turbulence in the vortex. Two injection configurations were tested in separate 10-in.-dia vortex tubes. In one configuration, air was injected tangentially through a single 0.182-in.-high slot which extended along the entire 30-in. length of the tube. In the second configuration, air was injected approximately tangentially through 2144 ports of 0.060-in. dia distributed over the surface of the peripheral wall. In both tubes, a controlled quantity of air was removed through ports located at the centers of the two end walls or was injected through a porous tube located on the centerline of the vortex; air was also removed through perforated plates in the peripheral wall. Hot-wire-anemometer measurements of tangential velocity profiles and root-mean-square velocity fluctuations were made near the peripheral wall at three circumferential stations at one axial location (the axial midplane).

The results indicated that the interior region of low-turbulence flow was larger for the 2144-port configuration than for the single-slot configuration. This was primarily because the turbulent peripheral wall boundary layer was thinner for the 2144-port configuration.

Johnson, B. V.: Analytical Study of Propellant Flow Requirements for Reducing Heat Transfer to the End Walls of Vortex-Stabilized Gaseous Nuclear Rocket Engines. UARL Report D-910091-6, September 1965.

SUMMARY

The propellant flow requirements for reducing heat transfer to the end walls of a vortex-stabilized gaseous nuclear rocket engine were estimated on the basis of three different analyses: an analysis involving only radiant heat transfer, an analysis involving only convective heat transfer, and an analysis in which heat is transferred by thermal radiation from the fuel-containment region to the end-wall boundary layer and by convection from the end-wall boundary layer to the wall. The analyses indicated that the propellant flow rates required because of radiant heat flux were greater than those required because of convective heat flux for the temperatures and heat flux rates expected to exist at the edge of the fuel-containment region in a full-scale engine.

Travers, A.: Experimental Investigation of Peripheral Wall Injection Techniques in a Water Vortex Tube. UARL Report D-910091-7, September 1965. Also issued as NASA CR-68866.

SUMMARY

An experimental investigation was conducted to determine the effects of the peripheral-wall injection technique used to drive a water vortex on the structure and thickness of the turbulent mixing region near the peripheral wall and on the flow patterns in the primary-flow region outside the peripheral and end-wall boundary layers. Three 10-in.-dia lucite vortex tubes having three different peripheral-wall injection configurations were tested: (1) tangential injection through a single 0.205-in.-high slot extending the entire 30-in. length of the tube, (2) tangential injection through four 0.050-in.-high slots, and (3) approximately tangential injection through 2144 ports of 0.060-in. diameter. In most tests, a controllable quantity of fluid was removed through one or more perforated screens in the peripheral wall and the remainder of the fluid was removed through 0.938-in.-dia thru-flow ports located at the centers of the two end walls. However, a few tests were conducted in which no fluid was removed through the thru-flow ports; instead, fluid was injected through a 1.0-in.-dia porous tube located along the centerline of the vortex tube.

Microflash photographs of dye patterns were taken through one of the end walls to observe the characteristics of the turbulent mixing region, and time-exposure photographs of dye patterns were taken through the side wall to observe the characteristics of the primary-flow region. Tangential velocity profiles in the primary-flow region were obtained by means of a photographic particle-trace method using small, neutrally buoyant polystyrene spheres.

The results of the tests indicate that the volume of low-turbulence flow in the primary-flow region was considerably larger for the 2144-port injection configuration than for the single-slot and four-slot injection configurations. This larger volume is attributable to the much thinner turbulent mixing region near the peripheral wall for the 2144-port injection configuration.

Johnson, B. V., and A. Travers: Analytical and Experimental Investigation of Flow Control in a Vortex Tube by End-Wall Suction and Injection. UARL Report D-910091-8, September 1965. Also issued as NASA CR-68927.

SUMMARY

Analytical and experimental studies were performed to investigate the effect of injection or suction through the end walls of a vortex tube on the secondary flow (flow in the end-wall boundary layers) and the primary flow (flow in the central portion of the vortex). The analytical study employed a momentum integral analysis to determine the injection flow distribution through the end walls required to prevent convection between the secondary-flow and the primary-flow regions. The analysis indicated that significant changes in the injection flow rate requirements resulted from changes in the following: the primary-flow tangential velocity distribution, the injection velocity distribution, the secondary flow at the radius where flow control is initiated, and the direction of the secondary flow (radially inward or outward).

Experiments were conducted in a 10-in.-dia by 30-in.-long water vortex tube to investigate the influence of end-wall injection and suction on flow characteristics. The experiments with end-wall injection were conducted in a basic vortex tube (without superimposed axial flow) and the experiments with end-wall suction were conducted in an axial-flow vortex tube. The results of the tests indicated that both end-wall suction and end-wall injection caused significant changes in the characteristics of the primary-flow region of the vortex.

Mensing, A. E., and J. S. Kendall: Experimental Investigation of the Effect of Heavy-to-Light-Gas Density Ratio on Two-Component Vortex Tube Containment Characteristics. UARL Report D-910091-9, September 1965. Also issued as NASA CR-68926.

SUMMARY

An experimental investigation of the containment of a heavy gas in a jet-driven light-gas vortex was conducted as part of a program to establish the feasibility of a vortex-stabilized gaseous nuclear rocket. Helium of air was employed as the light gas and was injected into the cylindrical vortex tube through a tangential injection slot extending the length of the vortex tube. A mixture of iodine and a heavy fluorocarbon was employed as the heavy gas and was injected into the vortex tube through a porous tube located on the vortex tube centerline. Tests were conducted in both the basic vortex tube (i.e., a vortex tube in which all the injected gas exhausted through a perforated plate on the vortex tube peripheral wall) and the axial-flow vortex tube (i.e., a vortex tube in which all the injected gas exhausted through an annulus in one end wall). The amount of heavy gas contained and the loss rate of this heavy gas were found to depend on the rate of its injection into the vortex tube, on the rate of injection of the light gas into the vortex tube and on the method of exhausting gas from the vortex tube. The highest ratios of average heavy-gas density to injection light-gas density (approximately 12) were obtained in tests in the basic vortex tube at low injection Reynolds numbers using helium as the light gas.

Williamson, H. A., H. H. Michels, and S. B. Schneiderman: Theoretical Investigation of the Lowest Five Ionization Potentials of Uranium. UARL Report D-910099-2, September 1965. Also issued as NASA CR-69002.

SUMMARY

Ionization potentials were calculated for uranium and its first four positive ions using approximate quantum mechanical methods. A range of values was obtained for each ionization potential, with the individual values depending upon the approximations entering into the calculations. The final suggested values are: U(I) - 6.11 e.v.; U(II) - 17.5 e.v.; U(III) - 37.5 e.v.; U(IV) - 61 e.v.; U(V) - 118 e.v.

Ionization potentials for U(I) through U(III), differing only slightly from these final suggested values, were employed in an evaluation of the following properties of equilibrium mixtures of hydrogen and uranium: species concentration, coefficients of viscosity and diffusion, and effective Schmidt number. The calculations were performed at pressures of 100, 500, and 1000 atm., temperatures of 20,000 K, 60,000 K, and 100,000 K, and fuel partial pressure fractions of 0.09, 0.1, 0.233, 0.367, 0.5, 0.633, 0.767, and 0.9. The results of these calculations indicate that the uranium ions of lower valency play an important role in the determination of the properties of the mixture up to temperatures higher than had been indicated in preceding studies, thereby raising significantly both the mixture viscosity and effective hydrogen-uranium binary diffusivity at temperatures below about 60,000 K. Since the changes in these two quantities are in the same direction, however, changes in the effective Schmidt number are small.

Krascella, N. L.: Theoretical Investigation of the Opacity of Heavy-Atom Gases. UARL Report D-910092-4, September 1965. Also issued as NASA CR-69001.

SUMMARY

A theoretical investigation was conducted to determine the composition, spectral absorption coefficients and Rosseland mean opacity of gaseous nuclear fuel and tungsten using a semi-empirical heavy-atom analytical model in order to obtain information applicable to gaseous nuclear rockets. The characteristics of the nuclear fuel were determined for a range of values of each of the following parameters which must be assumed in using the heavy-atom model; ionization potentials, energy level spacings, total oscillator strengths, and the ratio of partition functions for successive ionization species. Included in these ranges of values were calculated ionization potentials and partition function ratios. The greatest changes in Rosseland mean opacity at a given pressure and temperature resulted from the calculated changes in fuel ionization potentials. The Rosseland mean opacity of gaseous tungsten was calculated on the basis of completely overlapped lines (which would result from line broadening due to the presence of a perturbing gas at infinite pressure), and for finite-width spectral lines due to the presence of specified values of hydrogen partial pressure.

Kesten, A. S., and R. B. Kinney: Theoretical Effect of Changes in Constituent Opacities on Radiant Heat Transfer in a Vortex-Stabilized Gaseous Nuclear Rocket. UARL Report D-910092-5, September 1965.

SUMMARY

A theoretical investigation was conducted to determine the effect of changes in constituent opacities on the radiant heat transfer characteristics and temperature distributions in both the hydrogen-propellant and fuel-containment regions of a vortex-stabilized gaseous nuclear rocket. Two changes from preceding calculations were made which influenced primarily the opacities in the propellant region at temperatures between 10,000 and 15,000 R. The first change consisted of adding the opacity contribution of vaporized tungsten seeds whose spectral lines are broadened by the presence of high-pressure hydrogen propellant. The second change consisted of neglecting the opacity due to the Lyman-α line in hydrogen, and was made because of recent experimental information on opacity in the far line wings of monatomic gases. The results of the propellant-region calculations indicate that the inclusion of the opacity of vaporized tungsten seeds resulted in a substantial reduction in the distance required to absorb the incident radiant energy.

Temperature distributions in the fuel-containment region were determined for fuel opacities equal to half and twice those which have been employed in preceding calculations and for opacities which were determined from recent theoretical determinations of fuel ionization potentials. The fuel temperatures near the centerline of the vortex were found to be relatively insensitive to changes in fuel opacity.

Marteney, P. J., N. L. Krascella, and W. G. Burwell: Experimental Refractive Indices and Theoretical Small-Particle Spectral Properties of Selected Metals. UARL Report D-910092-6, September 1965. Also issued as NASA CR-68865.

SUMMARY

An applied research program was conducted to determine the absorption, scattering, and extinction parameters of small spherical metal particles which might be employed as seeding agents to control radiant heat transfer in gaseous nuclear rocket engines. This program consisted of both experimental and theoretical phases. Under the experimental phase of the program, measurements were made using an ellipsometric technique to determine the complex refractive indices of hafnium, molybdenum, nickel, and tungsten in the wavelength range between 0.2 and 0.7 microns. Under the theoretical phase of the program, calculations were made using the Mie theory to determine spectral absorption, scattering, and extinction parameters of small spherical particles made from nine different metals. These calculations were made using values of the complex refractive indices of the four metals investigated in the experimental phase of the program and the complex refractive indices for cobalt, iron, titanium, vanadium, and zirconium determined from the current literature. Calculations were also made of the Rosseland mean opacity parameter of 0.05μ-radius tungsten particles using spectral absorption parameters determined from the Mie theory.

McLafferty, G. H., H. H. Michels, T. S. Latham, and R. Roback: Analytical Study of Hydrogen Turbopump Cycles for Advanced Nuclear Rockets. UARL Report D-910093-19, September 1965.

SUMMARY

An analytical study was conducted to determine the characteristics of three different turbopump cycles which might be employed to obtain the high engine inlet pressures which are expected to exist in advanced nuclear rockets. The three cycles considered were: a topping cycle, in which the power required to drive the pump is obtained by passing all of the pump-exit flow through a turbine before this flow enters the engine; a bleed cycle, in which all of the pump power is obtained by discharging a fraction of the pump-exit flow through a bleed turbine with an expansion pressure ratio of 0.01; and a mixed cycle, in which half of the power to drive the pump is obtained from a primary turbine and half from a bleed turbine. The studies were conducted for a range of turbine inlet temperatures between 1400 and 3800 R, for a range of turbine inlet pressures between 200 and 5000 atm, for pressure drops between the pump exit and the turbine inlet of zero and 50 atm, and for three different combinations of pump and turbine efficiency. The results of the study indicate the effect of engine inlet pressure on the turbine pressure drop and/or the bleed flow fraction for each cycle.

Three studies not connected with hydrogen turbopumps are described in the Appendixes. These are: an analysis of the approximate temperature distribution in the fuel-containment region of a coaxial-flow gaseous nuclear rocket (APPENDIX I); a change in form of heavy-gas containment data obtained from NASA Lewis coaxial-flow tests (APPENDIX II); and an analysis of the heat generation rate in fuel passing through a fuel injection duct located in the moderator of a gaseous nuclear rocket engine (APPENDIX III).

McLafferty, G. H.: Analytical Study of the Performance Characteristics of Vortex-Stabilized Gaseous Nuclear Rocket Engines. UARL Report D-910093-20, September 1965.

SUMMARY

An analytical study of the performance characteristics of vortex-stabilized gaseous nuclear rocket engines was conducted to provide information for use in the evaluation of the results of vortex heavy-gas containment tests. An engine of this type is based on the transfer of energy by thermal radiation from gaseous nuclear fuel held in a vortex to seeded propellant passing over the fuel-containment region. The study included analysis of the effect on specific impulse and approximate engine weight of changes in the following: engine size, cavity pressure, engine power level (engine thrust-to-weight ratio), temperature of propellant injected into the cavity, fuel density ratio (ratio of the average fuel density required for criticality to the density of the light gas at the outside edge of the fuel-containment region), and the addition of a space radiator. Estimates were also made of payloads and direct mission costs which would result from use of some of the engine configurations with a Saturn S-IC launch vehicle for a mission requiring a total payload velocity 50,000 ft/sec greater than earth orbital velocity. The results of the calculations indicate that the payload per Saturn S-IC launch using a gaseous nuclear rocket will be five to ten times greater than those using solid-core nuclear rockets (and the direct cost per pound of payload approximately five times less) if fuel density ratios of approximately five and dimensionless fuel time constants of approximately 0.003 can be attained in the gaseous nuclear rocket at axial-flow Reynolds numbers of approximately 5×10^5.

Krascella, N. L.: Theoretical Investigation of the Absorptive Properties of Small Particles and Heavy-Atom Gases. UARL Report E-910092-7, September 1966. Also issued as NASA CR-693.

SUMMARY

A theoretical investigation was conducted to determine the spectral and mean absorption characteristics of solid and gaseous elemental materials which might be utilized to control the transfer of radiant energy in the propellant region of a gaseous nuclear rocket engine. Spectral extinction, absorption and scattering parameters were calculated, based on the Mie theory, for spherical molybdenum, niobium, tantalum and cadmium particles having radii of 0.01, 0.05, 0.10, and 0.50μ. Similar calculations were made for spherical tungsten particles at five temperatures between 1600 K (2880 R) and 2400 K (4320 R). The tungsten calculations were based on analytically extrapolated refractive indices for wavelengths between 0.1 and 30μ at each temperature. The Rosseland mean absorption parameter of spherical tungsten particles having a radius of 0.05 was calculated for temperatures between 1000 K (1800 R) and 5600 K (10,080 R). In addition, the spectral absorption parameters and normal spectral reflectivities of bulk aluminum, cadmium, carbon, cobalt, hafnium, iridium, iron, molybdenum, niobium, nickel, palladium, platinum, silicon, tantalum, thallium, titanium, tungsten, vanadium, and zirconium were calculated. The bulk absorption parameters apply to seeds in the form of thin plates and are generally higher than those for seeds in the form of spherical particles. Average reflectivities for normally incident radiation, determined by weighting the normal spectral reflectivities with respect to the black-body radiation function, were computed for aluminum, copper, gold, nickel, silver and tungsten.

The spectral absorption coefficients and Rosseland mean opacity of gaseous tungsten were re-evaluated using the UARL heavy-atom model with a modified oscillator strength distribution function. Additional average local line spacing and local line intensities for materials which might be used as gaseous seed agents were calculated. These materials included neutral iron, silicon, uranium, and vanadium as well as singly ionized niobium, tungsten, and vanadium.

Kinney, R. B.: Theoretical Effect of Seed Opacity and Turbulence on Temperature Distributions in the Propellant Region of a Vortex-Stabilized Gaseous Nuclear Rocket. UARL Report E-910092-8, September 1966. Also issued as NASA CR-694.

SUMMARY

A theoretical investigation was conducted to determine the effect on the temperature and radiant heat transfer distributions in the propellant region of a vortex-stabilized gaseous nuclear rocket which result from: the use of newly defined opacity characteristics of solid and vaporized tungsten seed; and the introduction of turbulence in the region adjacent to the peripheral wall. In determining the effect of turbulence level on the temperature distribution, values of trubulence level were used which bracket that which is expected in a specific vortex-stabilized gaseous nuclear rocket engine configuration under study at the Research Laboratories. The turbulence calculations include allowance for the stabilizing effect of radial temperature gradients and radial circulation gradients on the basis of hypotheses by G. I. Taylor and L. Prandtl concerning the effect of Richardson number on turbulence.

Kesten, A. S. and N. L. Krascella: Theoretical Investigation of Radiant Heat Transfer in the Fuel Region of a Gaseous Nuclear Rocket Engine. UARL Report E-910092-9, September 1966. Also issued as NASA CR-695.

SUMMARY

A series of calculations were made to determine temperature distributions in the fuel-containment region of gaseous nuclear rocket engines which are based on the transfer of energy by thermal radiation from the fuel to the propellant. Temperature distributions were determined for two sets of fuel opacities; the opacities in each of these sets were calculated from an analytical heavy-atom model using two recent theoretical estimates of fuel ionization potentials. The temperatures near the centerline of the fuel-containment region were found to be high and relatively insensitive to changes in fuel opacity.

McLafferty, G. H., H. E. Bauer and D. E. Sheldon: Preliminary Conceptual Design Study of a Specific-Vortex-Stabilized Gaseous Nuclear Rocket Engine. UARL Report E-910093-29, September 1966. Also issued as NASA CR-698.

SUMMARY

A study of a specific gaseous nuclear rocket engine configuration was made to determine the approximate weight of the primary components of the engine and to determine the dimensions necessary for the determination of the critical mass of nuclear fuel required. The vortex-stabilized engine concept considered is based on the transfer of heat by thermal radiation from gaseous nuclear fuel suspended in a vortex to seeded propellant passing axially over the fuel-containment region. The configuration employed in the study is assumed to have both a cavity diameter and cavity length of 6 ft and a moderator composed of successive layers of beryllium, beryllium oxide, graphite, and heavy water. The energy deposited in the moderator is assumed to be removed by a helium coolant and transferred through external heat exchangers to the propellant. The engine is estimated to have the following characteristics: specific impulse, 2186 sec; thrust, 1.45×10^6 lb; and weight of major components, between 113,000 and 211,000 lb. The analysis of the engine configuration covered only design-point operation.

The appendixes to the report include results of studies of the following: the approximate conditions in the engine during the start-up process; the effect of changes in critical mass and average cavity propellant enthalpy on engine characteristics; and a criteria for laminar-flow instability in the spiral-hole configuration employed for cooling the moderator.

Reference 26

Roback, R.: Theoretical Performance of Rocket Engines Using Gaseous Hydrogen in the Ideal State at Stagnation Temperatures up to 200,000 R. UARL Report E-910093-30, September 1966. Also issued as NASA CR-696.

SUMMARY

Theoretical performance parameters for rocket engines utilizing normal gaseous hydrogen in the ideal state were calculated using two different assumptions: first, that the chemical composition remained in equilibrium during the isentropic expansion through the engine exhaust nozzle; and, second, that the chemical composition remained fixed (frozen) during the expansion. Data are presented for stagnation temperatures ranging from 5000 to 200,000 R, stagnation pressures ranging from 1 to 2000 atm, and ratios of exhaust pressure to stagnation pressure ranging from 1 to 10^{-7}. The following performance parameters were calculated as a function of the ratio of nozzle exhaust pressure to stagnation pressure: temperature, enthalpy, entropy, molecular weight, density, velocity, Mach number, specific impulse and ratio of nozzle-exit area to throat area. Also calculated were several other properties of the gaseous mixture at the throat of the nozzle, such as the weight flow per unit area and a throat flow parameter defined as the product of the weight flow per unit area at the throat and the square root of the stagnation temperature divided by the stagnation pressure, $(W\sqrt{T_T}/A^* P_T)$.

Latham, T. S.: Nuclear Criticality Study of a Specific Vortex-Stabilized Gaseous Nuclear Rocket Engine. UARL Report E-910375-1, September 1966. Also issued as NASA CR-697.

SUMMARY

An analytical study was conducted using one- and two-dimensional diffusion theory to determine the critical mass requirements of a specific reference vortex-stabilized gaseous nuclear rocket engine configuration having a cavity length and diameter equal to 6 ft, a cavity liner composed of tubes made from W-184, and a surrounding moderator region made of successive layers of beryllium, beryllium oxide, graphite, and heavy water. The calculations made allowance for the following: an annular passage leading from the cavity to the exhaust nozzles, a fuel-injection duct passing through the moderator, voids and W-184 structure in the moderator, a radial distribution of hydrogen temperature in the cavity, and a radial fuel density distribution. In addition, the moderator was considered to be surrounded by layers of natural tungsten and iron to simulate the external piping and pressure vessel.

The results of the calculations indicate that a critical mass of 50.1 lb of U-233 fuel would be required for the reference engine design used in the present study. This mass could be reduced by a decrease in the volume of the nozzle-approach annulus, an increase in reflector-moderator mass, or a reduction in the volume of neutron-absorbing structure within the cavity liner and reflector-moderator. For instance, one-dimensional calculations indicate that the critical mass could be reduced by approximately 40% by substitution of beryllium wall liner tubes covered with niobium-carbide-coated graphite sleeves for the W-184 wall liner tubes assumed in the study.

One-dimensional calculations were performed to generate 4-group cross sections for subsequent two-dimensional calculations and also to provide information on trends in critical mass variation with variations in moderator void fractions, structure fractions, dimension of various regions, and selection of nuclear fuel. The two-dimensional calculations provide critical mass estimates for configurations with and without exhaust nozzles and fuel-injection duct, and with different amounts of structure within the exhaust nozzle region.

Travers, A.: Experimental Investigation of Flow Patterns in Radial-Outflow Vortexes Using a Rotating-Peripheral-Wall Water Vortex Tube. UARL Report F-910091-10, May 1967. Also issued as NASA CR-991.

SUMMARY

Experiments were conducted using a water vortex to investigate the conditions under which turbulence exists in radial-outflow vortexes with and without superimposed axial flow. The vortex test apparatus used had a 10-in.-dia by 30-in.-long rotating porous peripheral wall, a 1.0-in.-dia rotating inner porous tube located on the centerline, and end walls that could be rotated with the peripheral wall or held stationary. In the tests without superimposed axial flow (basic vortex configuration), plain end walls were used. Flow was injected through the inner porous tube, flowed radially outward, and was withdrawn through the rotating porous peripheral wall. In the tests with superimposed axial flow (axial-flow vortex configuration), one plain end wall and one end wall with a 3/4-in.-wide annulus near its outer edge were used. Flow was withdrawn through the annulus and was injected either (1) only through the inner porous tube, (2) through both the inner porous tube and the rotating porous peripheral wall, or (3) only through the rotating porous peripheral wall.

The characteristics of the flow were determined from observations and microflash photographs of dye patterns for different combinations of the flow conditions (values of tangential, radial and axial-flow Reynolds numbers) and the peripheral-wall, inner-porous-tube and end-wall rotation speeds. Tangential velocity profiles were measured for some basic-vortex flow conditions by means of a photographic particle-trace method using small, neutrally buoyant polystyrene spheres. Summary plots indicating criteria for the flow conditions that lead to laminar, alternating laminar and turbulent, and turbulent flow patterns were constructed for both vortex configurations.

The results of the tests indicate that radial-outflow vortexes are generally characterized by turbulence with large eddies that convect fluid from the central region of the vortex to near the peripheral wall. These flow patterns exist for both basic and axial-flow vortex configurations and for wide ranges of the flow conditions. Laminar flow was encountered only with low rates of radial outflow and low superimposed axial velocities. Rotation of the end walls had a significant effect on the flow patterns in the basic vortex configuration for a limited range of the flow conditions; rotation of the inner porous tube had no significant effect. Rotation of the inner porous tube and end walls had no significant effect on the flow patterns in the axial-flow vortex configuration.

Johnson, B. V.: Exploratory Flow and Containment Experiments in a Directed-Wall-Jet Vortex Tube with Radial Outflow and Moderate Superimposed Axial Flows. UARL Report F-910091-11, May 1967. Also issued as NASA CR-992.

SUMMARY

Exploratory fluid mechanics experiments were performed to obtain information applicable to an open-cycle, vortex-stabilized, gaseous-core nuclear rocket. The containment characteristics of confined radial-outflow vortexes with superimposed axial flow were studied to determine whether high average simulated-fuel densities and high ratios of simulated propellant-to-fuel flow rates could be obtained. The experiments concentrated on two factors that influence simulated-fuel containment: (1) simulated-propellant injection methods in which the flow is injected from the peripheral wall of an axial-flow vortex tube with both axial and tangential (circumferential) components of velocity, and (2) simulated-fuel injection methods. The experiments were performed in 10-in.-dia by 30-in.-long vortex tubes. Simulated propellant was injected at the peripheral wall through 600 directed wall jets that could be adjusted to any injection flow angle between the tangential and axial directions.

Flow visualization tests were performed using water with dye as a trace fluid. The dye patterns showed that large-scale turbulent mixing occurred between the central region and the peripheral-wall region when the simulated fuel was injected from ducts at the centers of both end walls (radial outflow). Velocity measurements were made using air as the working fluid. These measurements indicated that injection at the peripheral wall with both axial and tangential components of velocity will substantially decrease the average axial velocities in the central region and will create a larger volume within the vortex that is potentially available for containment of fuel. Containment tests to determine the average dwell time of simulated fuel in the vortex tube were performed using a heavy gas to simulate fuel and a light gas to simulate propellant. Compared with the containment times measured with no axial component of injection velocity, improvements in containment time of as much as a factor of three-and-one-half were obtained in this investigation using injection with both axial and tangential components of velocity. The improvements that can be obtained using different fuel injection methods are smaller. However, the maximum containment times that were measured were approximately one to two orders of magnitude less than the value now estimated to be required for an economically practical, open-cycle, gaseous-core nuclear rocket.

Kendall, J. S., A. E. Mensing, and B. V. Johnson: Containment Experiments in Vortex Tubes with Radial Outflow and Large Superimposed Axial Flows. UARL Report F-910091-12, May 1967. Also issued as NASA CR-993.

SUMMARY

An experimental investigation was conducted to determine the heavy-gas containment characteristics of radial-outflow vortexes for potential application to a vortex-stabilized, open-cycle gaseous nuclear rocket engine. Tests were conducted in a constant-temperature vortex with Reynolds numbers based on the superimposed axial flow up to those expected in a full-scale engine. Air was employed to simulate the seeded hydrogen propellant and a heavy fluorocarbon was used in most tests to simulate the gaseous nuclear fuel. The effects on heavy-gas containment of changes in the vortex tube length-to-diameter ratio, the light-gas injection geometry and area, the ratio of average heavy-gas density to light-gas density, and the density of the heavy gas at injection were studied.

The heavy-gas containment parameters obtained were one to two order of magnitude less than are presently estimated to be required for an economically practical open-cycle engine. The containment parameters varied significantly only with vortex tube length-to-diameter ratio and the ratio of average heavy-gas density to light-gas density. The results of some tests using helium injected near the centerline of the vortex indicated that the presence of a light gas in the central region of the vortex has a significant favorable effect on containment characteristics; these results have potential application to the nuclear light bulb engine.

Clark, J. W., J. S. Kendall, B. V. Johnson, A. E. Mensing, and A. Travers: Summary of Gaseous Nuclear Rocket Fluid Mechanics Research Conducted Under Contract NASw-847. UARL Report F-910091-13, May 1967.

SUMMARY

An extensive experimental and analytical investigation of the characteristics of vortex flows was conducted to obtain information required for evaluating the feasibility of two vortex-stabilized gaseous nuclear rocket engine concepts. While most of the fluid mechanics research was directed toward the vortex-stabilized open-cycle concept, the results are also applicable to the closed-cycle nuclear light bulb concept. Both of these concepts are based on the transfer of energy by thermal radiation from gaseous nuclear fuel contained in a vortex to seeded hydrogen propellant. In the open-cycle engine, propellant is injected at the peripheral wall of the cavity to drive the vortex and then spirals axially around the fuel-containment region toward the exhaust nozzle. Nuclear fuel is injected into the central region of the cavity where it is contained for a period of time by the vortex flow field. In the nuclear light bulb engine, the propellant and vortex regions are separated by an internally cooled transparent wall. Neon collant is injected tangent to the inner surface of the transparent wall to drive the vortex and to provide a buffer region to isolate the gaseous nuclear fuel from the transparent wall. The purpose of this report is to summarize the principal results of the fluid mechanics investigation and to interpret them in terms of the requirements of these two engines.

Containment tests were conducted using gases having different molecular weights to simulate the gaseous nuclear fuel and either the propellant or the neon coolant. In addition, flow visualization tests were conducted and flow-field velocity measurements were made using water and air vortexes to obtain fundamental information on vortex flow patterns. The principal geometrical parameters investigated in the program were (1) the length-to-diameter ratio of the vortex tube, (2) the geometry of the system used to inject light gas at the peripheral wall, (3) the geometry of the system used to inject heavy gas, (4) the locations and sizes of the ports for removing flow (an annulus at the outer edge of one end wall, ports at the centers of the end walls, and ports at the peripheral wall), and (5) end-wall boundary layer control. The flow conditions tested included Reynolds numbers up to those estimated to be required for full-scale engines.

Travers, A.: Experimental Investigation of Radial-Inflow Vortexes in Jet-Injection and Rotating-Peripheral-Wall Water Vortex Tubes. UARL Report F-910091-14, September 1967. Also issued as NASA CR-1028.

SUMMARY

Experiments were conducted in water vortex tubes to determine the effects of peripheral-wall injection area and axial bypass on the flow pattern and location of the radial stagnation surface in radial-inflow vortexes. The particular type of flow pattern investigated contains a central cell region which is bounded on the outside by a radial stagnation surface which appears to be laminar. At the radius of the radial stagnation surface, all radial flow passes through the end wall boundary layers. The flow in the vortex is laminar for radii less than that of the radial stagnation surface and is turbulent at larger radii.

Two 10-in.-dia by 30-in.-long lucite vortex tubes were used: a jet-injection vortex tube and a rotating-peripheral-wall vortex tube. In tests with the jet-injection vortex tube, flow was injected through the peripheral-wall and was removed (1) through two axial bypass exhaust annuli (a 1/8-in.-wide annulus was located at the outer edge of each end wall) and two 1.0-in.-dia thru-flow ports located at the centers of the end walls, or (2) through only the thru-flow ports. This vortex tube was tested with different peripheral-wall injection areas. In tests with the rotating-peripheral-wall vortex tube where there was no provision for axial bypass, the flow was injected through the rotating peripheral wall and was withdrawn through the thru-flow ports.

Tests were conducted with different combinations of tangential injection and radial Reynolds numbers, different amounts of bypass flow, and different peripheral-wall injection areas. The characteristics of the flow and the radius of the radial stagnation surface were determined from observations and photographs of dye patterns. The results of the experiments were compared with the results of a previous theoretical investigation of confined vortex flows.

Kendall, J. S.: Experimental Investigation of Heavy-Gas Containment in Constant-Temperature Radial-Inflow Vortexes. UARL Report F-910091-15, September 1967. Also issued as NASA CR-1029.

SUMMARY

An experimental investigation was conducted to determine the containment characteristics of radial-inflow vortexes for potential application to a vortex-stabilized nuclear light bulb engine. This engine concept is based on the transfer of energy by thermal radiation from gaseous nuclear fuel contained in a vortex through an internally cooled transparent wall to seeded hydrogen propellant. A transparent buffer gas would be injected at the inner surface of the transparent wall to drive the vortex and to isolate the wall from the fuel and fission products.

Tests were conducted using 10-in.-dia by 30-in.-long vortex tubes. Air used to simulate the buffer gas was injected through ports in the peripheral walls of the vortex tubes. Iodine mixed with one of four other gases (helium, nitrogen, sulfur hexafluoride or a heavy fluorocarbon, FC-77) was used to simulate the gaseous nuclear fuel. The simulated fuel was injected at several different locations: at one end wall without swirl through 10 small tubes; at one end wall with swirl through 10 wall jets; or radially inward from the peripheral wall through 12 small tubes at the axial mid-plane of the vortex tube. Flow was removed through 1.0-in.-dia thru-flow ports at the center of one or both end walls. Flow also was removed through 1/8-in.-wide annuli at the outer edges of both end walls (axial bypass) or through ports at the peripheral wall (peripheral bypass). The amount and radial distribution of simulated fuel contained in the vortex were determined using an axial light beam absorption technique.

The effects on containment of changes in the following were investigated: (1) the geometry of the simulated-fuel injection configurations, (2) the number of thru-flow ports used, (3) the radial Reynolds number (a measure of the amount of flow withdrawn through the thru-flow ports) and the corresponding amount of bypass flow, and (4) the molecular weight of the simulated fuel.

Reference 34

Douglas, F. C., R. Gagosz, and M. A. DeCrescente: Optical Absorption in Transparent Materials Following High-Temperature Reactor Irradiation. UARL Report F-910485-2, September 1967. Also issued as NASA CR-1031.

SUMMARY

An experimental investigation was conducted to determine the optical absorption levels induced in fused silica as a result of exposure to nuclear reactor irradiation over a range of fast neutron fluxes, fast neutron doses, and reactor temperatures. Also included in the investigation were a limited number of specimens made from alumina, hot-pressed beryllia, and single crystal beryllia. Measurements of the ultraviolet transmittance spectrum were made prior to the reactor irradiation, after the reactor irradiation, and after a series of cobalt-60 gamma irradiations. Measurements were also made during and after heat treatments at elevated temperatures. The induced absorption coefficients were determined from these measurements at the centers of absorption bands located at 0.215 and 0.163 microns.

Gagosz, R., J. Waters, F. C. Douglas, and M. A. DeCrescente: Optical Absorption in Fused Silica During TRIGA Reactor Pulse Irradiations. UARL Report F-910485-1, September 1967. Also issued as NASA CR-1032.

SUMMARY

An experimental investigation was conducted to determine the spectral transmission characteristics of fused silica before, during and after exposure to reactor irradiation pulses. The transmission measurements were carried out at three wavelengths (0.215, 0.625 and 1.0 microns) and at a range of temperatures from ambient to 900 C. Corning 7940 fused silica specimens in a corner cube configuration were mounted next to the reactor core face of the University of Illinois' TRIGA Mark II reactor. Peak neutron and gamma fluxes obtained from this reactor were approximately 5.4×10^{15} n/cm^2-sec and 6.1×10^{7} R/sec, respectively. Neutron and gamma doses associated with these pulses were 2.3×10^{14} n/cm^2 and 2.6×10^{6} R, respectively. The effective time of the pulse obtained by dividing the total dose by the peak flux was approximately 0.043 sec. The transmission measurements were made immediately before, during and after the reactor pulses to monitor both the creation of irradiation induced absorption and the decay of the induced absorption after the pulse.

Latham, T. S.: Nuclear Criticality Studies of Specific Nuclear Light Bulb and Open-Cycle Gaseous Nuclear Rocket Engines. UARL Report F-910375-2, September 1967.

SUMMARY

Analytical studies were conducted to determine the U-233 critical mass requirements for two specific vortex-stabilized gaseous nuclear rocket engines: a nuclear light bulb engine and an open-cycle engine. The specific open-cycle engine employs a single cylindrical cavity having both a length and a diameter of 6 ft. The specific nuclear light bulb engine employs seven separate cavities, each having a length of 6 ft; the total volume of all seven cavities approximately equals the volume of the single cavity of the open-cycle engine. The nuclear light bulb engine employs beryllium oxide between the unit cavities, layers of beryllium oxide and graphite surrounding the assembly of seven unit cavities, a relatively large amount of neutron-absorbing structural material in the end walls, seven separate exhaust nozzles, fuel and propellant injection ducts, and hot gases in the propellant and fuel regions. The open-cycle engine employs layers of beryllium oxide, graphite, and heavy water surrounding the cavity; various structural materials; an annular exhaust nozzle; fuel and propellant injection ducts; and hot gases in the propellant and fuel regions.

Studies were also made to determine the effect on criticality of various modifications to a reference configuration for each of the specific engines. For the nuclear light bulb engine, these included addition of impurities to the moderator materials, changes in the end-wall portions of the moderator, and changes in material and gas temperatures. For the open-cycle engine, these included changes in the nozzle-approach configuration, changes in the cavity liner materials, elimination of heavy water from the reflector-moderator, and substitution of hydrogen for helium in the moderator coolant circuit.

The analyses of the nuclear light bulb engine were made using 4-group two dimensional transport theory and 24-group one-dimensional transport theory. The analyses of the open-cycle engine were made using 4-group two-dimensional diffusion theory and 24-group one-dimensional diffusion and transport theories.

McLafferty, G. H. and H. E. Bauer: Studies of Specific Nuclear Light Bulb and Open-Cycle Vortex-Stabilized Gaseous Nuclear Rocket Engines. UARL Report F-910093-37, September 1967. Also issued as NASA CR-1030.

SUMMARY

Analytical studies were conducted to determine the characteristics of two specific vortex-stabilized gaseous nuclear rocket engines: a nuclear light bulb engine and an open-cycle engine. Both engines are based on the transfer of energy by thermal radiation from gaseous nuclear fuel suspended in a vortex to seeded hydrogen propellant. The two engines differ in that the nuclear light bulb engine employs an internally-cooled transparent wall to separate the fuel-containing vortex region from the propellant region, while the open-cycle engine relies entirely on fluid mechanics containment for preferential retention of the nuclear fuel. The majority of the work has been directed toward the nuclear light bulb engine, since recent fluid mechanics results indicate that the fuel retention characteristics of an open-cycle vortex-stabilized engine are insufficient to provide economic fuel containment. The nuclear light bulb engine offers the possibility of providing essentially perfect containment of the nuclear fuel.

One specific nuclear light bulb engine and one specific open-cycle engine have been selected for study. Both engines have a cavity volume of 170 cu ft. The open-cycle engine employs a single cavity having both a diameter and a length of 6 ft; the nuclear light bulb engine employs seven separate cavities, each having a length of 6 ft. The studies indicate approximate values of the thrust, weight, and specific impulse of both configurations. The studies have been made only in sufficient detail to provide information necessary for guidance of the research efforts which are being conducted to determine the feasibility of the engines.

The appendixes to the report describe: an analysis by the United Technology Center, a division of United Aircraft Corporation, of the weight of a filament-wound pressure vessel for a nuclear light bulb engine, and an analysis of the radiant energy emitted from the propellant stream of a nuclear light bulb engine.

Gagosz, R. M. and J. Waters: Optical Absorption and Fluorescence in Fused Silica During TRIGA Pulse Irradiation. UARL Report G-910485-3, April 1968. Also issued as NASA CR-1191.

SUMMARY

An experimental investigation was conducted at the University of Illinois' TRIGA Mark II pulse reactor to determine the spectral transmission characteristics during and after an irradiation pulse and to determine the cause of the apparent increase in transmission during the pulse and the apparent decrease of transmission after the pulse which had been observed in the previous test program. A total of 91 experiments were performed on six specimens at a range of temperatures from 500 to 900 C. Transmission measurements were made at two wavelengths, 2150 and 3021 Å. Corning 7940 fused silica specimens in a corner cube configuration were mounted next to the reactor core face at the internal end of a reactor beam port. Peak neutron and gamma fluxes obtained from this reactor were approximately 5.4×10^{15} n/cm^2-sec and 6.1×10^7 R/sec, respectively. Neutron and gamma doses associated with these pulses were 2.3×10^{14} n/cm^2 and 2.0×10^6 R, respectively. In addition to the transmittance tests, bypass and optical instrumentation tests were conducted to examine the influence of the optical alignment parameters upon system operation. Fluorescent tests were also conducted to obtain an applicable correction to the transmittance runs.

Johnson, B. V.: Experimental Study of Multi-Component Coaxial-Flow Jets in Short Chambers. UARL Report G-910091-16, April 1968. Also issued as NASA CR-1190.

SUMMARY

Fluid mechanics experiments were performed to obtain information applicable to an open-cycle, coaxial-flow, gaseous nuclear rocket engine. In this engine concept, gaseous nuclear fuel and a surrounding stream of seeded hydrogen propellant pass coaxially through a reactor chamber. The flow was simulated in the present experiments by multi-component, constant-temperature, coaxial-flow jets in short chambers. The flow was studied using flow visualization techniques and concentration measurements.

All tests were performed in 10-in.-dia chambers having lengths (from inlet plane to exhaust nozzle throat) between 7.5 and 12.5 in. The following flow and geometric variables were investigated: (1) an intermediate-velocity buffer stream between the high-velocity outer-stream (simulated propellant) and the low-velocity inner jet (simulated fuel), (2) the ratio of average outer-stream and buffer-stream velocity to inner-jet velocity, (3) the absolute inlet velocities of the outer stream, buffer stream and inner jet, (4) the ratio of inner-jet gas density to outer-stream and buffer-stream gas density, (5) the ratios of buffer-gas density to outer-stream gas density and to inner-jet gas density, (6) the ratios of inner-jet inlet radius and buffer-stream inlet radius to chamber radius, (7) the ratio of chamber length to diameter, and (8) the ratio of exhaust nozzle throat diameter to chamber diameter. Air was used as the outer-stream gas; air and Freon-11 were used as buffer-stream gases; and air, Freon-11 and FC-77 were used as inner-jet gases. The tests were conducted at Reynolds numbers up to those expected for a full-scale engine.

The results indicate that the containment of inner-jet gas is strongly affected by the occurrence of recirculation or reverse flow in the inner-jet region. For a high ratio of average outer-stream and buffer-stream inlet velocity to inner-jet inlet velocity, the flow reciruclates behind the inner jet like flow behind a bluff body, and the containment is poor. For flow conditions with moderate values of this velocity ratio (on the order of 20), a reduced level of turbulent mixing occurs between the outer stream, buffer stream and inner jet, and the inner-jet core extends to the exhaust nozzle; under these conditions, the amount of inner-jet gas contained approached the amount that would be contained in a cylinder of radius equal to the inner-jet inlet radius and length equal to the chamber length.

Kendall, J. S., W. C. Roman, and P. G. Vogt: Initial Radio-Frequency Gas Heating Experiments to Simulate the Thermal Environment in a Nuclear Light Bulb Reactor. UARL Report G-910091-17, September 1968. Also issued as NASA CR-1311.

SUMMARY

Initial experiments were conducted to develop an intense radiant energy source which would eventually be capable of producing radiant energy fluxes equal to those expected in a full-scale nuclear light bulb engine. The test program was conducted using the UARL 1.2-megw r-f induction heater at d-c input power levels up to approximately 250 kw to supply energy to the simulated fuel-containment region of a vortex. The primary objective of the experimental program was to determine the effect of various parameters on the power radiated from the vortex, the power deposited in the peripheral wall of the vortex tube, and the power carried away by convection from the vortex. Both argon discharges with no seed and argon discharges seeded with submicron carbon and tungsten particles were employed. Tests were conducted at discharge pressures up to 6.0 atm abs and with up to 85 kw of power deposited in the discharge; of this, 35 kw was radiated through a water-cooled transparent wall surrounding the discharge. The 35 kw of radiant energy represents a radiant energy flux of about 12.0 kw/in.^{2} (1.86 kw/cm^2), which corresponds to an equivalent black-body radiating temperature of 7600 R. For comparison, the design radiant flux level at the edge of the fuel-containment region of a representative nuclear light bulb engine is 178 kw/in.^{2}, which corresponds to an equivalent black-body radiating temperature of 15,000 R.

A second objective of the investigation was to design, fabricate, and test thin, internally-cooled transparent-wall models. Several different types of models were tested around the radiant energy source. Additional supporting research was conducted using the UARL 80-kw r-f induction heater, the two-component isothermal gas vortex test facility, and various small water vortex models. This supporting research is described in the appendixes of the report.

Mensing, A. E., and L. R. Boedeker: Theoretical Investigation of R-F Induction Heated Plasmas. UARL Report G-910091-18, September 1968. Also issued as NASA CR-1312.

SUMMARY

Theoretical analyses were made to investigate the power deposition and energy removal in radio-frequency induction heated plasmas. These investigations were directed toward the high-power, high-pressure, radiating r-f plasmas that are being used to simulate the thermal environment of the nuclear light bulb reactor.

Two related investigations are described in this report. In one, the power deposition and energy dissipation characteristics of infinite-cylinder r-f heated argon plasmas at pressures of 1.0 and 10 atm were studied. It was assumed that the thermal and electrical conductivities varied with temperature, that the gas radiation per unit volume varied with both temperature and pressure, and that the plasma was optically thin. The electromagnetic field equations, energy equation, and heat conduction equation were integrated numerically starting with specified values of temperature and axial magnetic field at the centerline. Generalized curves suitable for design and analysis of experiments were constructed. These curves show the relationships between the radius of the plasma, the axial magnetic field external to the plasma, the power radiated, and the radiation efficiency (the power radiated divided by the sum of the power radiated and the power conducted away from the plasma). The results also show the importance of gas radiation on the characteristics of the plasmas.

In the second investigation, the coupling between the plasma discharge and the r-f generator was studied using an infinite-cylinder, constant-conductivity model. Analyses performed by other investigators were combined and extended to develop an analysis more useful in the nuclear light bulb reactor simulation program. The analysis was used to investigate the effects of discharge power, reactive power, and discharge size on the surface radiation heat flux and to examine the effect of r-f frequency shifts on matching. In addition, an expression was derived from which the magnetic pressure at the center of an r-f discharge can be calculated.

Krascella, N. L.: Theoretical Investigation of the Composition and Line Emission Characteristics of Argon-Tungsten and Argon-Uranium Plasmas. UARL Report G-910092-10, September 1968. Also issued as NASA CR-1313.

SUMMARY

A theoretical investigation was conducted to determine the composition and integrated line emission characteristics of various ionization species of tungsten, uranium, and argon. The study was made to facilitate radiant heat transfer analysis in the seeded propellant and nuclear fuel regions of gaseous-core nuclear rocket engines and to provide a basis of comparison for a concurrent experimental program designed to examine line emission characteristics of gaseous tungsten and uranium over a wide spectral range.

Estimates were made of the composition as a function of temperature for mixtures of Ar with tungsten hexafluoride and uranium hexafluoride using an existing UARL machine composition program to ascertain the decomposition products of WF_6 and UF_6. For temperatures greater than 5000 K, a machine program was written to describe the concentrations of heavy-metal ionization species present based on the Saha equations. Calculations were made for mass ratios of W or U to Ar of 1.0×10^{-3}, 1.0×10^{-5}, and 1.0×10^{-7} for a total pressure of 1.0 atm and for temperatures in the range from 3000 to 10,000 K.

Data generated with the composition routines were used as input to a line intensity machine program designed to compute the integrated line intensities for classified W, U, and Ar spectral lines of known or estimated oscillator strength. Lines from two ionization species of Ar (neutral argon and singly ionized argon) as well as the corresponding species in W and U were considered in the line intensity program. Integrated line intensities summed over wavelength intervals of 100 Å were calculated in the spectral region between wavelengths of 1700 and 10,000 Å. W-to-Ar or U-to-Ar mass ratios of 1.0×10^{-3}, 1.0×10^{-5}, and 1.0×10^{-7} were considered at temperatures of 5000, 7000, and 9000 K. The total pressure in all cases was 1.0 atm.

Marteney, P. J., A. E. Mensing, and N. L. Krascella: Experimental Investigation of the Spectral Emission Characteristics of Argon-Tungsten and Argon-Uranium Induction Heated Plasmas. UARL Report G-910092-11, September 1968. Also issued as NASA CR-1314.

SUMMARY

An experimental study was conducted to determine the emission characteristics of gaseous tungsten and uranium located in an rf induction-heated, vortex-stabilized argon discharge. The tungsten and uranium were introduced into the discharge in the form of tungsten hexafluoride or uranium hexafluoride at heavy-atom to argon mass ratios of approximately 1.0×10^{-4} and a total pressure of one atmosphere.

Temperatures in the heavy-atom seeded discharges were determined to be approximately 8500 deg K, and were ascertained by measuring neutral argon atom relative line intensity ratios by the Boltzmann method. Temperatures determined by this method were confirmed by measurements of absolute neutral argon atom line intensities and absolute argon ion continuum intensities.

Spectra were obtained for pure argon, tungsten hexafluoride-argon, and uranium hexafluoride-argon systems in the wavelength region from 1250 Å (0.125 micron) to 100,000 Å (10 micron). The experimental data were reduced to obtain integrated continuum and line intensities over intervals of 100 Å for pure argon. Integrated line intensities were obtained over wavelength intervals of 100 Å for tungsten and uranium after correcting the experimental results for the contribution to total intensity due to argon continuum and lines.

Experimental integrated line intensities over 100 Å wavelength intervals for argon, tungsten and uranium were subsequently compared to similar analytical results calculated for the visible region of the spectrum (2000 Å to 10,000 Å). The correlation between experimental and analytical results for tungsten was generally poor, particularly at wavelengths less than approximately 4000 Å, although fairly poor agreement was noted between 4000 Å and 6000 Å. The correlation between experimental and analytical results for uranium is somewhat better than that for tungsten, and is best in the region between approximately 2000 Å and 4000 Å. The agreement between experimental and analytical results for argon is excellent in all wavelength intervals of comparison.

Latham, T. S.: Nuclear Studies of the Nuclear Light Bulb Rocket Engine. UARL Report.G-910375-3, September 1968. Also issued as NASA CR-1315.

SUMMARY

Analytical studies were conducted to determine U-233 critical mass requirements, neutron kinetic behavior, and neutron and gamma ray heating rates for the nuclear light bulb rocket engine. The nuclear light bulb is a multiple-cavity gaseous nuclear rocket engine in which energy is transferred by thermal radiation from gaseous nuclear fuel through internally cooled transparent walls to seeded hydrogen propellant. The engine considered in this report employs seven separate cavities, each having a length of 6 ft and an average diameter of 2.3 ft. Beryllium oxide is employed between the unit cavities, and layers of BeO and graphite surround the seven units to provide neutron reflection.

The criticality analysis allowed the effects of engine design changes on critical mass to be investigated. Among the factors that were varied were the total moderator mass, the amount of BeO between unit cavities, the distribution of moderator mass, the amount of tungsten seed in the hydrogen propellant, and the amount of hafnium required to shield the fuel injection and recirculation system ducts. The analysis also considered factors affecting the kinetic behavior of a nuclear light bulb engine. The effects of variations in fuel region radius, mixed-mean propellant temperature, nominal system operating temperature, system operating pressure, and the proportion by weight of tungsten seed in the hydrogen propellant were investigated. For one specific nuclear light bulb engine configuration, prompt neutron lifetime was calculated, and comparisons of critical masses were made for U-233, U-235, and Pu-239.

Neutron kinetic equations were formulated which allowed for variable loss rates of both nuclear fuel and delayed neutron precursors. Power level responses to step, ramp, and oscillatory variations in both reactivity and fuel loss rate were obtained.

Neutron and gamma ray heating rates were calculated for a specific nuclear light bulb engine to provide information on requirements for cooling engine components and the location and design of heat exchangers. Radiation dose rates in the transparent wall materials were calculated and compared with the dose rates of various test reactors. Dosages in the filament-wound fiberglass pressure vessel were also calculated to evaluate the potential for degradation of pressure vessel strength due to radiation damage.

Roman, W. C., J. F. Klein, and P. G. Vogt: Experimental Investigations to Simulate the Thermal Environment, Transparent Walls and Propellant Heating in a Nuclear Light Bulb Engine. UARL Report H-910091-19, September 1969. To be issued as NASA CR report.

SUMMARY

Experiments were conducted to develop an intense radiant energy source capable of producing radiant energy fluxes within the range expected in nuclear light bulb engines. Concurrently, small-scale internally cooled fused silica models similar to the transparent walls proposed for the engine were developed and tested. Experiments to demonstrate heating of a seeded simulated propellant by thermal radiation passing through the transparent wall were also initiated.

The major portion of the test program was conducted using the UARL 1.2-megw radio-frequency induction heater at d-c input power levels up to approximately 600 kw. R-F energy was supplied to an argon plasma within a radial-inflow vortex. The effects of several important parameters on the power radiated from the plasma, the power deposited in the surrounding water-cooled transparent peripheral wall, and the power carried away from the vortex by convection were investigated. Tests were conducted with argon at pressures up to 16 atm and with up to 216 kw of power deposited in the steady-state plasma discharge. A maximum of 156 kw was radiated through a 2.24-in. inside diameter water-cooled transparent peripheral wall. The maximum radiant energy flux at the edge of the plasma was 36.7 kw/in.^{2}, which corresponds to an equivalent black-body radiating temperature of 10,200 R. For reference, the range of edge-of-fuel radiant energy fluxes of interest for full-scale nuclear light bulb engines is from 177.8 kw/in.^{2} for a reference engine to 14.4 kw/in.^{2} for a derated engine; the corresponding equivalent black-body radiating temperatures are 15,000 R and 8000 R, respectively.

Transparent-wall models having multiple axial coolant tubes up to 10 in. long and peripheral-wall vortex injection were fabricated and tested in the 1.2-megw r-f induction heater. These models, with inside diameters of 1.26 and 0.95 in., were constructed from many individual tubes having internal diameters of 0.040 in. and wall thicknesses down to 0.005 in., the estimated thickness required in the full-scale engine. One of these models was tested at power levels up to 55 kw; higher power levels resulted in localized melting of the argon-cooled vortex injectors.

Both the UARL 1.2-megw r-f induction heater and the d-c arc heater were used in the propellant heating tests. The propellant heating configurations used were generally similar to the geometries of the components expected to be employed in the nuclear light bulb engine. Argon seeded with micron-sized carbon particles was used as the simulated propellant. At the low radiant energy source power levels of up

to 3 kw that were used in these initial tests, temperature rises up to 223 R were obtained. Further increases in simulated propellant temperature rise will be obtained primarily by means of increased power, improved particle deagglomeration to increase absorption, and more effective buffer layers to reduce the coating of particles on the transparent walls.

Reference 46

Mensing, A. E., and J. F. Jaminet: Experimental Investigations of Heavy-Gas Containment in R-F Heated and Unheated Two-Component Vortexes. UARL Report H-910091-20, September 1969. To be issued as NASA CR report.

SUMMARY

Experimental investigations were conducted in which the amount of heavy gas contained in light-gas vortexes was measured for both heated and unheated (isothermal) vortex flows. In the vortex flows with heat addition, power was added to the flow by r-f induction heating of the gas within the vortex chamber. The light gas, argon, was injected in a tangential direction either from the end walls or from the peripheral wall of the vortex chamber. The vortex flow rates, plasma diameter, and power addition were such as to provide a radial gradient of temperature of approximately 50,000 deg K/in. near the outer edge of the plasma. Xenon was employed as the heavy gas and was injected into the vortex at several different locations. Spectroscopic techniques were used to determine both the temperature distribution and the xenon partial pressures within the plasma.

Tests conducted with unheated vortex flows employed a vortex tube much larger than, but geometrically similar to, the vortex tube used in the heated tests. Air was used as the light gas and mixtures of iodine with helium, nitrogen or sulfur hexafluoride were used as heavy gases. Several different heavy- and light-gas injection configurations were used, and the weight flow rates of both the heavy and light gases were varied. The volume-averaged partial pressures of the heavy gas within the vortexes were determined, as were the radial distributions of the heavy-gas partial pressure.

Comparisons were made of the heavy-gas partial pressures in the heated and unheated flows. For similar geometries and the same light-gas weight flows, the heated vortexes had larger values of the heavy-gas partial pressure in the central regions of the vortex, but less heavy-gas partial pressure at the greater radii. Under the same conditions, the volume averaged heavy-gas partial pressures were about equal in both heated and unheated flows. Radial gradients of static pressure in the heated vortexes were much less than in unheated vortexes having the same flow rates.

Krascella, N. L.: Theoretical Investigation of the Radiant Emission Spectrum from the Fuel Region of a Nuclear Light Bulb Engine. United Aircraft Research Laboratories Report H-910092-12, September 1969. To be issued as NASA CR report.

SUMMARY

A theoretical investigation was conducted to determine the spectral emission characteristics of the fuel region of a nuclear light bulb engine and hence the spectral radiative flux incident upon the transparent containment walls or upon the reflective end walls of such an engine. The analysis was performed for a specified engine configuration and for a specific nuclear fuel partial pressure distribution. Estimates of the spectral radiative flux emanating from the nuclear fuel region were made for a total radiated flux of 24,300 Btu/ft^2-sec (2.757 x 10^{11} erg/cm^2-sec), which corresponds to an effective black-body radiating temperature of 15,000 R (8333 K).

Six cases were considered in which the effects of changes in the heavy-atom absorption coefficient model parameters, the addition of a seeding gas, and changes in end-wall reflectivities on the spectral radiative flux emitted from the nuclear fuel region were examined. Three cases involved parametric variations of the heavy-atom model in either the fuel species ionization potentials or in the oscillator strength distribution functions describing line transitions. In the fourth case, the effect of hydrogen as a seed gas on the emitted spectral radiative flux was studied. The effect on the emitted flux of a uniform end-wall spectral reflectivity of 0.5 was examined in the fifth case; similar calculations were made in the sixth case using the spectral reflectivity of aluminum.

Latham, T. S., H. E. Bauer, and R. J. Rodgers: Studies of Nuclear Light Bulb Start-up Conditions and Engine Dynamics. UARL Report H-910375-4, September 1969. To be issued as NASA CR report.

SUMMARY

Analytical studies were conducted to determine the operating conditions of a nuclear light bulb engine during start-up and the transient response of the engine to various perturbations at the nominal full-power operating level. The basic nuclear light bulb engine design was refined, where necessary, to include modifications which resulted from recent criticality studies and test program results.

The start-up study was performed using a simplified analytical model of the basic engine. Three linear power ramps were used and the general engine response, auxiliary power requirements and thermal stress levels were investigated. The calculated responses in temperature and pressure were similar for all of the power ramps. It appears that there will be no major problems with engine control or with excessive thermal stress levels during start-up. Some type of auxiliary power will be required for the turbopump unit during start-up.

Finite-difference approximations to the time-dependent thermal, fluid dynamics and neutron kinetics equations were used to describe the operating characteristics of the engine. These equations were programmed on a UNIVAC 1108 digital computer to construct a dynamic simulation for predicting the response of the engine to selected perturbations occurring at the nominal full-power operating condition. A preliminary transient analysis was performed using the model, which simulates an uncontrolled engine, to determine the basic stability characteristics and to identify the parameters which would provide the most effective control mechanisms. Responses to perturbations in the uncontrolled system can be characterized by either steady-state or damped oscillations with a characteristic frequency of about 1 cycle/sec. It was concluded that control of the engine could be achieved primarily by control of fuel injection rate.

Reference 49

Johnson, B. V.: Exploratory Experimental Study of the Effects of Inlet Conditions on the Flow and Containment Characteristics of Coaxial Flows. UARL Report H-910091-21, September 1969. To be issued as NASA CR report.

SUMMARY

Fluid mechanics experiments were performed to investigate the factors which influence the formation and growth of the large eddy structure in developing coaxial shear flows. Information from these experiments was used to develop inlet configurations and inlet flow conditions in order to improve containment of the inner-jet gas for application to the open-cycle gaseous-core nuclear rockets and to improve film cooling flow characteristics for application to closed-cycle nuclear light bulb rockets.

The tests were performed in a 10-in.-dia chamber with lengths of 10 in. and 30 in. The inlet to the chamber had provision for two- or three-stream operation. Air or Freon-11 was used for the inner-jet gas, and air was used for the buffer-stream gas (if used) and outer-stream gas. Flow visualization was obtained by coloring the inner-jet gas with iodine gas and photographing the flow with high-speed motion pictures. Hot-wire and pitot probes were used to obtain average and fluctuating velocity data in the chamber. Film-cooling flow visualization tests were also performed with a 5-in.-dia cylinder in the center of the 10-in.-dia chamber.

The results from these tests indicate that the large eddies, characteristic of the interface between coaxial flows, could be essentially eliminated for flows in short chambers. This was done by decreasing the velocity gradient between the two streams at the coaxial-flow inlet so that any disturbances in the system would be convected from the chamber before developing into large waves or eddies. The best apparent inner-jet gas containment obtained with a modified inlet configuration in the short chamber was better than was obtained from previous tests. Tests with the centerbody and 30-in.-length configuration indicated that the disturbances from both the inlet and the exhaust systems need to be damped to prevent noticeable waves from forming in the chamber and developing into eddies.

Palma, G. E. and R. M. Gagosz: Measurement of Optical Transmission During Reactor Irradiation. UARL Report H-930709-1, October 1969. To be issued as NASA CR report.

SUMMARY

In situ optical experiments were conducted to determine the level of irradiation-induced optical absorption that exists in Corning Grade 7940 fused silica at elevated temperatures during 1.5-Mev electron irradiation and during nuclear reactor irradiation. The optical absorption was measured at the peak of the strong irradiation-induced absorption band in fused silica centered at 2150 Å over a range of specimen temperatures from 170 to 900 C. Several additional measurements were made at longer wavelengths (2700 and 4500 Å) to investigate the width of the absorption band and to check the absorption where strong absorption bands are not expected to exist.

The electron irradiation experiments were conducted at the NASA Langley Research Center using a Dynamitron electron accelerator as a source of 1.5 Mev electrons. The accelerator provided current densities in the range 20 to 150 microamp/cm^2 corresponding to estimated ionizing dose rates of 2.7 to 20 x 10^6 R/sec deposited in the specimen. The induced absorption and specimen temperature were measured before, during, and after the irradiation and transient, as well as steady state, data were obtained. The nominal irradiation time for the electron irradiation experiments was 1000 sec.

The reactor irradiation experiments were conducted at the Air Force Institute of Technology using a 10 megw, swimming pool reactor as a source of fast neutrons and gamma rays. The fast neutron flux ($E > 0.75$ Mev) and ionizing dose rate at full power were 1.7 x $10^{12}/cm^2$-sec and 0.02 x 10^6 R/sec, respectively, at the location of the specimen. The induced absorption was measured during the irradiation at constant reactor power and specimen temperature in order to obtain equilibrium values. The nominal irradiation time for the reactor experiments was 3.5 x 10^5 sec.

TABLE I

TOPICS COVERED IN REPORTS FROM
UARL AND OTHER AGENCIES

References	Referenced Reports Contain Information on Following Subjects				
	Vortex Fluid Mechanics	Coaxial Fluid Mechanics	Opacity and Radiant Heat Transfer	Radiation Damage to Transparent Material	Engine Design
Reports issued under Contract NASw-847 (Refs. 1 - 50)	1-4, 10-15, 28-33, 40-42, 45, 46	38, 49	5-7, 12, 16-19, 22-24, 42, 43, 47	34, 35, 39, 50	8, 9, 20, 21, 25-27, 31, 36, 37, 44, 48
Other United Aircraft Research Laboratories Reports (Refs. 51 - 97)	53-56, 58-64, 68-70, 74, 77, 79-81, 83, 84, 94, 95	93	51, 52, 56, 57, 61, 65-67, 71, 75, 85, 88, 89	72, 90-92	70, 72, 73, 76-78, 82, 84, 86, 87, 96, 97
NASA Lewis Research Center Reports (Refs. 98 - 136)	98, 100	99, 101-121	99, 101, 103, 111, 114, 122-131	132	98, 99, 101, 103, 111, 114, 133-136
Reports from other agencies (Refs. 137 - 235)	137-163	164-177	178-185	186-192	141, 143, 145, 153, 191, 193-235

FIG. 1

SKETCHES ILLUSTRATING PRINCIPLE OF OPERATION OF NUCLEAR LIGHT BULB ENGINE

a) OVERALL CONFIGURATION

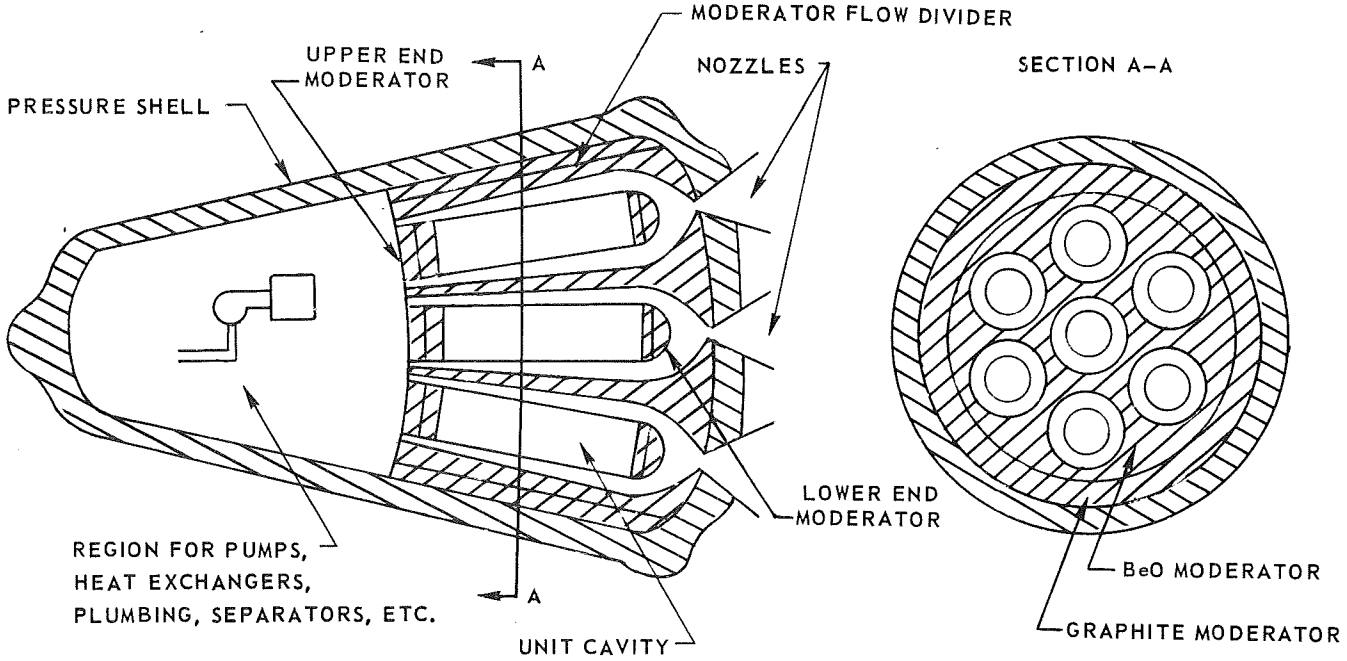

b) CONFIGURATION OF UNIT CAVITY

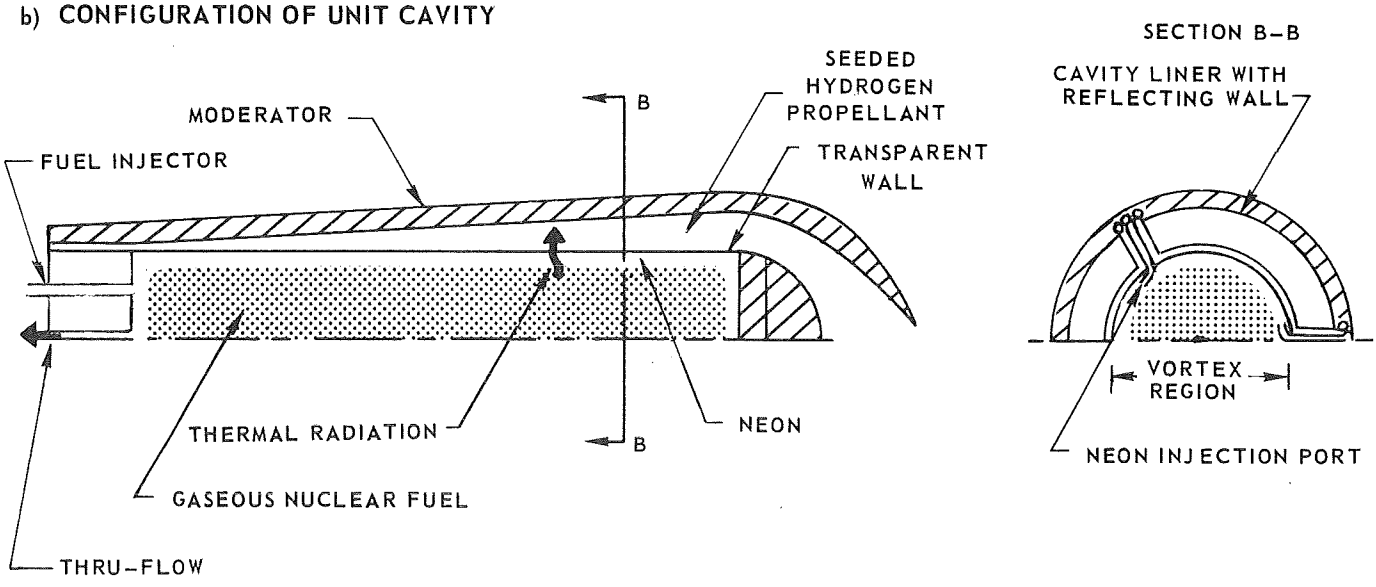

DIMENSIONS OF UNIT CAVITY IN REFERENCE NUCLEAR LIGHT BULB ENGINE

COMPLETE ENGINE COMPOSED OF SEVEN UNIT CAVITIES

ALL DIMENSIONS IN FT

VOLUME OF UNIT CAVITY = $\frac{\pi}{2}((0.911)^2 + (1.32)^2)\ (6.0) = 24.2\ FT^3$

VOLUME WITHIN UNIT VORTEX = $\pi\ (0.802)^2\ (6.0) = 12.1\ FT^3$

FLOW CONDITIONS GIVEN IN FIG. 3

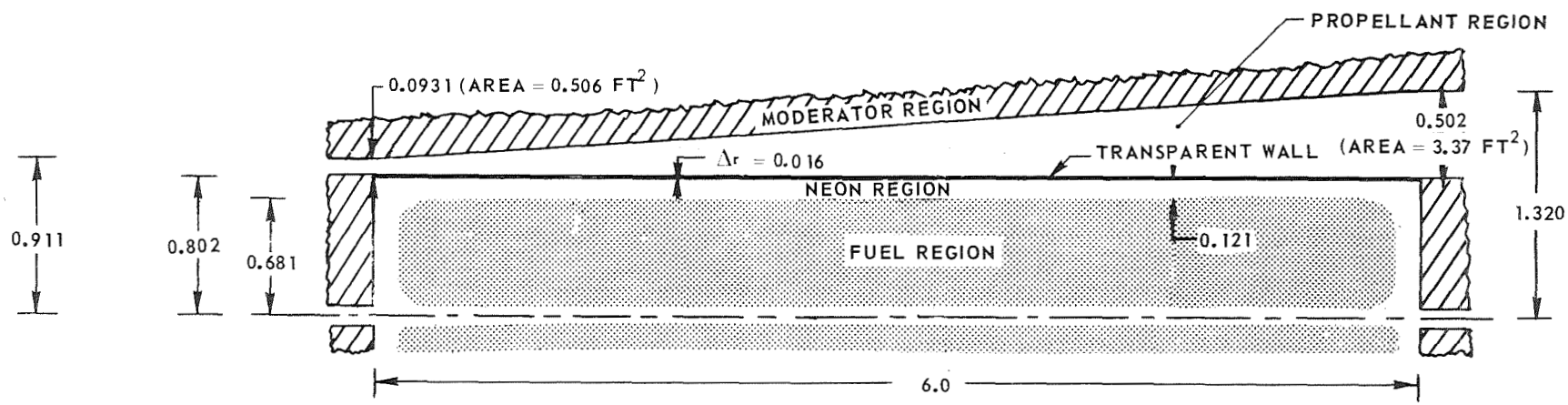

FIG. 2

FLOW CONDITIONS IN UNIT CAVITY OF REFERENCE NUCLEAR LIGHT BULB ENGINE

PRESSURE = 500 ATM

DIMENSIONS GIVEN IN FIG. 2

FLOW RATES THROUGH EACH UNIT:
HYDROGEN – 6.04 LB/SEC
NEON – 2.96 LB/SEC
FUEL – 0.19 LB/SEC

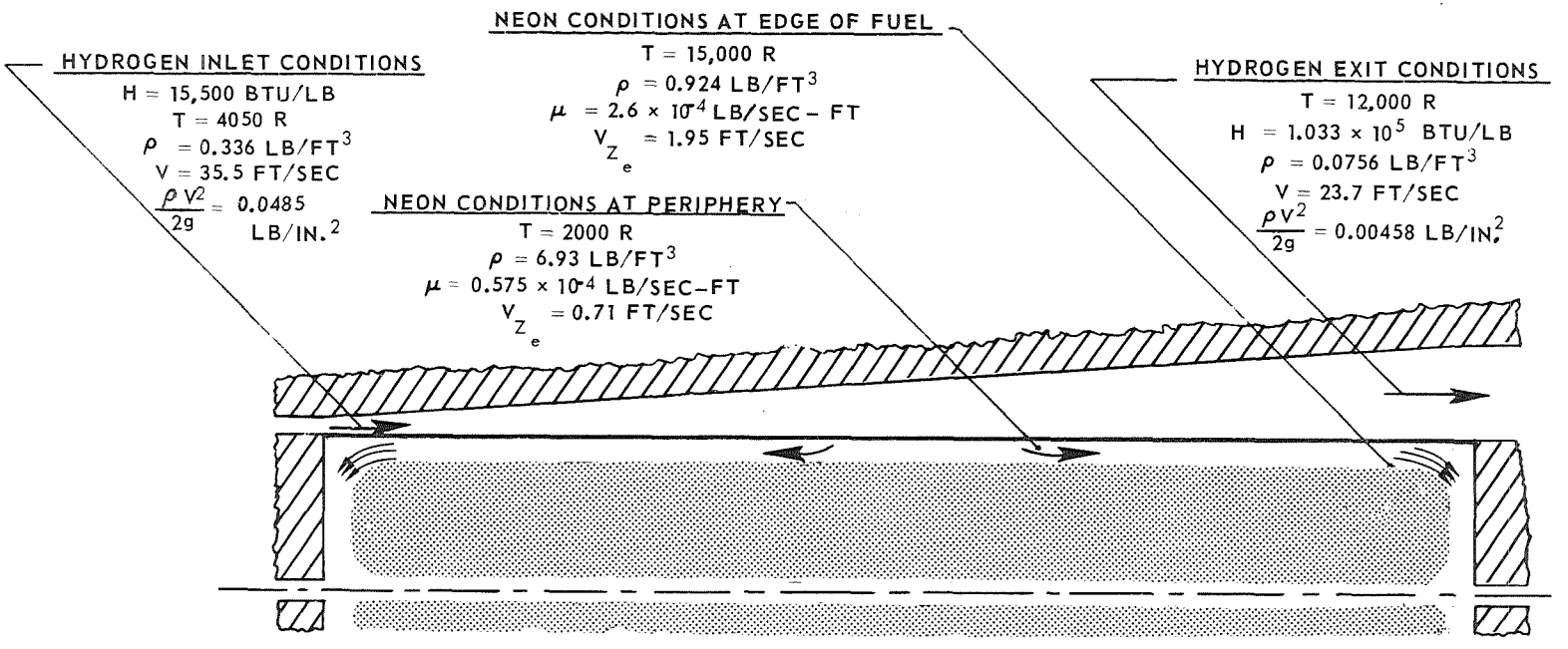

FIG. 3

FIG. 4

SIDE VIEW OF REFERENCE NUCLEAR LIGHT BULB ENGINE CONFIGURATION

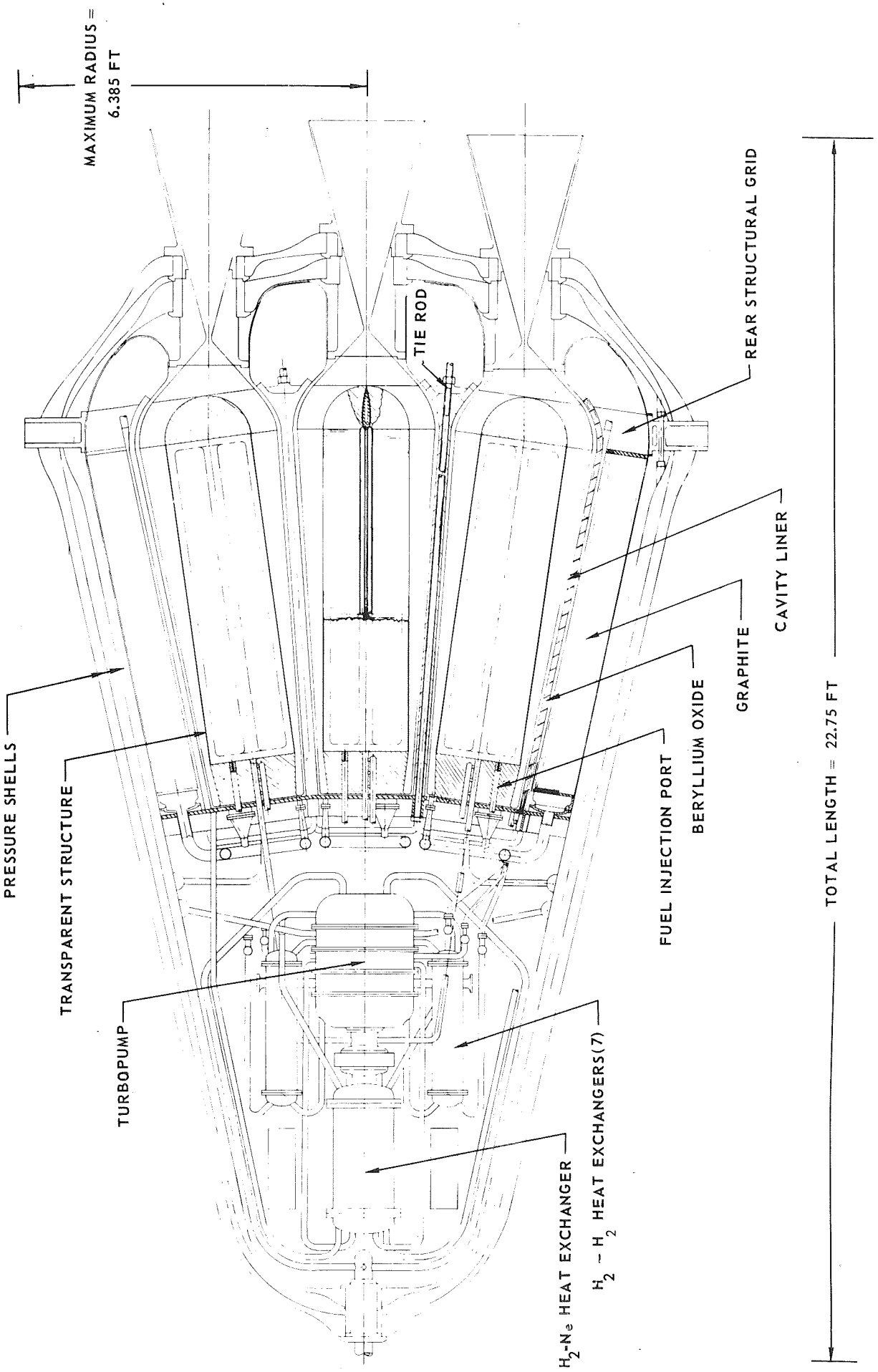

FIG. 5

EFFECT OF PROPELLANT HEATING MECHANISM AND PROPELLANT INLET TEMPERATURE ON SPECIFIC IMPULSE

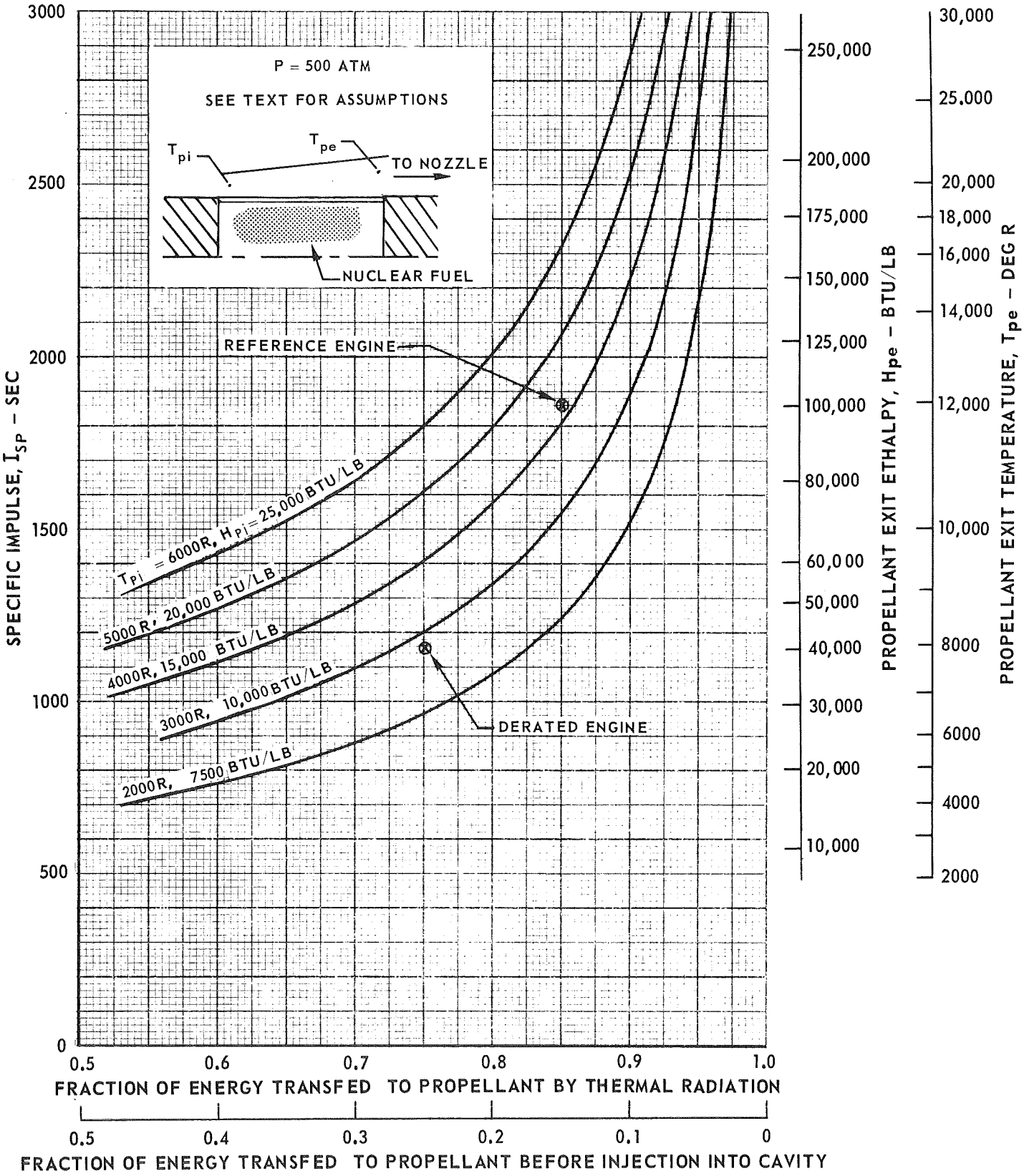

PHOTOGRAPHS OF DYE PATTERNS IN RADIAL - INFLOW WATER VORTEXES

PHOTOGRAPHS FROM REF. 13 TAKEN AT INDICATED TIMES AFTER CESSATION OF DYE INJECTION THROUGH END WALLS

SINGLE-SLOT INJECTION - 3.0 MIN

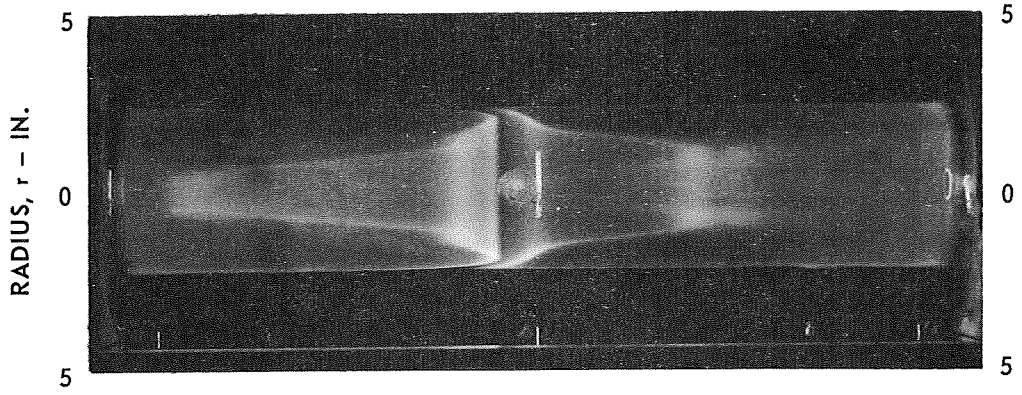

2144 - PORT INJ ECTION - 3.0 MIN

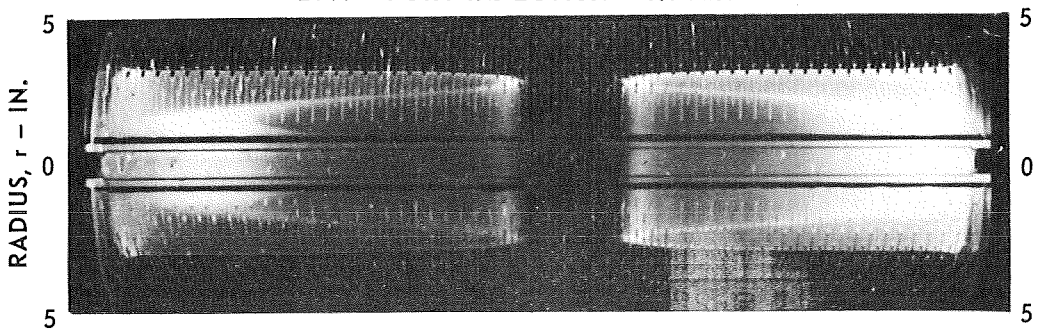

FIG. 7

EFFECT OF SIMULATED-FUEL DENSITY AT INJECTION ON THE RADIAL DISTRIBUTION OF SIMULATED-FUEL PARTIAL PRESSURE IN AN AIR VORTEX

DATA FROM REF. 31

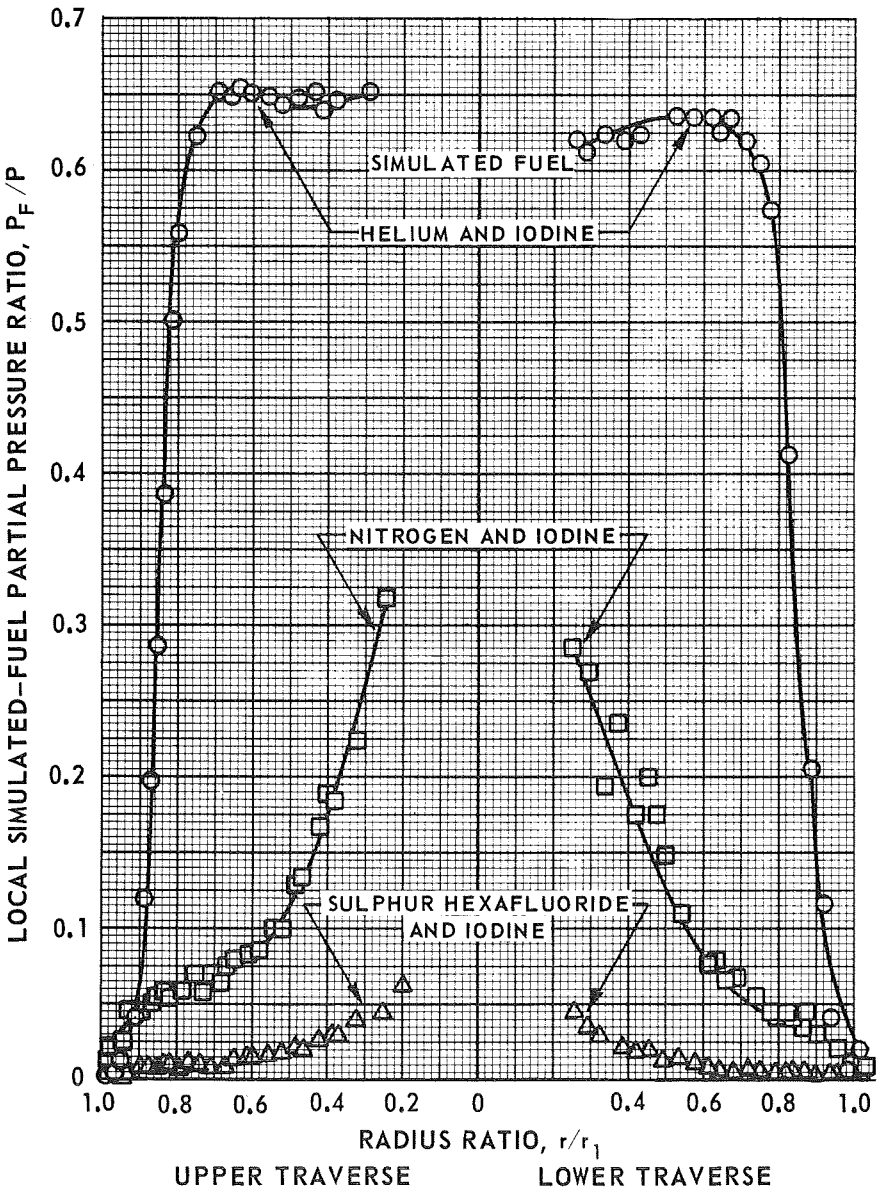

FIG. 8

SKETCH OF END WALLS AND R-F PLASMA DISCHARGE SHOWING POWER LOSSES FOR HIGHEST POWER OPERATING POINT

1.2-MEGW R-F INDUCTION HEATER
DATA FROM REF. 45

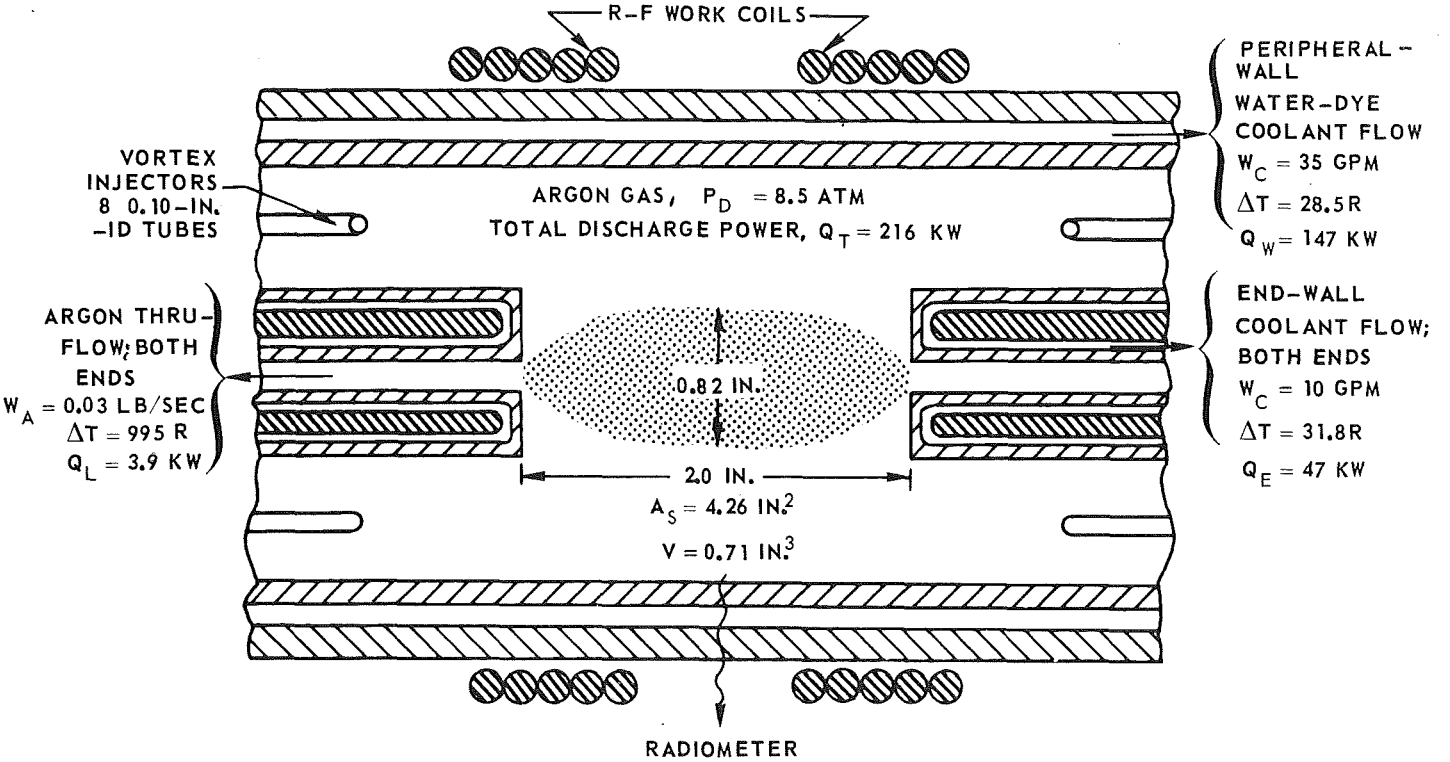

READING = 2.09×10^3 MV

$Q_R = (8.6 \times 10^{-3}$ KW/MV) $(2.09 \times 10^3$ MV) = 18 KW

TOTAL D-C INPUT POWER, Q_I = 600 KW AT 5.51 MHz

TOTAL DISCHARGE POWER, $Q_T = 147 + 47 + 3.9 + 18 = 216$ KW

R-F SYSTEM COUPLING EFFICIENCY, $\eta = 216/600 = 36\%$

PROBABLE MAXIMUM POWER CONDUCTED THROUGH PERIPHERAL WALL, Q_C = 9.0 KW (SEE REF. 45)

TOTAL POWER RADIATED THROUGH INNER PERIPHERAL WALL, $Q_{R,T} = 147 - 9 + 18 = 156$ KW

$\phi_R = Q_{R,T}/A_S = 156/4.26 = 36.7$ KW/IN.^{2} ($T^* = 10{,}200$ R)

FRACTION OF DISCHARGE POWER RADIATED THROUGH INNER PERIPHERAL WALL

$Q_{R,T}/Q_T = 156/216 = 0.72$

VARIATION OF RADIANT ENERGY FLUX WITH TOTAL R-F DISCHARGE POWER

1.2-MEGW R-F INDUCTION HEATER
RANGE OF CHAMBER PRESSURE, P_D = 2 TO 16 ATM
RANGE OF ARGON WEIGHT FLOW, W_A = 0.010 TO 0.041 LB/SEC
DATA FROM REF. 45

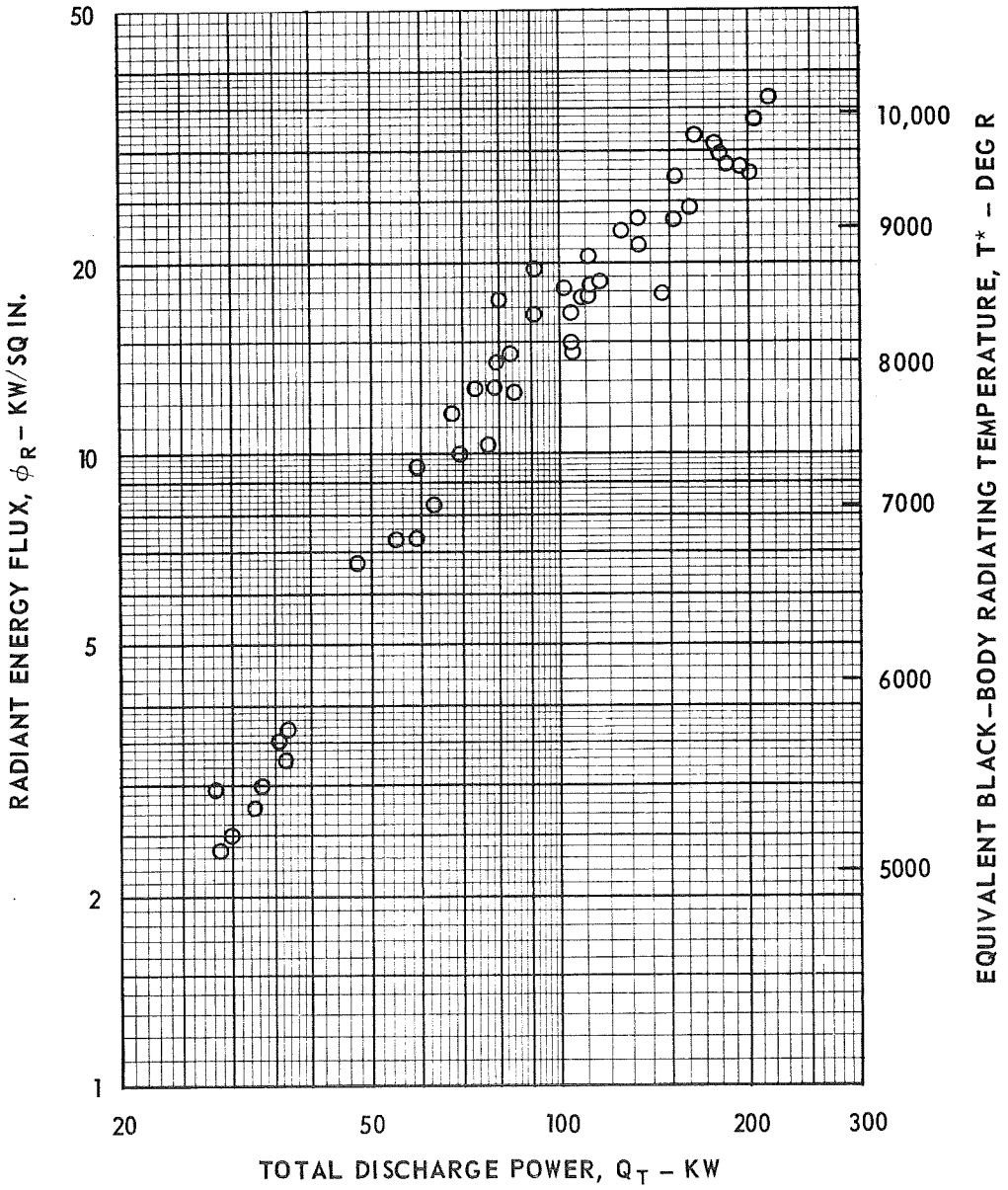

FIG. 10

PHOTOGRAPHS OF TRANSPARENT-WALL AXIAL COOLANT-TUBE MODELS EMPLOYED IN R-F PLASMA TESTS

MODELS EMPLOYED IN TESTS DESCRIBED IN REF. 45

a) DETAILS OF 1.26-IN.-ID MODEL

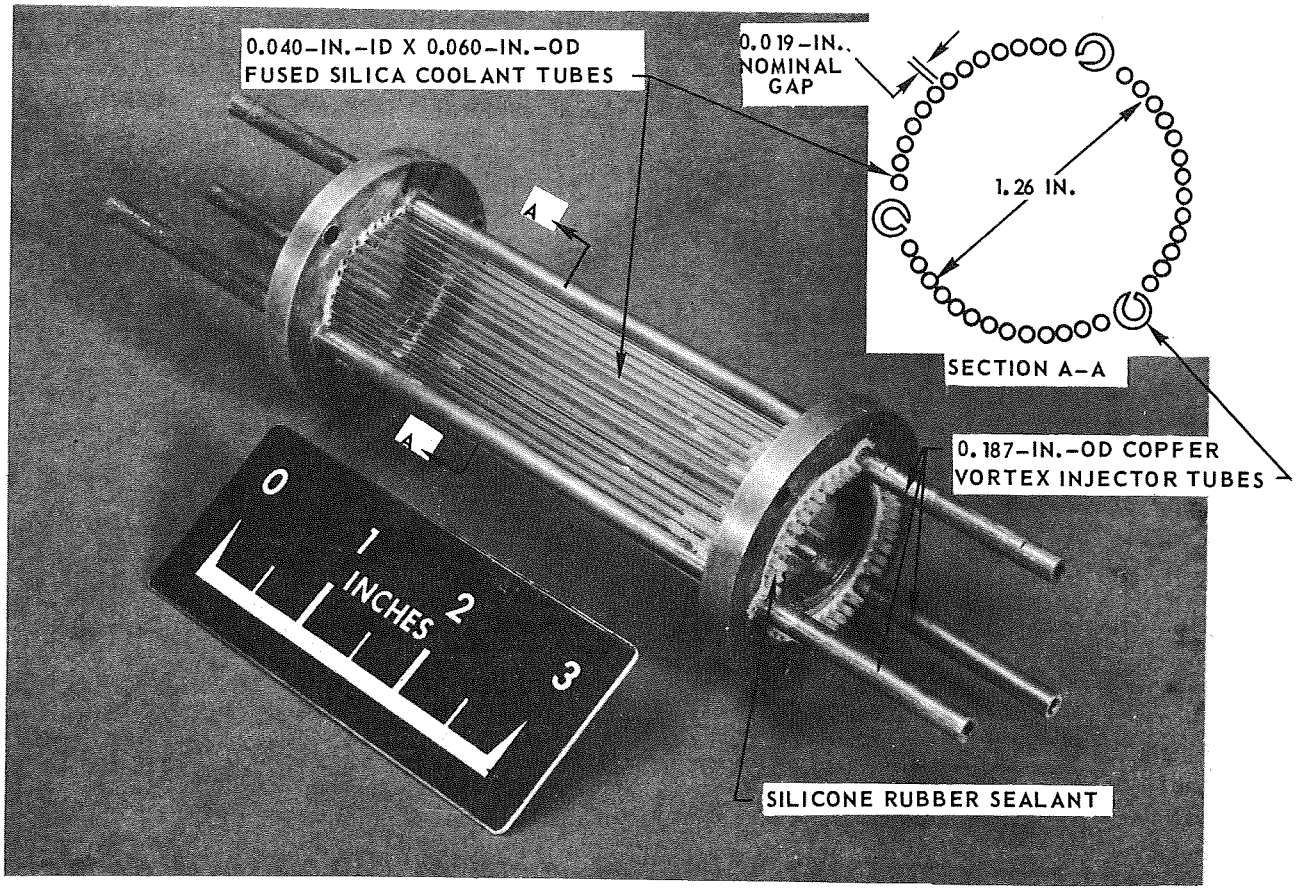

b) DETAILS OF 0.95-IN.-ID MODEL

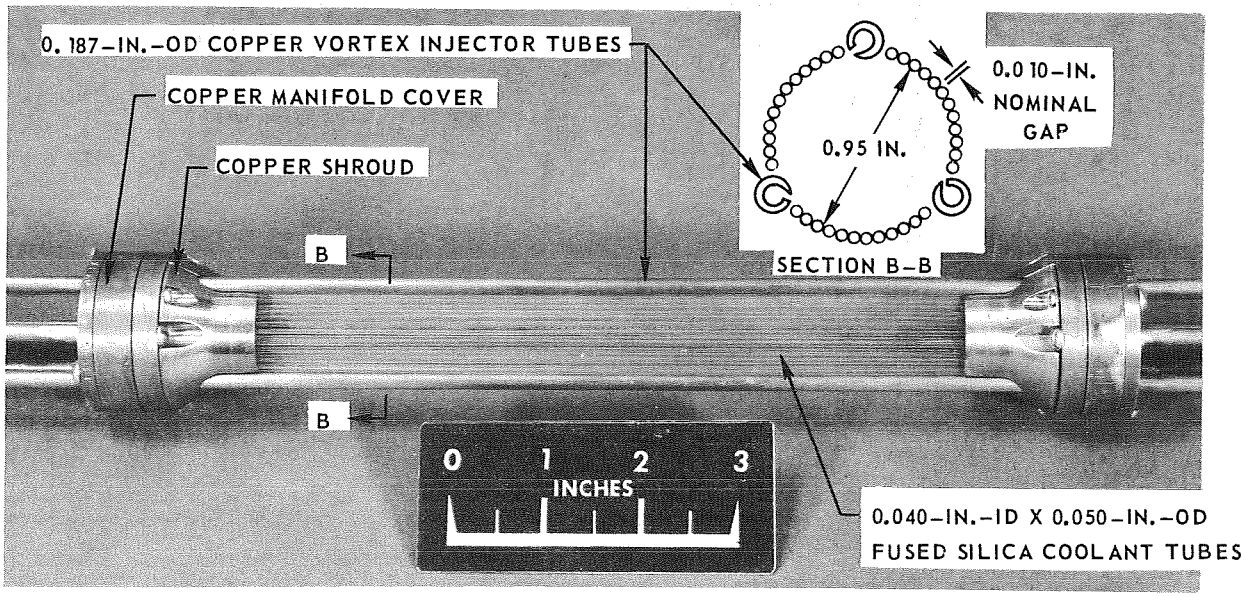

FIG. 11

EFFECT OF INLET FLOW CONDITIONS ON WAVE DISTURBANCE CHARACTERISTICS FOR COAXIAL JETS

PHOTOGRAPHS FROM REF. 49

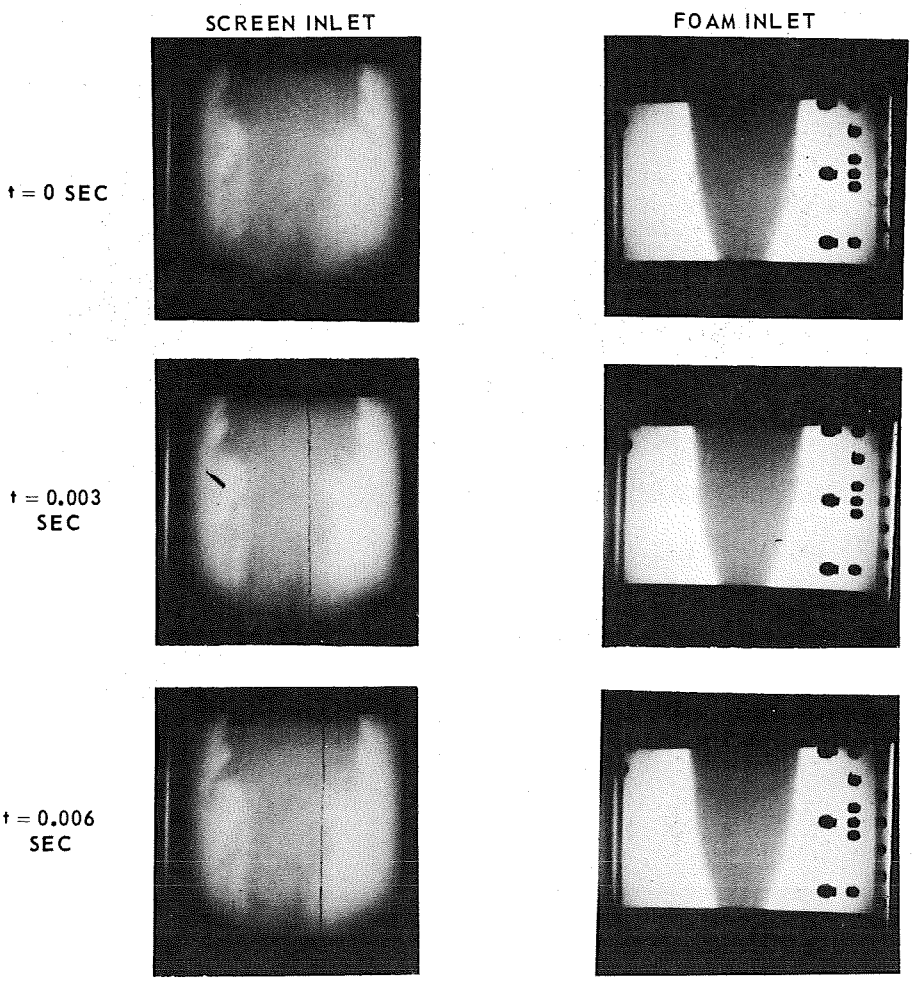

FIG. 12

COMPARISON OF THE EFFECT OF AVERAGE FUEL DENSITY ON FUEL CENTERLINE TEMPERATURES FOR DIFFERENT IONIZATION POTENTIALS USED IN THE HEAVY ATOM MODEL

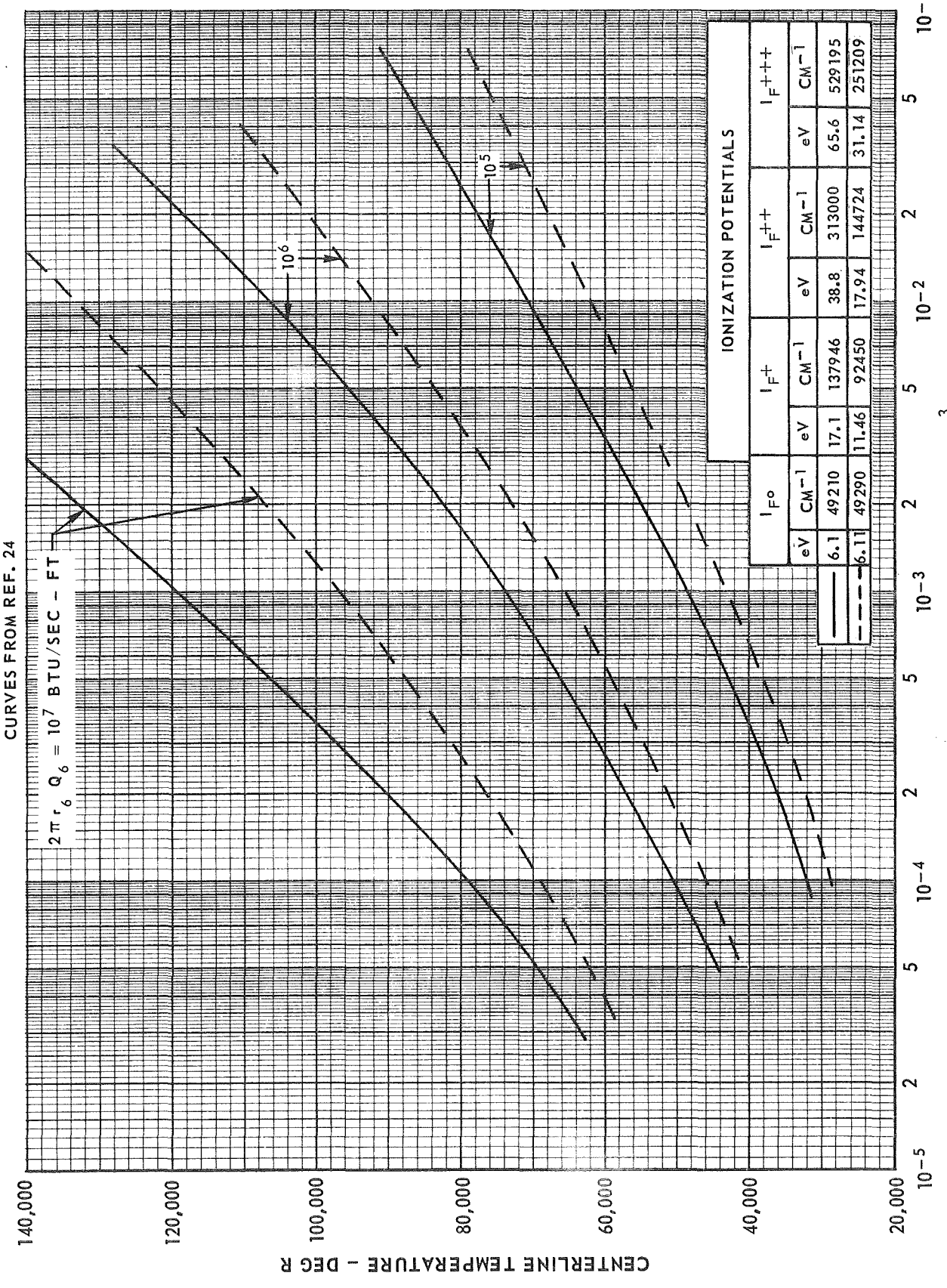

EFFECT OF RESERVOIR PRESSURE ON THE EXTINCTION PARAMETER OF DISPERSED TUNGSTEN POWDER AT A WAVELENGTH OF 0.435 MICRONS

DATA FROM REF. 6

NOMINAL PARTICLE RADIUS, R_P = 0.01 MICRONS

PASSAGE DIAMETER = 0.020 IN.

○ – HELIUM CARRIER GAS

△ – NITROGEN CARRIER GAS

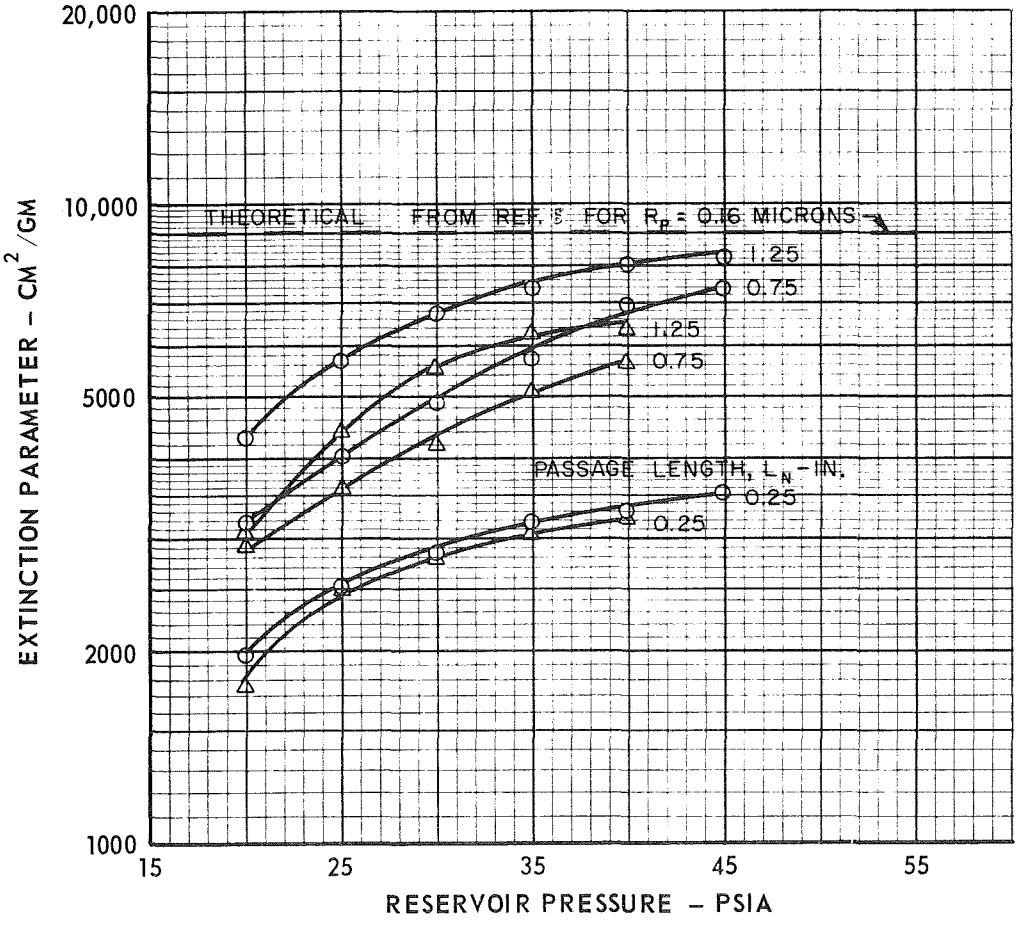

FIG. 14

FRACTIONAL DISTRIBUTION OF BLACK-BODY ENERGY SPECTRUM FOR SEVERAL RADIATING TEMPERATURES

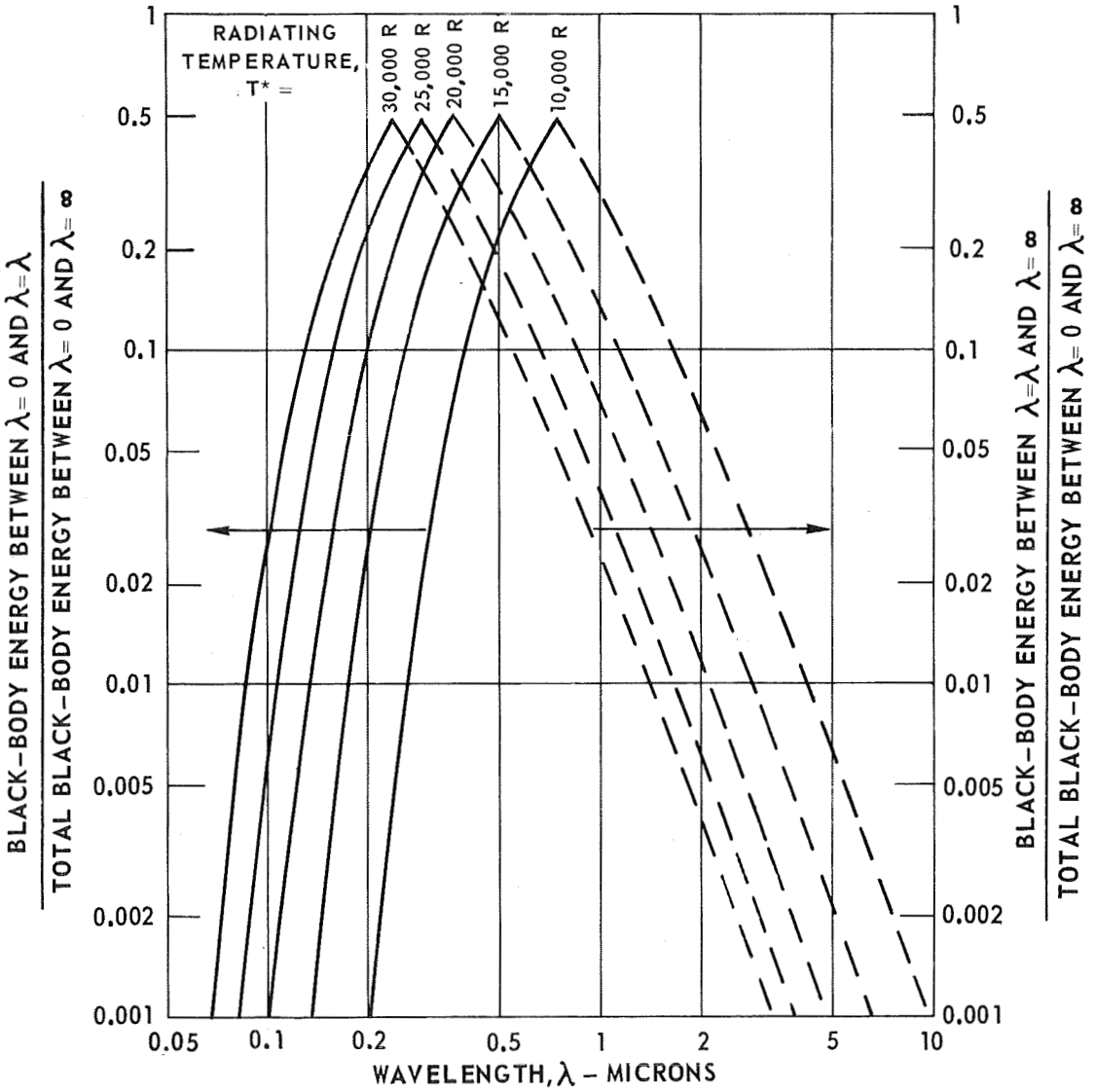

FIG. 15

MEASURED TRANSMISSION CHARACTERISTICS OF FUSED SILICA

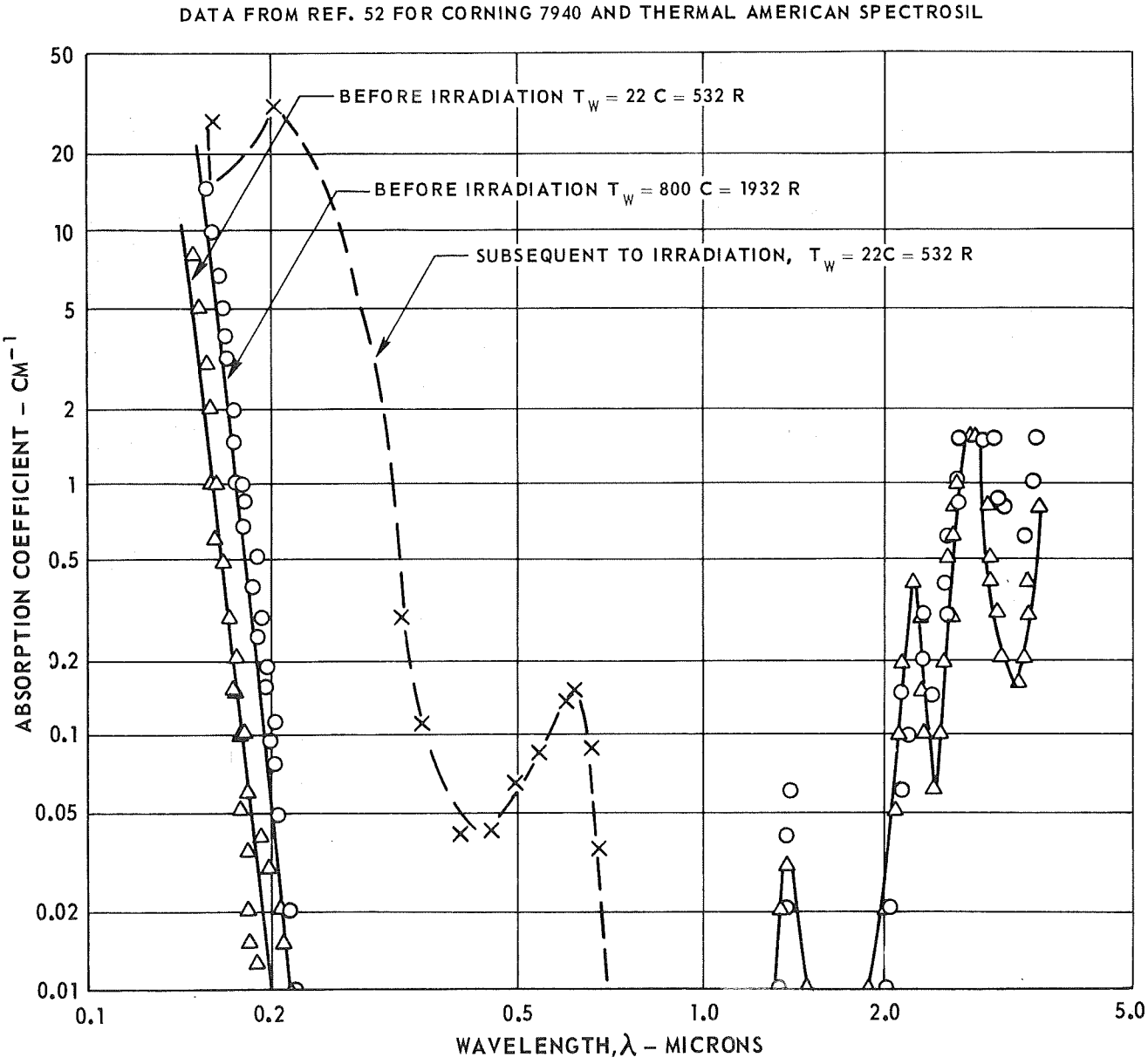

COMPARISON OF EXPERIMENTAL AND CALCULATED ABSORPTION COEFFICIENTS IN FUSED SILICA

SYMBOL	MATERIAL TEMPERATURE
○	700 C
●	800 C
▲	900 C

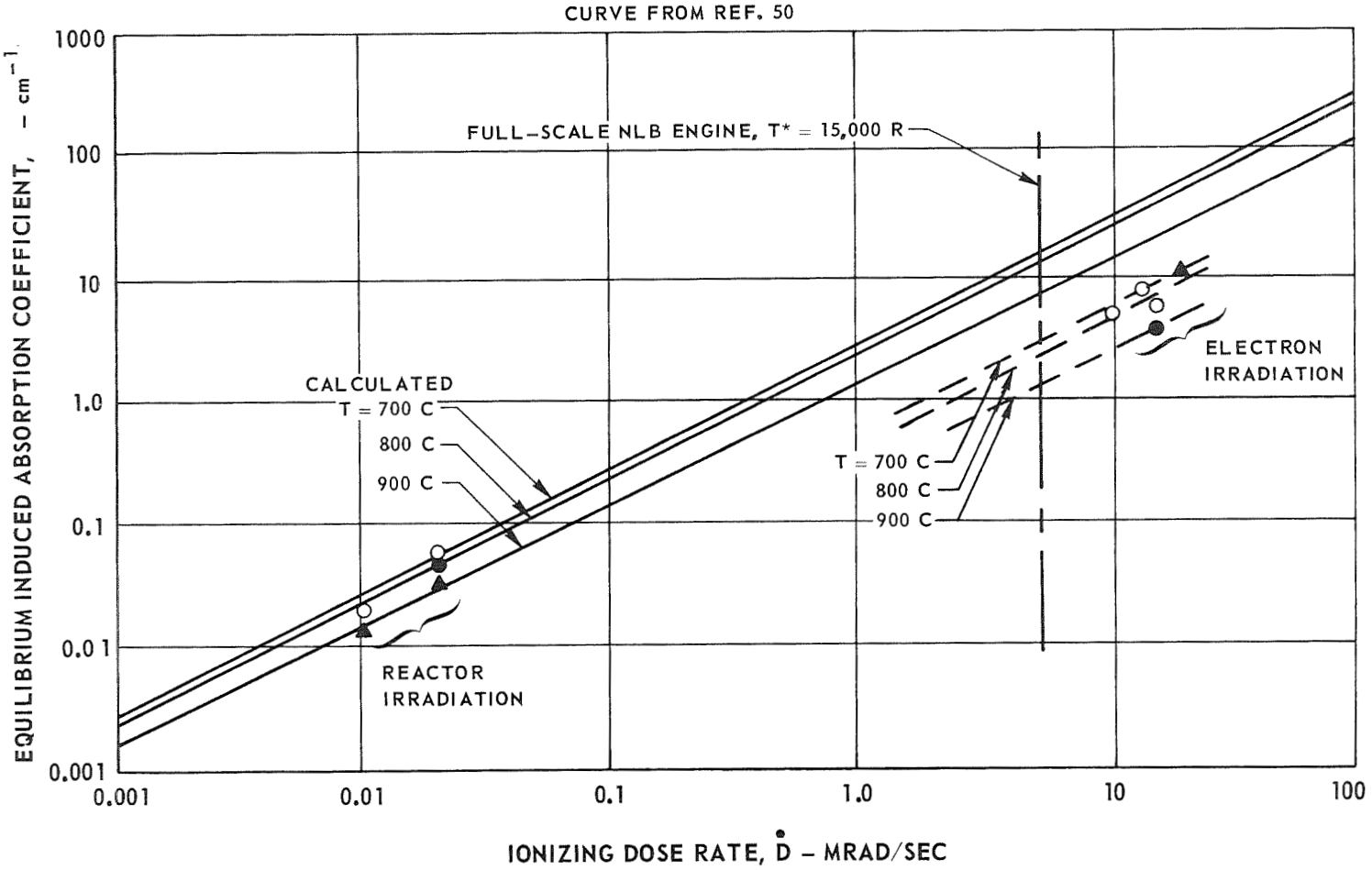

FIG. 16

DISTRIBUTION LIST

Government	Copy No.
Mr. Milton Klein Space Nuclear Propulsion Office U. S. Atomic Energy Commission Washington, D. C. 20545	1
Mr. F. C. Schwenk Space Nuclear Propulsion Office U. S. Atomic Energy Commission Washington, D. C. 20545	2
Captain C. E. Franklin Space Nuclear Propulsion Office U. S. Atomic Energy Commission Washington, D. C. 20545	3
Mr. R. F. Dickson Director of Technical Division Space Nuclear Propulsion Office c/o Nevada Operations Office U. S. Atomic Energy Commission Las Vegas, Nevada	4
Mr. Frank E. Rom Nuclear Systems Division Mail Stop 106-1 NASA Lewis Research Center 21000 Brookpark Road Cleveland, Ohio 44135	5
Mr. Robert G. Ragsdale Nuclear Systems Division Mail Stop 106-1 NASA Lewis Research Center 21000 Brookpark Road Cleveland, Ohio 44135	6
Dr. Richard W. Patch Nuclear Systems Division Mail Stop 106-1 NASA Lewis Research Center 21000 Brookpark Road Cleveland, Ohio 44135	7

Copy No.

Dr. J. C. Evvard
Associate Director
Mail Stop 3-5
NASA Lewis Research Center
21000 Brookpark Road
Cleveland, Ohio 44135 — 8

National Aeronautics and Space Administration
Office of Scientific and Technical Information
Washington, D. C. 20546
Attention: AFSS-LL — 9

Dr. A. J. Eggers, Jr.
Office of Advanced Research and Technology
NASA Headquarters
1520 H Street, NW
Washington, D. C. 20546 — 10

Mr. A. E. Gessow
NASA Headquarters
Office of Advanced Research and Technology
Washington, D. C. 20546 — 11

Dr. Robert F. Trapp
Chief, Research Division
Weapons Evaluation and Control Bureau
Arms Control and Disarmament Agency
320 21st Street, N.W.
Washington, D. C. 20451 — 12

NASA Headquarters
Washington, D. C. 20546
Attention: OART — 13

National Aeronautics and Space Administration
Washington, D. C. 20546
Attention: Office of Technical Information
and Educational Programs, Code ETL — 14

Mr. R. W. Ziem (RPS)
National Aeronautics and Space Administration
Washington, D. C. 20546 — 15

Mr. D. R. Bartz
Manager, Research and Advanced Concepts Section
Propulsion Division
Jet Propulsion Laboratory
Pasadena, California 91103 — 16

Copy No.

Mr. Jerry P. Davis 17
Building 122-3
Jet Propulsion Laboratory
4800 Oak Grove Drive
Pasadena, California 91103

Jet Propulsion Laboratory/CALTECH 18
4800 Oak Grove Drive
Pasadena, California 91103
Attn: Library Section 111-113

Dr. Clifford J. Heindl 19
Building 180-805
Jet Propulsion Laboratory
4800 Oak Grove Drive
Pasadena, California 91103

Dr. Robert V. Meghreblian 20
Jet Propulsion Laboratory
4800 Oak Grove Avenue
Pasadena, California 91103

Mr. L. E. Newlan 21
Chief, Reports Groups
Jet Propulsion Laboratory
4800 Oak Grove Drive
Pasadena, California 91103

Mr. H. Hornby 22
NASA Ames Research Center
Mission Analysis Division
Moffett Field, California 94035

Mr. C. A. Syvertson 23
Associate Director for Astronautics
NASA Ames Research Center
Moffett Field, California 94035

	Copy No.
Mr. Ronald J. Harris Chief, Planetary & Nuclear Systems Group Advanced Systems Office R-AS Marshall Space Flight Center Huntsville, Alabama 35812	24
National Aeronautics and Space Administration George C. Marshall Space Flight Center Huntsville, Alabama 35812 Attention: Library	25
NASA Goddard Space Flight Center Glenn Dale Road Greenbelt, Maryland Attention: Librarian	26
National Aeronautics and Space Administration Manned Spacecraft Center P. O. Box 1537 Houston, Texas Attention: Library	27
National Aeronautics and Space Administration Langley Research Center Langley Air Force Base Virginia Attention: Library	28
Dr. George Grover N-5 Los Alamos Scientific Laboratory P. O. Box 1663 Los Alamos, New Mexico 87544	29
Dr. William Kirk University of California Los Alamos Scientific Laboratory P. O. Box 1663 Los Alamos, New Mexico 87544	30
Los Alamos Scientific Laboratory P. O. Box 1663 Los Alamos, New Mexico 87544 Attention: N Division	31

Copy No.

Mr. John D. Orndoff 32
N Division
Los Alamos Scientific Laboratory
Los Alamos, New Mexico 87544

U. S. Atomic Energy Commission 33
Headquarters Library, Reports Section
Mail Station G-017
Washington, D. C. 20545

Atomic Energy Commission 34
Division of Technical Information Extension
P. O. Box 62
Oak Ridge, Tennessee

Mr. A. P. Fraas 35
Oak Ridge National Laboratory
P. O. Box Y
Oak Ridge, Tennessee 37831

Mr. E. A. Franco-Ferreira 36
Metals & Ceramics Division
Oak Ridge National Laboratory
P. O. Box X
Oak Ridge, Tennessee 37831

Dr. John J. Keyes, Jr. 37
Reactor Division
Oak Ridge National Laboratory
P. O. Box Y
Oak Ridge, Tennessee 37831

Dr. A. J. Miller 38
Oak Ridge National Laboratory
P. O. Box Y
Oak Ridge, Tennessee 37831

Mr. P. Patriarca 39
Oak Ridge National Laboratory
P. O. Box X
Oak Ridge, Tennessee 37831

Copy No.

Mr. John Marchaterre 40
Argonne National Laboratory
9700 South Cass Avenue
Argonne, Illinois

Mr. L. P. Hatch 41
Brookhaven National Laboratory
Upton, Long Island, New York 11101

Dr. Charles Beckett 42
Heat Division
National Bureau of Standards
Washington, D. C.

Mr. Keith Boyer 43
N Division
Los Alamos Scientific Laboratory
Los Alamos, New Mexico 87544

National Aeronautics and Space Council 44
Attention: W. E. Berg
Executive Office of the President
Washington, D. C. 20502

Dr. Charles J. Bridgman 45
Associate Professor of Physics
Air Force Institute of Technology
Wright-Patterson Air Force Base, Ohio 45433

The Rand Corporation 46
1700 Main Street
Santa Monica, California 90406

Mr. G. Sayles (RPRRA) 47
Air Force Rocket Propulsion Laboratory
Edwards Air Force Base
California 93523

Copy No.

Aerospace Corporation 48
P. O. Box 95085
Los Angeles, California 90045
Attention: Library-Documents

Dr. Robert H. Fox 49
Institute for Defense Analysis
400 Army Navy Drive
Arlington, Virginia 22202

Mr. J. E. Jackson 50
DDR&E (OAP)
Washington, D. C.

DDR&E (WSEG) 51
Washington, D. C.
Attention: OSD

AFSC (SCTD) 52
Andrews Air Force Base
Washington, D. C.

Dr. Theodore B. Taylor 53
Defense Atomic Support Agency
The Pentagon
Washington, D. C. 20301

Dr. J. F. Masi (SREP) 54
Department of the Air Force
Air Force Office of Scientific Research
1400 Wilson Boulevard
Arlington, Virginia 22209

Commander 55
AFSC
Foreign Technology Division
Wright-Patterson Air Force Base, Ohio 45433
Attention: RTD (TD-E3b)

Dr. Hans von Ohain 56
Aerospace Research Laboratories (ARD-1)
Wright-Patterson Air Force Base
Ohio 45433

	Copy No.
Mr. E. C. Perkins AUL (AUL3T-7143) Maxwell Air Force Base Alabama	57
Mr. Ben Pinkel Rand Corporation 1700 Main Street Santa Monica, California 90406	58
Mr. Frederick C. Durant, III Assistant Director, Astronautics National Air Museum Smithsonian Institute Washington, D. C. 20560	59
Captain E. N. Kemler Office of Research Analysis Holloman Air Force Base New Mexico	60
Superintendent U. S. Naval Postgraduate Naval Academy Monterey, California	61
Mr. George T. Lalos U. S. Naval Ordnance Laboratory White Oaks, Silver Springs Maryland 20900	62
HQ-SAMSO (SMAAP/Capt. Yepp) Air Force Unit Post Office Los Angeles Air Force Station California 90045	63

Copy No.

NASA Scientific and Technical Information Facility (2 copies) 64
Post Office Box 33 65
College Park, Maryland 20740

NASA Headquarters 66
Washington, D. C. 20546
Attention: New Technology Representative, Code UT

Dr. K. Thom 67
Code RRE
NASA Headquarters
Washington, D. C. 20546

Lt. N. Kuehn 68
Defense Intelligency Agency
Attention: DIA ST-2C2
Washington, D. C. 20301

Universities

Dr. C. C. Chang 69
Head, Space Sciences & Applied Physics
Catholic University of America
Washington, D. C. 20017

Professor Abraham Hyatt 70
1700 E. Imperial Highway
El Segundo, California 90246

Professor Robert A. Gross 71
School of Engineering & Applied Science
Columbia University
New York, New York 10027

Dr. Peter Chiarulli 72
Head, Mechanics Department
Illinois Institute of Technology
Chicago, Illinois 60616

Copy No.

Dr. Andrew Fejer — 73
Head, Mechanical & Aerospace Engineering Department
Illinois Institute of Technology
Chicago, Illinois 60616

Dr. Zalman Lavan — 74
Illinois Institute of Technology
M. A. E. Department
Technology Center
Chicago, Illinois 60616

Dr. T. P. Torda — 75
Illinois Institute of Technology
M. A. E. Department, Technology Center
Chicago, Illinois 60616

Dr. Herbert Weinstein — 76
Chemical Engineering Department
Illinois Institute of Technology
Chicago, Illinois 60616

Dr. Joseph Clement — 77
Nuclear Engineering Department
Georgia Institute of Technology
Atlanta, Georgia 30332

Professor Clyde Orr, Jr. — 78
Chemical Engineering Department
Georgia Institute of Technology
Atlanta, Georgia 30332

Professor Elias P. Gyftopoulos — 79
Room 24-109
Massachusetts Institute of Technology
Cambridge, Massachusetts 02139

Professor J. L. Kerrebrock — 80
Room 33-115
Massachusetts Institute of Technology
Cambridge, Massachusetts 02139

Professor Edward Mason — 81
Room NW12
Massachusetts Institute of Technology
Cambridge, Massachusetts 02139

Copy No.

Professor E. P. Wigner
Department of Physics
Princeton University
Princeton, New Jersey 08540
82

Professor M. J. Zucrow
Atkins Professor of Engineering
Mechanical Engineering Department
Purdue University
Lafayette, Indiana 49707
83

Dr. A. V. Grosse
Research Institute of Temple University
4150 Henry Avenue
Philadelphia, Pennsylvania 19144
84

Professor H. C. Perkins
Energy, Mass & Momentum Transfer Laboratory
Aerospace & Mechanical Engineering Department
University of Arizona
Tucson, Arizona 85721
85

Professor Rafael Perez
Nuclear Engineering Department
University of Florida
Gainesville, Florida 32601
86

Professor Terence Cool
Thermal Engineering Department
Cornell University
Ithaca, New York 14850
87

Dr. Franklin K. Moore, Head
Thermal Engineering Department
Cornell University
Ithaca, New York 14850
88

Professor Chieh Ho
Division of Nuclear Science
Room 287, Mudd Building
Columbia University
New York, New York 10027
89

Copy No.

Dr. W. S. Lewellen 90
Room 33-119
Massachusetts Institute of Technology
Cambridge, Massachusetts 02139

Dr. Bruce A. Reese, Director 91
Jet Propulsion Center
Mechanical Engineering Department
Purdue University
Lafayette, Indiana 47907

Professor Glen J. Schoessow 92
Department of Nuclear Engineering Sciences
202 Nuclear Sciences Building
University of Florida
Gainesville, Florida 32601

Dr. J. Richard Williams 93
Nuclear Engineering Department
Georgia Institute of Technology
Atlanta, Georgia 30332

Dr. Robert Uhrig 94
Chairman, Department of Nuclear Engineering
University of Florida
Gainesville, Florida 32601

Dr. Paul T. Bauer 95
Research Institute
University of Dayton
300 College Park
Dayton, Ohio 45409

Professor Ron Dalton 96
Department of Nuclear Engineering
University of Florida
Gainesville, Florida 32601

Dr. George Nelson 97
University of Arizona
Nuclear Engineering Department
Tucson, Arizona 85721

Copy No.

Dr. Richard T. Schneider — 98
202 Nuclear Sciences Building
Department of Nuclear Engineering Sciences
University of Florida
Gainesville, Florida 32601

Professor C. N. Shen — 99
Rensselaer Polytechnic Institute
Troy, New York

Dr. Herman E. Unger — 100
Assistant Professor
Engineering Sciences
Northwestern University
Evanston, Illinois 60201

Industry

Mr. James Carton — 101
Advanced Concepts
REON Division
Aerojet-General Corporation
Sacramento, California 95801

Mr. A. B. Longyear — 102
New Technology - NRO
Aerojet-General Corporation
P. O. Box 15847
Sacramento, California 95813

Mr. William J. Houghton — 103
Department 7040, Building 2019A2
Aerojet-General Corporation
P. O. Box 1947
Sacramento, California 95809

Mr. W. L. Snapp — 104
Aerojet-General Corporation
20545 Center Ridge Road
Cleveland, Ohio 44116

	Copy No.
Mr. C. K. Soppet, Manager Engine Test Operations NERVA Test Operations P. O. Box 2027 Jackass Flats, Nevada 89023	105
Dr. J. J. Stewart Department 7040, Building 2019A2 Aerojet-General Corporation Sacramento, California 95809	106
Aerojet-General Corporation P. O. Box 1947 Sacramento, California 95809 Attention: Technical Information Office	107
Florence Walsh, Librarian Aerojet-General Corporation 11711 South Woodruff Avenue Downey, California	108
B. Probert Aerojet-General Nucleonics P. O. Box 78 San Ramon, California	109
R. R. Blackwell Allison Division - GMC P. O. Box 24013 Indianapolis, Indiana 46206	110
Mr. David Mallon Allison Division General Motors Corporation 2355 S. Tibbs Avenue Indianapolis, Indiana 46206	111
Dr. Richard Rosa AVCO Everett Research Laboratory 2385 Revere Beach Parkway Everett, Massachusetts 02149	112

Copy No.

Mr. Jack Ravets 113
Westinghouse Astronuclear Laboratory
P. O. Box 10864
Pittsburgh, Pennsylvania 15236

Mr. Jerrold M. Yos 114
AVCO Corporation
Research & Advanced Development Division
201 Lowell Street
Wilmington, Massachusetts 01887

Bell Aerosystems 115
Box 1
Buffalo 5, New York
Attention: T. Reinhardt

Mr. R. R. Barber 116
Boeing Company
Aerospace Division
P. O. Box 3707
Seattle, Washington 98124

Mr. J. A. Brousseau 117
Chief, Propulsion Systems Technology
Mail Stop 47-18
The Boeing Company
Seattle, Washington 98124

Chrysler Corporation 118
Defense Operations Division
Box 757
Detroit 31, Michigan

Dr. Ralph S. Cooper 119
Donald W. Douglas Laboratories
2955 George Washington Way
Richland, Washington 99352

Mr. J. S. Cory 120
Donald W. Douglas Laboratories
2955 George Washington Way
Richland, Washington 99352

Copy No.

Dr. D. E. Knapp 121
Donald W. Douglas Laboratories
2955 George Washington Way
Richland, Washington 99352

Dr. R. J. Holl 122
Missiles & Space Systems Division
Douglas Aircraft Company
Santa Monica, California 90405

Mr. J. L. Waisman 123
Douglas Aircraft Company
Santa Monica, California 90405

Dr. Kurt P. Johnson 124
Advanced Space Technology, A2-263
Douglas Missiles & Space Systems Division
Santa Monica, California 90405

Dr. J. R. Beyster 125
General Atomic
P. O. Box 608
San Diego, California 92112

Mr. James Nance 126
General Atomic
P. O. Box 608
San Diego, California 92112

General Atomics Division 127
General Dynamics Corporation
P. O. Box 1111
San Diego, California 92110

Mr. Richard W. Carkeek 128
The Boeing Company
P. O. Box 3868
Mail Stop 85-85
Seattle, Washington 98124

Dr. J. F. Kunze, Manager 129
Operations & Analysis
Idaho Test Station
Idaho Nuclear Corporation
P. O. Box 2147
Idaho Falls, Idaho 83401

Copy No.

Mr. John Peak — 130
General Atomics Division
General Dynamics Corporation
P. O. Box 608
San Diego, California 92112

Mr. Louis Canter — 131
General Dynamics/Astronautics
Technical Library
San Diego, California 92112

General Electric Company — 132
MSVD Library Documents Group, RM 3446
3198 Chestnut Street
Philadelphia, Pennsylvania 19101

Dr. S. M. Scala — 133
Manager, Theoretical Fluid Physics Section
General Electric Company
Space Sciences Laboratory
P. O. Box 8555
Philadelphia, Pennsylvania 19101

Mr. J. W. Stephenson — 134
General Electric Co., NMPO
P. O. Box 15132
Cincinnati 15, Ohio

General Electric Company — 135
Cincinnati 15, Ohio
Attention: Technical Information Center

Dr. Jerry Grey — 136
Grey-Rad Corporation
61 Adams Street
Princeton, New Jersey 08540

Mr. M. O. Friedlander — 137
Engineering Library, Plant 5
Grumman Aircraft Engineering Corporation
Bethpage, Long Island, New York

Mr. Holmes F. Crouch — 138
Lockheed Missiles & Space Company
Space System Division, Dept. 62-90, Building 104
Sunnyvale, California 94408

Copy No.

Mr. Maxwell Hunter — 139
Department 50-01, Building 102
Lockheed Missiles & Space Company
P. O. Box 504
Sunnyvale, California 94408

Mr. H. F. Plank — 140
Building 153, DCS-G
Lockheed Missile & Space Company
Sunnyvale, California 94408

Miss Belle Berlad, Librarian — 141
Lockheed Propulsion Company
P. O. Box 111
Redlands, California

Dr. Larry Kaufman — 142
Director of Research
Manlabs, Inc.
21 Erie Street
Cambridge, Massachusetts 02139

Martin Nuclear, A Division of Martin-Marietta Corporation — 143
P. O. Box 5042
Middle River 3, Maryland
Attention: Library

Mr. J. J. Norton — 144
Marquardt Corporation
16555 Saticoy Street
Van Nuys, California

Naval Plant Representative Office — 145
c/o UAC Pratt & Whitney Aircraft Division
East Hartford, Connecticut 06108
Attention: Mr. R. N. Schuster
Contracts Division

North American Aviation, Inc. — 146
Space and Information Systems Division
12214 Lakewood Boulevard
Downey, California
Attention: Technical Information
Center (L. M. Foster)

Copy No.

Mr. W. H. Morita — 147
North American Aviation, Inc.
Space & Information Systems Division
12214 Lakewood Boulevard
Downey, California

Mr. C. C. Bennett — 148
Rocketdyne
P. O. Box 552
Canoga Park, California 91303

Mr. Robert Dillaway — 149
Nucleonics Department
Rocketdyne
6633 Canoga Avenue
Canoga Park, California 91303

Dr. S. V. Gunn — 150
Rocketdyne
6633 Canoga Avenue
Canoga Park, California 91303

Mr. Carmen Jones — 151
H63 - General Electric Co.
North I-75
Cincinnati, Ohio 45215

Rocketdyne — 152
6633 Canoga Park, California 91303
Attention: Library , Dept. 596-306

Space Technology Laboratories — 153
One Space Park
Redondo Beach, California 90277
Attention: STL Technical Library Doc.
Acquisitions

Thompson Ramo Wooldridge — 154
23555 Euclid Avenue
Cleveland, Ohio
Attention: Librarian

Copy No.

Mr. Walter F. Krieve 155
Building S
TRW Systems
One Space Park
Redondo Beach, California 90278

Dr. D. W. Drawbaugh 156
Astronuclear Laboratory
Westinghouse Electric Corporation
Pittsburgh, Pennsylvania 15236

Mr. F. McKenna 157
Astronuclear Laboratory
Westinghouse Electric Corporation
P. O. Box 10864
Pittsburgh, Pennsylvania 15236

Dr. John Romanko, Staff Scientist 158
Y-128, Building 197
General Dynamics
Ft. Worth Division, Box 740
Ft. Worth, Texas 76101

Dr. J. W. Hilborn 159
Reactor Physics Branch
Advanced Projects & Reactor Physics Division
Atomic Energy of Canada Limited
Chalk River, Ontario, Canada

Dr. Jacob B. Romero 160
The Boeing Company
Mail Stop 84-66
Kent, Washington

Mr. Merle Thorpe 161
TAFA Division
Humphreys Corporation
180 North Main Street
Concord, New Hampshire 03301

Copy No.

Dr. Henry Stumpf 162
Astronuclear Lab
Westinghouse Electric Corporation
Pittsburgh, Pennsylvania 15236

Dr. J. W. Morfitt, Manager 163
Idaho Test Station
Idaho Nuclear Corporation
P. O. Box 2147
Idaho Falls, Idaho 83401